TSC-FAA-80-21

REPORT NO. FAA-RD-80-133

ANALYSIS OF GROUND-WIND VORTEX SENSING SYSTEM DATA FROM O'HARE INTERNATIONAL AIRPORT

T.E. Sullivan
J.N. Hallock
B.P. Winston

U.S. DEPARTMENT OF TRANSPORTATION
RESEARCH AND SPECIAL PROGRAMS ADMINISTRATION
Transportation Systems Center
Cambridge MA 02142

SEPTEMBER 1980

FINAL REPORT

Prepared for

U.S. DEPARTMENT OF TRANSPORTATION
FEDERAL AVIATION ADMINISTRATION
Systems Research and Development Service
Washington DC 20591

NOTICE

This document is disseminated under the sponsorship of the Department of Transportation in the interest of information exchange. The United States Government assumes no liability for its contents or use thereof.

NOTICE

The United States Government does not endorse products or manufacturers. Trade or manufacturers' names appear herein solely because they are considered essential to the object of this report.

Technical Report Documentation Page

1. Report No.	2. Government Accession No.	3. Recipient's Catalog No.
FAA-RD-80-133		

4. Title and Subtitle	5. Report Date
ANALYSIS OF GROUND-WIND VORTEX SENSING SYSTEM DATA FROM O'HARE INTERNATIONAL AIRPORT	SEPTEMBER 1980
	6. Performing Organization Code
7. Author(s) T.E. Sullivan, J.N. Hallock, and B.P. Winston	8. Performing Organization Report No. DOT-TSC-FAA-80-21
9. Performing Organization Name and Address U.S. Department of Transportation Research and Special Programs Administration Transportation Systems Center Cambridge MA 02142	10. Work Unit No. (TRAIS) FA086/R1116
	11. Contract or Grant No.
12. Sponsoring Agency Name and Address U.S. Department of Transportation Federal Aviation Administration Systems Research and Development Service Washington DC 20591	13. Type of Report and Period Covered Final Report July 1976-Sep. 1977
	14. Sponsoring Agency Code

15. Supplementary Notes

16. Abstract

From July 1976 through September 1977, aircraft wake vortex data were collected on the approach to runways 14R, 27R, and 32L at O'Hare International Airport. The vortices from over 21,000 aircraft were tracked using the propeller anemometer Ground-Wind Vortex Sensing System (GWVSS), and the vortex behavior was correlated with the associated ambient meteorological conditions. The primary purpose of the tests was the evaluation of the Vortex Advisory System (VAS) concept. The elliptical wind criterion used in the VAS was verified using the vortex data.

17. Key Words	18. Distribution Statement
- Aircraft Wake Vortices Vortices Vortex Sensors Vortex Decay Meteorology Vortex Transport	DOCUMENT IS AVAILABLE TO THE PUBLIC THROUGH THE NATIONAL TECHNICAL INFORMATION SERVICE, SPRINGFIELD, VIRGINIA 22161

19. Security Classif. (of this report)	20. Security Classif. (of this page)	21. No. of Pages	22. Price
Unclassified	Unclassified	116	

Form DOT F 1700.7 (8-72) Reproduction of completed page authorized

PREFACE

It is the objective of the Aircraft Wake Vortex Program to increase capacity at the major high-density air terminals. Analysis of many thousands of vortex tracks led to the concept of a Vortex Advisory System (VAS); the VAS has been proposed as a first or interim step toward meeting the objective of the Program. Vortex-tracking data were collected at Stapleton, Kennedy, Heathrow, and O'Hare International Airports. This report addresses the data collected at Chicago O'Hare.

The authors would like to thank Ed Scharres (Illinois Institute of Technology Research Institute, field engineer for the O'Hare test site) and Dick Uram and Buzz Lowe (O'Hare FAA Facilities Sector); their assistance and cooperation assured the successful installation and operation of the test site at O'Hare. We also acknowledge the cooperation of the Dispatch Offices of United, TWA, and American Airlines in the identification of the Heavy B-707 and DC-8 aircraft.

METRIC CONVERSION FACTORS

Approximate Conversions to Metric Measures

Symbol	When You Know	Multiply by	To Find	Symbol
	LENGTH			
in	inches	2.5	centimeters	cm
ft	feet	30	centimeters	cm
yd	yards	0.9	meters	m
mi	miles	1.6	kilometers	km
	AREA			
in^2	square inches	6.5	square centimeters	cm^2
ft^2	square feet	0.09	square meters	m^2
yd^2	square yards	0.8	square meters	m^2
mi^2	square miles	2.6	square kilometers	km^2
	acres	0.4	hectares	ha
	MASS (weight)			
oz	ounces	28	grams	g
lb	pounds	0.45	kilograms	kg
	short tons (2000 lb)	0.9	tonnes	t
	VOLUME			
tsp	teaspoons	5	milliliters	ml
Tbsp	tablespoons	15	milliliters	ml
fl oz	fluid ounces	30	milliliters	ml
c	cups	0.24	liters	l
pt	pints	0.47	liters	l
qt	quarts	0.95	liters	l
gal	gallons	3.8	liters	l
ft^3	cubic feet	0.03	cubic meters	m^3
yd^3	cubic yards	0.76	cubic meters	m^3
	TEMPERATURE (exact)			
°F	Fahrenheit temperature	5/9 (after subtracting 32)	Celsius temperature	°C

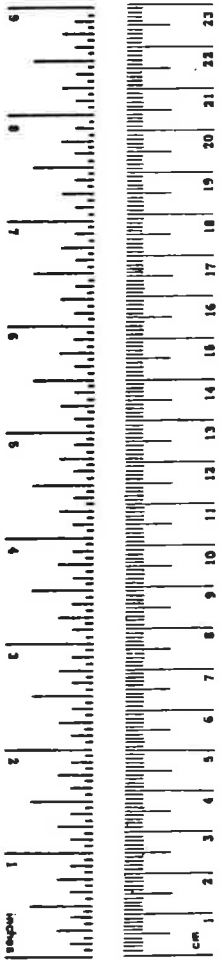

Approximate Conversions from Metric Measures

Symbol	When You Know	Multiply by	To Find	Symbol
	LENGTH			
mm	millimeters	0.04	inches	in
cm	centimeters	0.4	inches	in
m	meters	3.3	feet	ft
m	meters	1.1	yards	yd
km	kilometers	0.6	miles	mi
	AREA			
cm^2	square centimeters	0.16	square inches	in^2
m^2	square meters	1.2	square yards	yd^2
km^2	square kilometers	0.4	square miles	mi^2
ha	hectares (10,000 m^2)	2.5	acres	
	MASS (weight)			
g	grams	0.035	ounces	oz
kg	kilograms	2.2	pounds	lb
t	tonnes (1000 kg)	1.1	short tons	
	VOLUME			
ml	milliliters	0.03	fluid ounces	fl oz
l	liters	2.1	pints	pt
l	liters	1.06	quarts	qt
l	liters	0.26	gallons	gal
m^3	cubic meters	35	cubic feet	ft^3
m^3	cubic meters	1.3	cubic yards	yd^3
	TEMPERATURE (exact)			
°C	Celsius temperature	9/5 (then add 32)	Fahrenheit temperature	°F

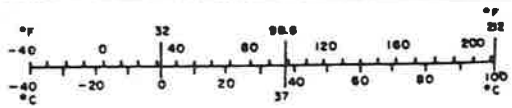

TABLE OF CONTENTS

TABLE OF CONTENTS (CONTINUED)

LIST OF ILLUSTRATIONS

LIST OF ILLUSTRATIONS (CONTINUED)

LIST OF ILLUSTRATIONS (CONTINUED)

LIST OF ILLUSTRATIONS (CONTINUED)

LIST OF TABLES

1. INTRODUCTION

The restricted capacity and the resulting airline and passenger delay costs at the high density air terminals are major problems confronting the United States air transportation system. The need to increase airport landing and takeoff capacity under all weather conditions without degrading current high levels of safety is therefore of prime importance. When the major air terminals operate at or near saturation in the current capacity-demand environment, aircraft delays are commonplace and poor weather only compounds the delay problem. Since capacity relief through construction of new airports or runways is not likely, some other means must be pursued to permit increased aircraft operations into and out of the major air terminals. One such solution would be to decrease the longitudinal or inter-aircraft spacings between successive aircraft operations.

Prior to 1970, landing aircraft were separated by a minimum of 3 nautical miles during Instrument Flight Rules (IFR) operations. The minimum was based primarily on radar operating limits and to a lesser extent on runway occupancy limitations. Concern about the possible pernicious effects of aircraft wake vortices arose with the introduction of jet transports into airline service in 1959. It was the introduction of the jumbo jet that finally led in 1970 to the establishment of wake vortex separation standards which were added to the IFR separations. These additive separations varied from 0 nautical miles (for a B-727 following another B-727, for instance) to 3 nautical miles (for a King Air following a B-747, for instance) at the runway threshold.

Under the sponsorship of the Federal Aviation Administration (FAA), the Transportation Systems Center (TSC) has been collecting data on the behavior of wake vortices, particularly on how they move and decay near the ground. The data indicate that, most of the time, the separation criteria are overly conservative. Using knowledge of vortex behavior, systems could be developed to provide information on the presence or absence of potentially

hazardous vortices in the flight corridors around an airport. Since separation criteria are often overly conservative, and since systems can be developed to identify those times when vortices do not present a safety problem, longitudinal spacings could often be decreased permitting a concurrent reduction in air traffic delays.

The collection of data on the transport and decay of vortices in the approach region from middle marker to runway threshold has been underway for some time. At Stapleton International Airport in Denver, Colorado, the approach region of runway 26L was equipped to monitor vortices from landing aircraft. The test program lasted from August through November of 1973, and vortex tracks from approximately 7000 aircraft landings were recorded (Refs. 1-3). The approach zone of runway 31R at Kennedy International Airport in Jamaica, New York, was established as a vortex test site in June 1973 until its closing in January 1977. Over 15,000 landings were recorded at Kennedy (Refs. 1-3). In a joint venture with the British Civil Aviation Authority, approximately 13,000 landings were monitored between May 1974 and June 1975 on runway 28R at Heathrow International Airport near London, England (Refs. 4 and 5).

Thousands of vortex tracks are required as meteorology, aircraft characteristics, and the proximity of the ground all affect the motion and decay of wake vortices. The characteristics of the wake vortices are established initially by factors related to the aircraft such as gross weight, flight speed, configuration (flap settings), and wingspan. Subsequently, the vortex characteristics are altered and eventually dominated by interactions between the vortices and the ambient atmosphere. Reference 1 reviews the current understanding of the vortex phenomenon.

Detailed analyses of the 35,000 vortex tracks collected at Stapleton, Kennedy, and Heathrow indicated that a wind-rose criterion might be used to determine when interarrival separations could be uniformly reduced to 3 nautical miles for all aircraft (i.e., when the vortex separation standards can be ignored). A simple system, known as the Vortex Advisory System (VAS), was

designed to take advantage of the wind-rose criterion (Refs. 6-9). The VAS is based on comparing the measured wind magnitude and direction (with respect to the runway heading) with the wind criterion.

It was decided to test the VAS concept at an airport under actual operating conditions. Since the main objective of the VAS is to decrease delays, the major high density terminals with a significant percentage of jumbo jet operations and with capacity at or near saturation were considered for the feasibility tests. [It should be noted that the feasibility tests were to be done without ever actually altering aircraft separations. The operation of the VAS equipment and the potential delay reductions were to be examined.] Chicago O'Hare was the airport selected.

This report addresses the analysis of the vortex behavior from over 21,000 aircraft landings at O'Hare. The feasibility tests lasted from July 1976 through September 1977. Data were collected both prior to July 1976 and after September 1977, but the approximately 14,000 aircraft landings are not included in the analysis described herein. The purposes of the 14,000 cases were algorithm development, testing averaging time techniques, and meteorological sensor tests; the vortex data were not subjected to the same extensive analysis as the 21,000 cases -- with respect to vortex behavior, only possible violations of the VAS wind criterion were sought.

The VAS as implemented at O'Hare consists of a network of instrumented meteorological towers placed near the middle marker (and about 1000 feet to one side) of each runway (Refs. 6 and 7). The report will often refer to the VAS instrumentation. Reference 6 describes in detail the major subsystems of the VAS: a Meteorological Subsystem for the measurement of the meteorological conditions existing in the landing corridors of the airport; a Data Processing Subsystem which processes all meteorological data and, based on the VAS wind-rose criterion, determines when separations between landing aircraft can be reduced; a Data Display Subsystem for the display of separation requirements and meteorological

conditions to the air traffic controllers; and a VAS Performance Monitoring and Data Recording Subsystem which monitors system performance, indicates failures and displays these to maintenance personnel, and records all VAS input and output data for archival purposes.

Section 2 describes the sensors used in the data collection emphasizing the anemometer arrays of the Ground-Wind Vortex Sensing System. Section 3 describes the O'Hare test sites. The data collection hardware and data formats are presented in Section 4. Data processing techniques are outlined in Section 5.

Section 6 describes the meteorology of the O'Hare site. The analysis techniques and the results of the data analysis are presented in Section 7; this section covers vortex behavior vis-a-vis vortex motion and decay near the ground. Section 8 summarizes the results of the O'Hare data collection effort.

2. SENSORS

Two types of vortex sensors were deployed during the Chicago O'Hare (ORD) tests, the Ground-Wind Vortex Sensing System (GWVSS) and the Monostatic Acoustic Vortex Sensing System (MAVSS). This report discusses only the results from the GWVSS. The data obtained from the MAVSS are discussed in a separate report (Ref. 10). The main function of the GWVSS was to provide data on vortex transport characteristics. The detection of the vortex by the GWVSS gives little direct information on the strength or height of the vortex, but does locate a vortex within the sensor systems. Aircraft detectors provided trigger signals for the time of aircraft passage over each of the GWVSS lines. Analysis of the data depended on accurately measuring the ambient wind velocity which has been empirically determined to be the most important parameter for characterizing vortex transport.

2.1 GROUND-WIND VORTEX SENSING SYSTEM

The GWVSS consisted of an array of Gill propeller anemometers arranged along a line oriented perpendicular to the runway centerline. All the anemometers pointed in the same direction. A typical array at the O'Hare test site (Fig. 1) consisted of fifteen anemometers located symmetrically about the extended runway centerline with an inter-sensor spacing of 50 feet. The lateral extent of the GWVSS lines was limited to $\pm$ 350 feet; this value was chosen as being necessary and sufficient to determine that vortices had either decayed or transported away from the extended runway centerline.

The propeller is directly coupled to a miniature d.c. generator whose output voltage level is proportional to the component of the wind along the anemometer axis. When a vortex is within about 150 feet of the ground, the vortex flow field can be detected by the GWVSS. The vortices rotate in opposite directions and, therefore, one vortex (downwind) causes an increase while the other vortex (upwind) causes a decrease in the wind

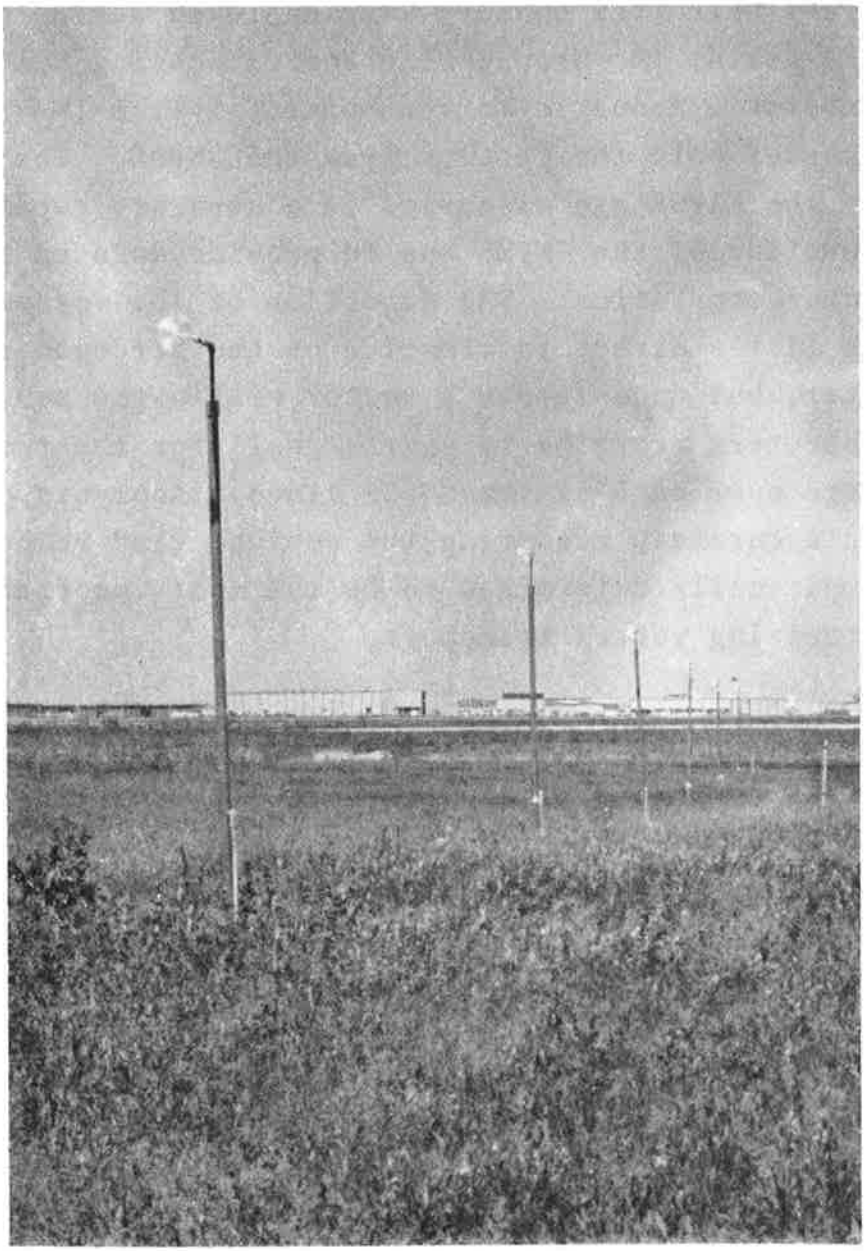

FIGURE 1. ANEMOMETER ARRAY AT O'HARE

measured by the anemometers as shown in Fig. 2. As a vortex pair transported across the array of sensors, the output voltage from each sensor would be expected to increase above the level of the ambient wind as the first vortex passed and to decrease below the level of the ambient wind as the second vortex passed as shown in Fig. 3. By displaying the outputs of several anemometers simultaneously, the transport of the vortices could be observed (Fig. 4). The location of each vortex was determined by a computer algorithm which simultaneously inspected all the anemometers in an array and selected the candidate locations with the highest and lowest signal strengths.

2.2 AMBIENT WIND SENSOR

The ambient wind was measured in the vicinity of each GWVSS with three Climatonics® Mark III wind sensors mounted on a 50-foot tower. Wind speed was measured by a three-cup anemometer coupled to a light chopper which converted the speed of rotation of the cups to a voltage whose frequency was proportional to the wind speed. Wind direction was measured by a vane coupled to a potentiometer, the d.c. voltage output being proportional to the wind direction. One sensor was mounted on the top of the tower at the 50-foot level and two sensors were mounted on a crossarm at the 40-foot level as shown in Figure 5. The sensor threshold (minimum wind which would result in sensor movement) was 0.7 knots and the accuracy was $\pm$ 0.2 knots or 1.5 percent for wind speed and $\pm$ 1.5° for wind direction.

2.3 AIRCRAFT DETECTOR

An acoustic aircraft detector, consisting of a miniature speaker mounted on a printed circuit board with electronics for signal conditioning (Fig. 6), was mounted in an environmental enclosure on each GWVSS line. The electrical signal produced by the speaker as an aircraft passed overhead was amplified, rectified, and integrated, resulting in a smoothed Gaussian-shape signal roughly proportional to the noise level produced by the

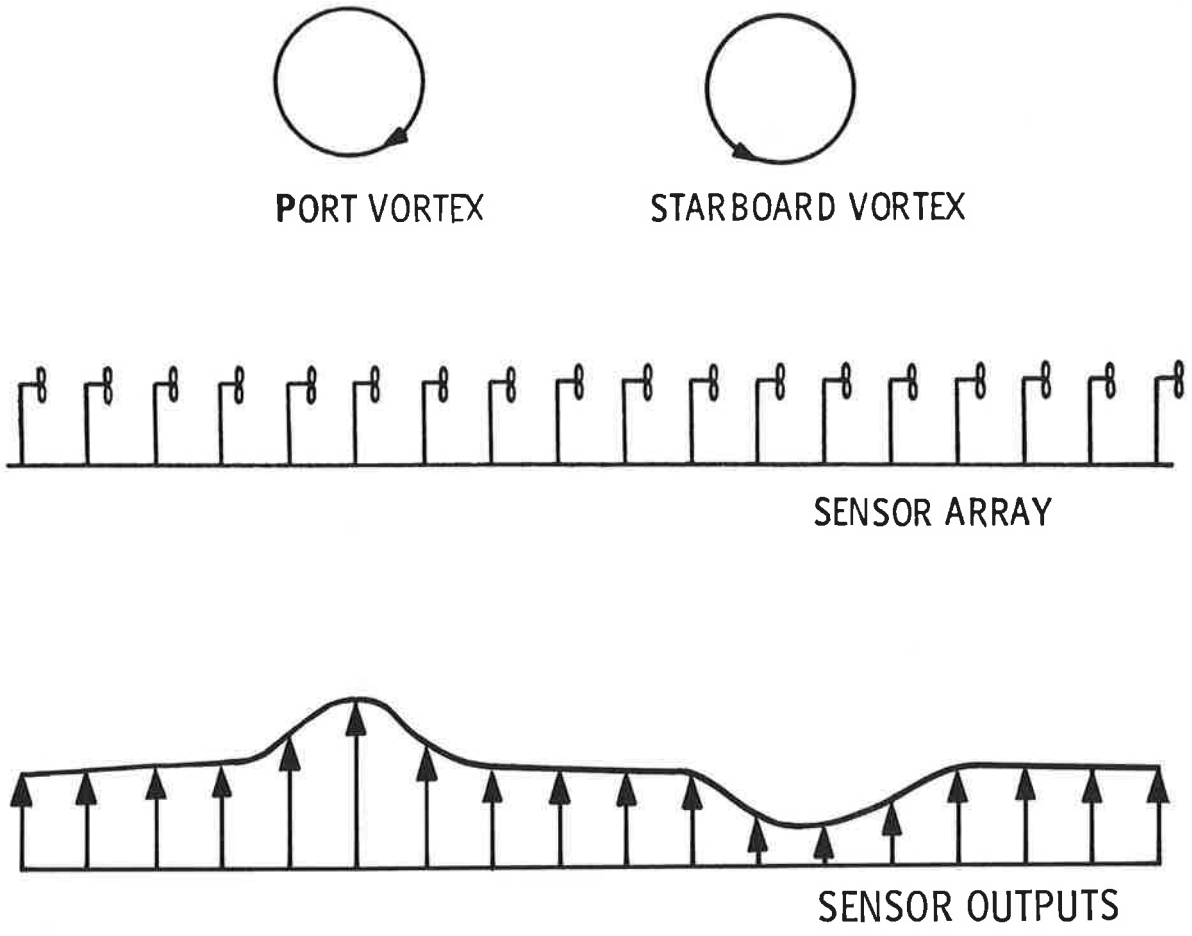

FIGURE 2. SCHEMATIC VIEW OF GWVSS ANEMOMETER ARRAY AND SIGNAL OUTPUTS

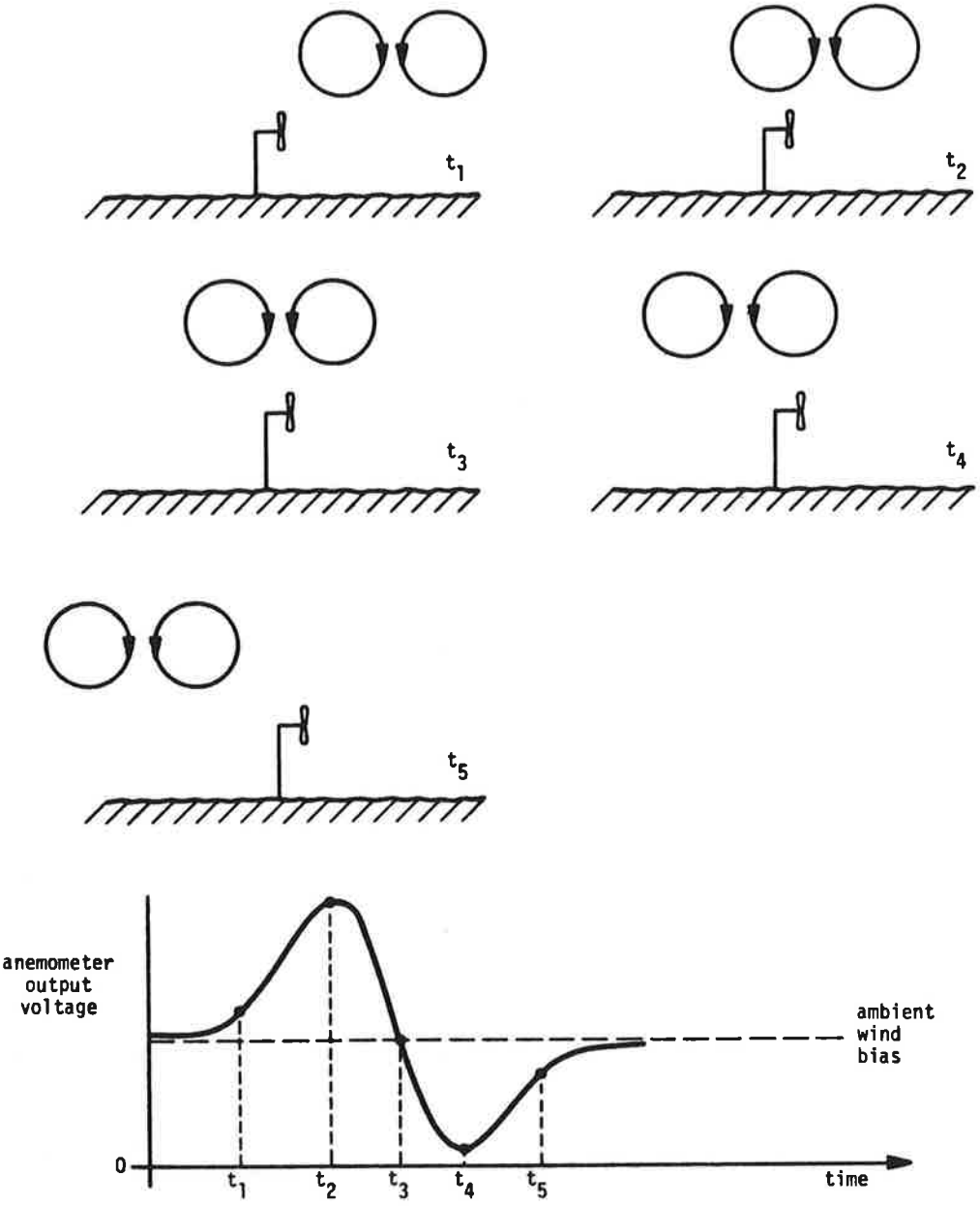

FIGURE 3. ANEMOMETER OUTPUT VOLTAGE AS A VORTEX PAIR PASSES OVERHEAD

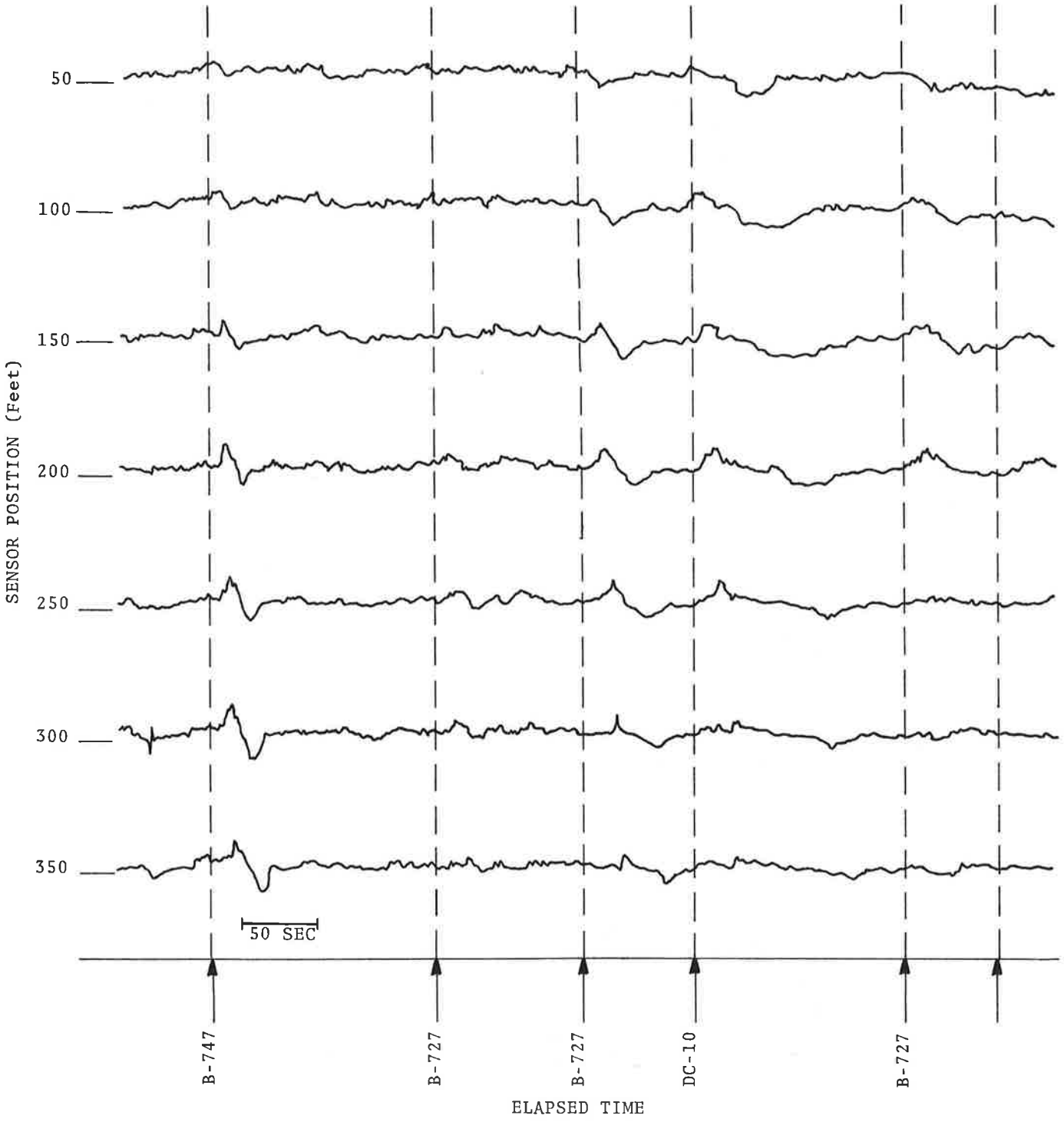

FIGURE 4. ANEMOMETER ARRAY DATA (HEADWIND, 5-8 KNOTS; CROSSWIND, 2-10 KNOTS)

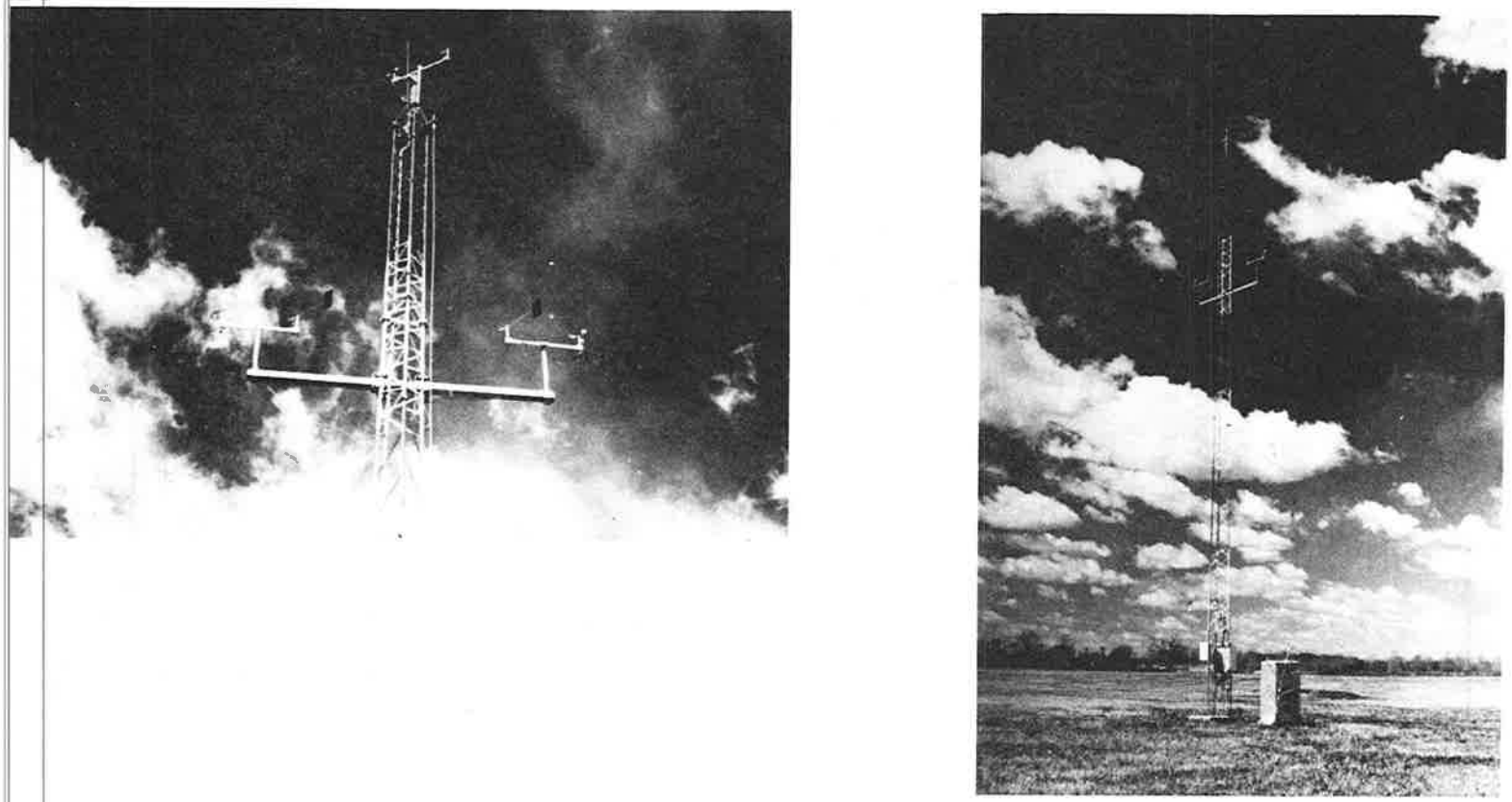

FIGURE 5. TRIAD OF CLIMATRONICS® WIND SENSORS ON 50-FOOT METEOROLOGICAL TOWER

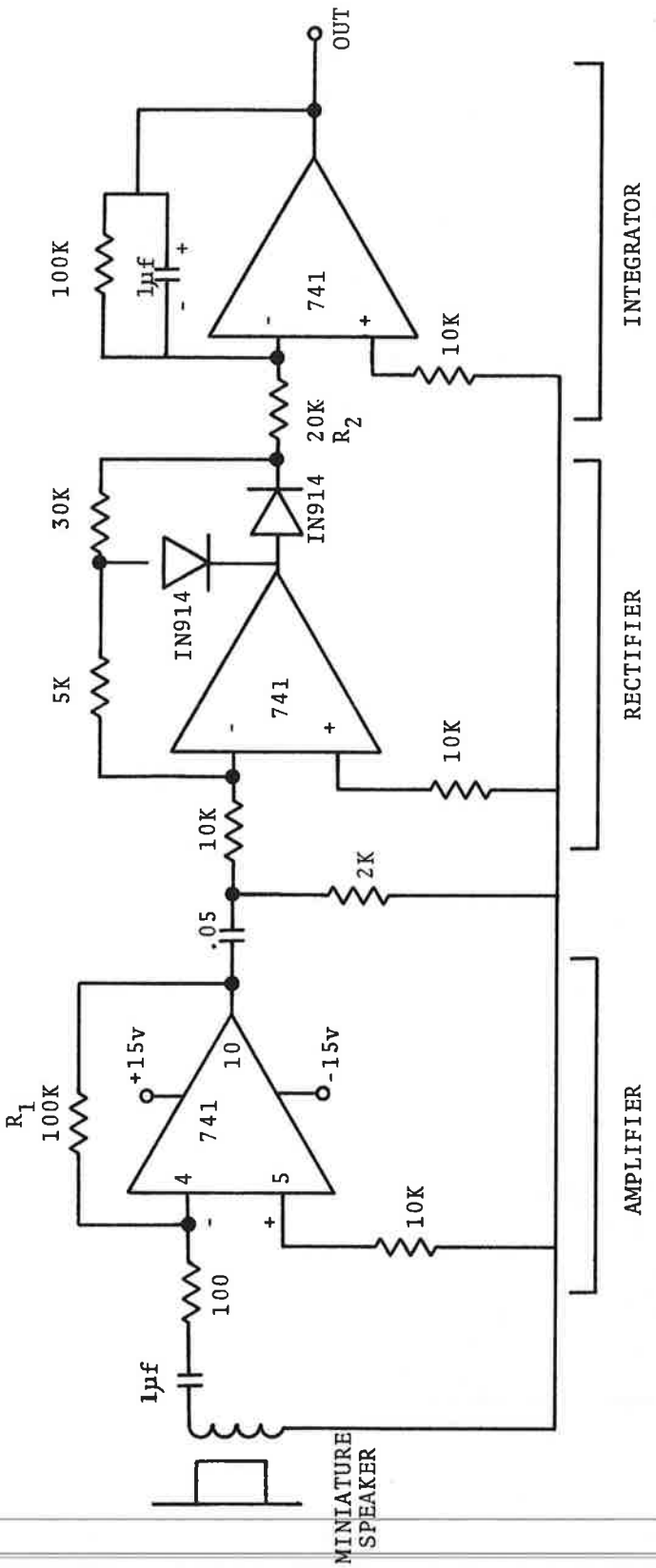

FIGURE 6. AIRCRAFT DETECTOR CIRCUIT

aircraft. The peak in this signal was detected and defined to be the time at which the aircraft was overhead and thus provided a zero time reference for the data collection and analysis.

3. TEST SITE

The GWVSS arrays were located on the approach to runways 14R, 27R, and 32L. At the time of these tests, runway-use statistics indicated that these runways were the most heavily used landing runways at O'Hare. An overall plan view of the test site is shown in Fig. 7.

The sign convention adopted in this report is defined as follows: the direction to the right of the runway centerline as viewed by a pilot of a landing aircraft is defined as positive. Thus, distances to the right (left) of the centerline are called positive (negative). A wind component from the negative side to the positive side is defined as a positive crosswind.

The GWVSS locations are given in Table 1. The baselines were located in the region where vortices have the highest probability of lingering near the extended runway centerline for the longest time. The meteorological data for each GWVSS were obtained from the nearest VAS tower as given in Table 2.

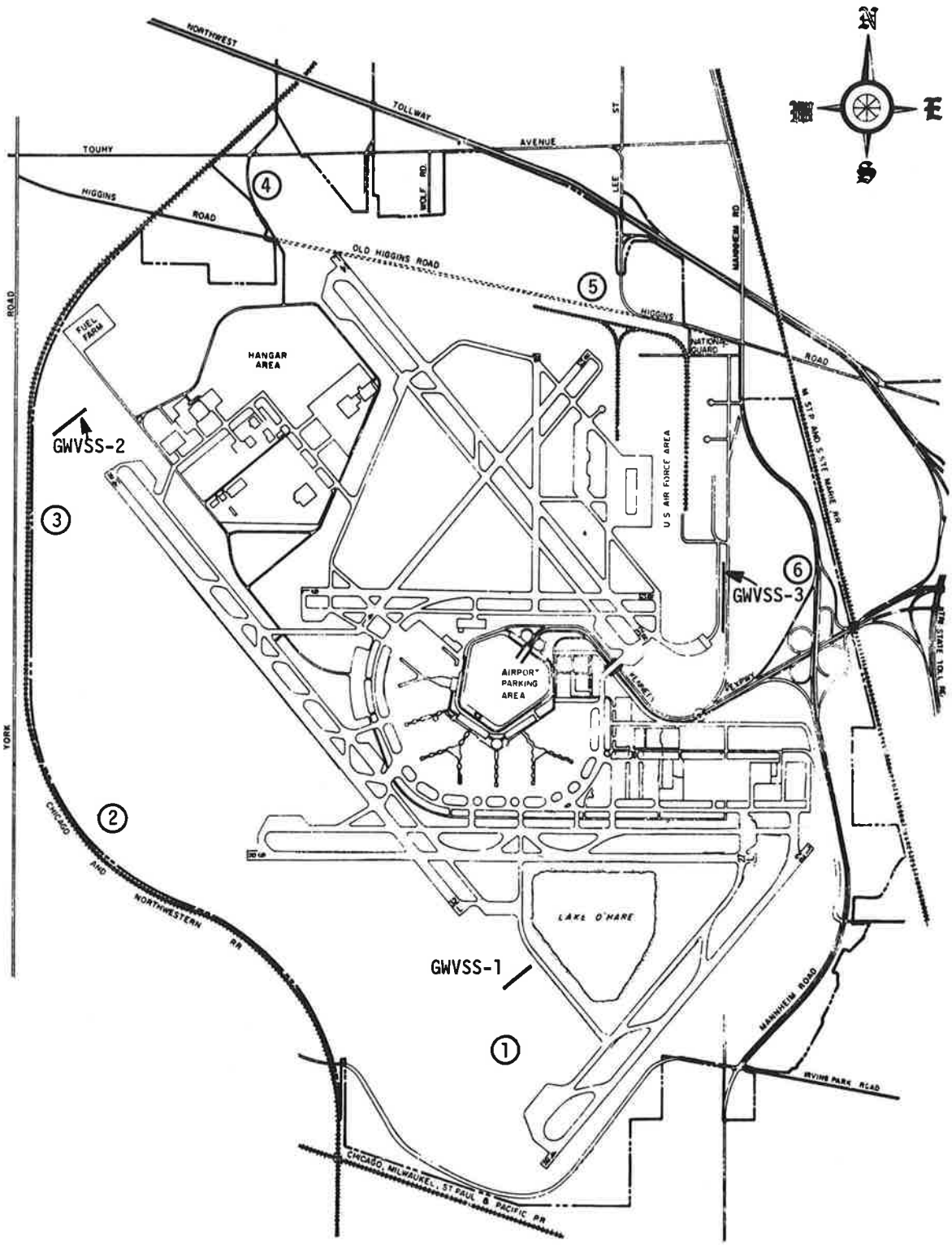

FIGURE 7. LAYOUT MAP OF CHICAGO O'HARE INTERNATIONAL AIRPORT

TABLE 1. LOCATION OF GWVSS ARRAYS

GWVSS Baseline	Runway	Distance from Runway Threshold
		Feet
1	32L	1550
2	14R	1550
3	27R	1350

TABLE 2. LOCATION OF METEOROLOGICAL TOWERS

GWVSS Baseline	Tower No.	Distance from Runway Threshold	Distance Offset from Runway Centerline
		Feet	Feet
1	1	3350	-300
2	3	-40	1200
3	6	3000	-300

4. DATA COLLECTION

Data were collected for aircraft landing on runways 14R, 27R, and 32L at O'Hare Airport. Recording of meteorological data was continuous while recording of ground-wind data was initiated by the aircraft detector when aircraft were landing on the runway.

4.1 SYSTEM HARDWARE

The system hardware consisted of meteorological and vortex sensors (discussed in Section 2), field electronics, processing electronics, and data recording equipment as shown in Figure 8.

The field electronics for the meteorological systems and the GWVSS were similar. In each system the sensor analog voltages were sampled with a 16-channel sequential-scan multiplexer. The sampling rates were 4 times a second for the GWVSS and 2 times per second for the meteorological data. The analog output of the multiplexer was converted to a serial digital signal and transmitted first through direct-earth-burial cable to an FAA field facility (a glide-slope building, for example) and then through FAA signal cables to the equipment room in the base of the control tower. The data streams from each GWVSS were converted from serial to parallel digital data, reformatted, and combined for transmission to the data recording facility where all the processing of the data was performed. Conversely, all the processing of the meteorological data was performed at the equipment room and then transmitted to the data collection facility to be combined with the GWVSS data.

Microprocessors were used to process and format the meteorological data. A simplified electronics block diagram is given in Figure 9. A complete description of the VAS system can be found in Reference 6. Since the wind data are so important to the vortex characteristics, some of the salient features of the meteorological data processing are discussed below.

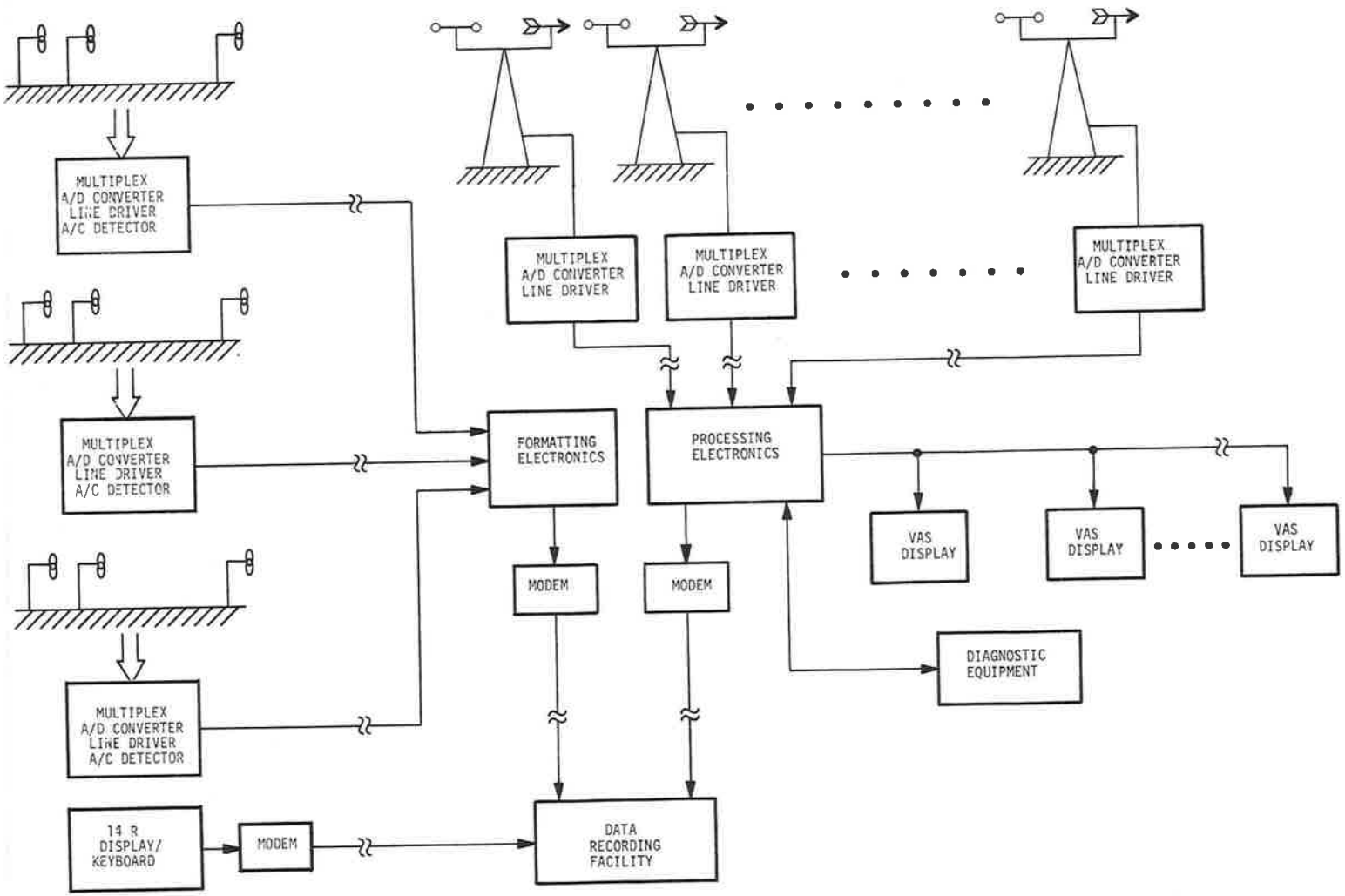

FIGURE 8. DATA ACQUISITION SYSTEM HARDWARE

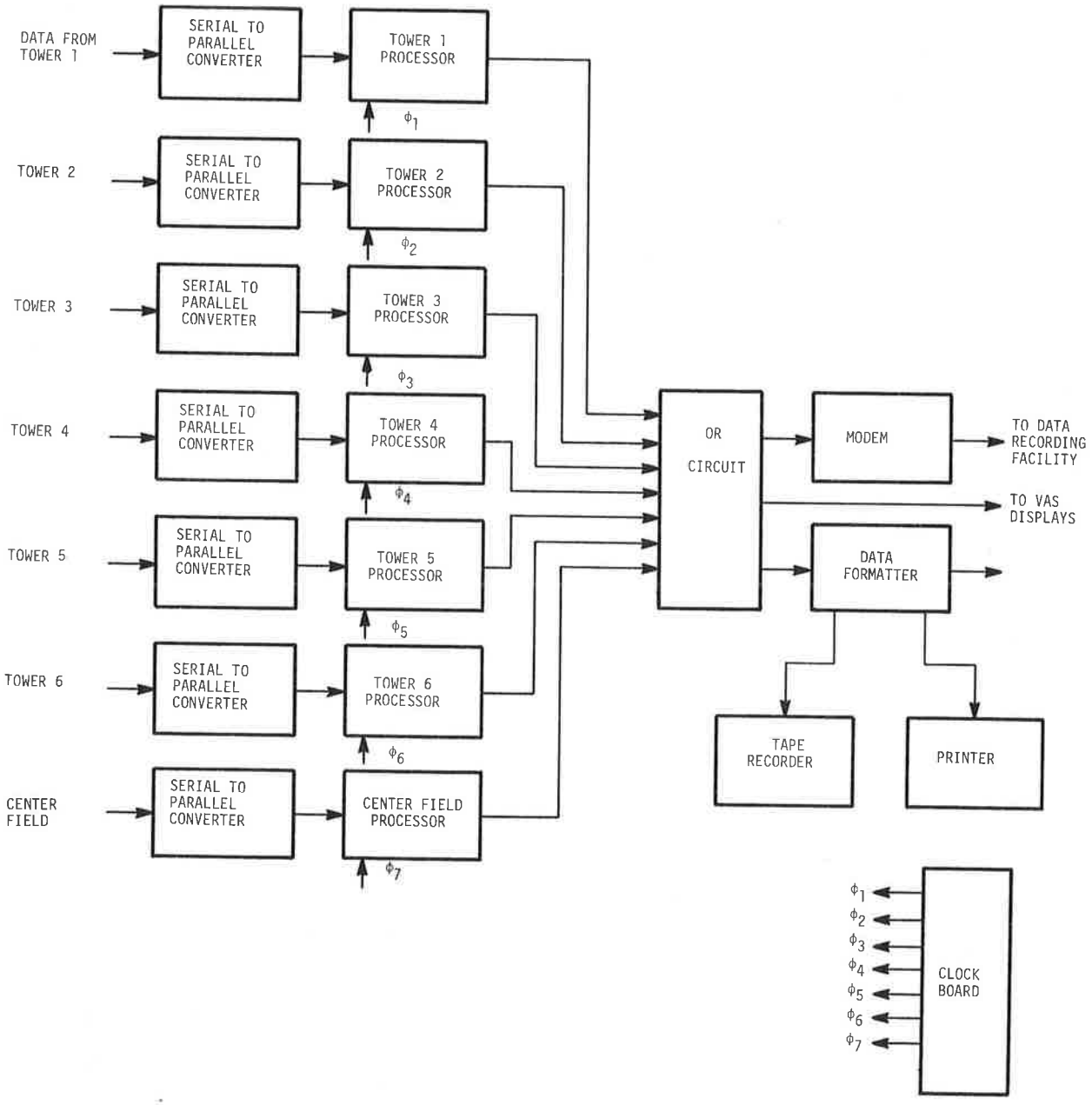

FIGURE 9. METEOROLOGICAL DATA PROCESSING ELECTRONICS

The first task of the microprocessor was to select the wind sensor to be used. For a data set to be considered valid, at least two of the three sensors must have agreed within ± 3 knots in wind speed and ± 20 degrees in wind direction. If the data met these criteria and the reading from the top sensor (at the 50-foot level) agreed with either of the other two sensors, the data from the top sensor were selected. If only the lower two sensors agreed (see Fig. 5), then the upwind sensor values were selected. The tower microprocessor calculated the North and East components of the wind. A 64-second (128-sample) sliding average of each component was then computed. At each half-second interval the results were recombined to form an average wind magnitude and direction for each tower. Sensor failures and detectable systematic errors were recorded. A VAS status indication was also determined for each runway serviced by the meteorological tower. All sensor, error, wind average, and VAS status data were formatted and transmitted by the microprocessors at half-second intervals to the data collection computer which recorded the data for off-line processing.

4.2 DATA COLLECTION FACILITY

The data collection equipment was installed in the Mobile Vortex Data Acquisition Facility (MVDAF) located next to the 32L ALS substation. The hardware consisted of a Data General NOVA® 2/10 minicomputer, a cathode ray tube (CRT) display/terminal, a time-code generator, and a digital magnetic tape drive as shown in Figure 10. The VAS data and the three lines of GWVSS data were transmitted from the control tower to the MVDAF by separate 4800 baud modems in the control tower. These data were entered into the computer through a modem interface, checked for integrity, converted to appropriate engineering units, and formatted for display and recording.

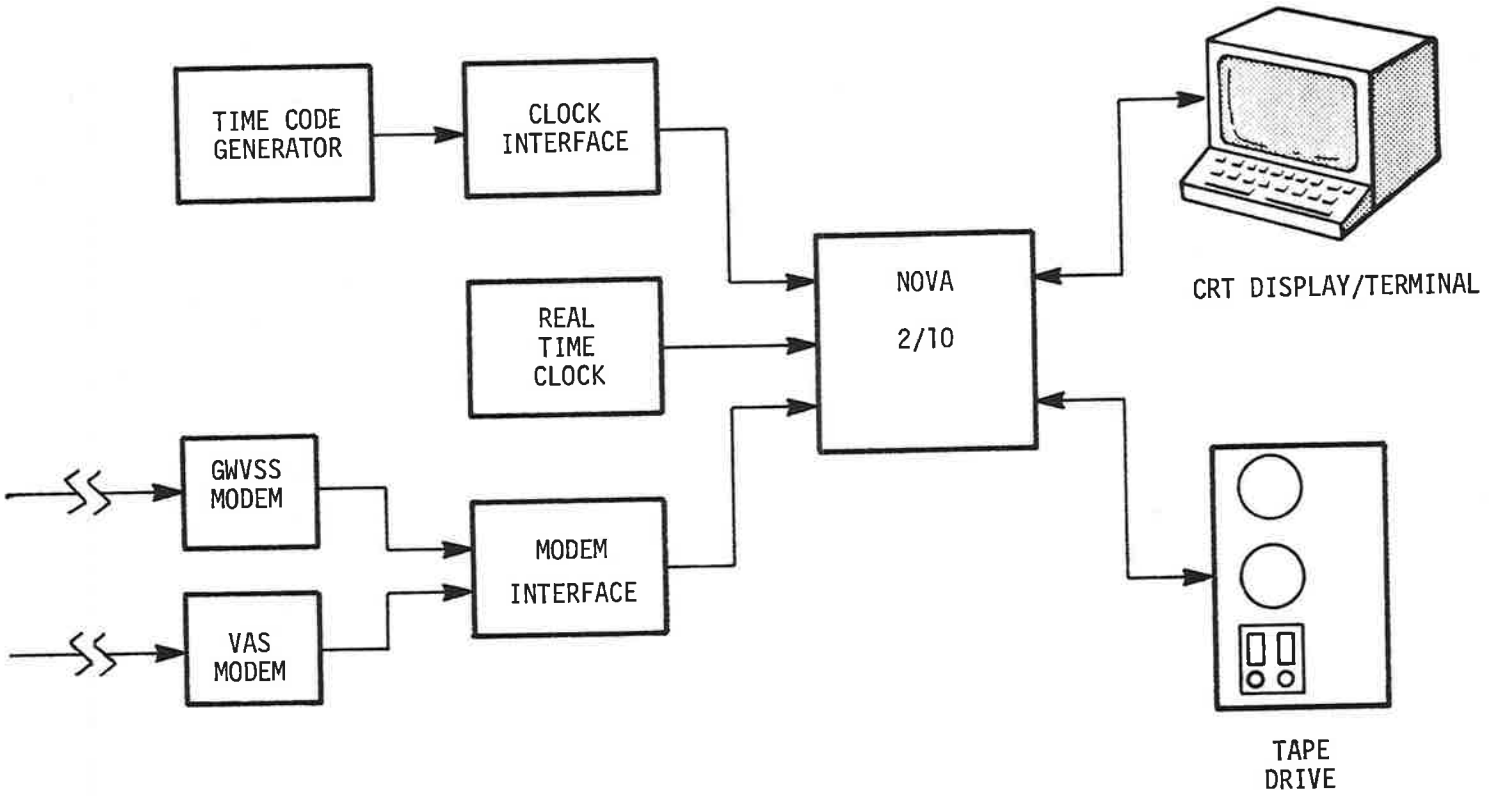

FIGURE 10. MOBILE VORTEX DATA ACQUISITION FACILITY HARDWARE

A CRT display/terminal was used for system input and as a real-time display of data collection parameters. The CRT was divided into six areas as shown in Figure 11. General system status was displayed in the upper right area and included the following information:

a. Data collection mode for each of the GWVSS arrays and VAS meteorological towers (e.g., mode 1 indicated data would be collected continuously, mode 2 applied only to GWVSS and indicated that data would be collected only after an aircraft detector was triggered, etc.).

b. Codes for errors detected in the GWVSS and meteorological data transmission.

c. Indication that an aircraft detector has triggered.

d. Echo of the aircraft identification selected by the operator.

An area to the left of the status zone contained the time code when the last trigger of an aircraft detector was observed. The bottom line of the display echoed the terminal key strokes and responses from the executive software operating system. The remaining area was divided into three zones for displaying meteorological data in tabular form and GWVSS data in graphical form as selected by the operator through keyboard commands. Both GWVSS and meteorological data could be displayed in Zone 1 (however, this area was most often used to display GWVSS data), while only meteorological data could be displayed in Zones 2 and 3. The GWVSS display consisted of the anemometer analog voltages in a spatial bar-graph display. The voltages were quantized by the CRT display software which provided means for viewing all anemometers simultaneously thus helping to identify malfunctioning sensors. The meteorological data display consisted of the speed and direction from the three wind sensors on a given tower, pressure, turbulence, temperature, VAS display status, averaged wind speed and direction, gust, and sensor failure codes. A typical display is shown in Figure 12.

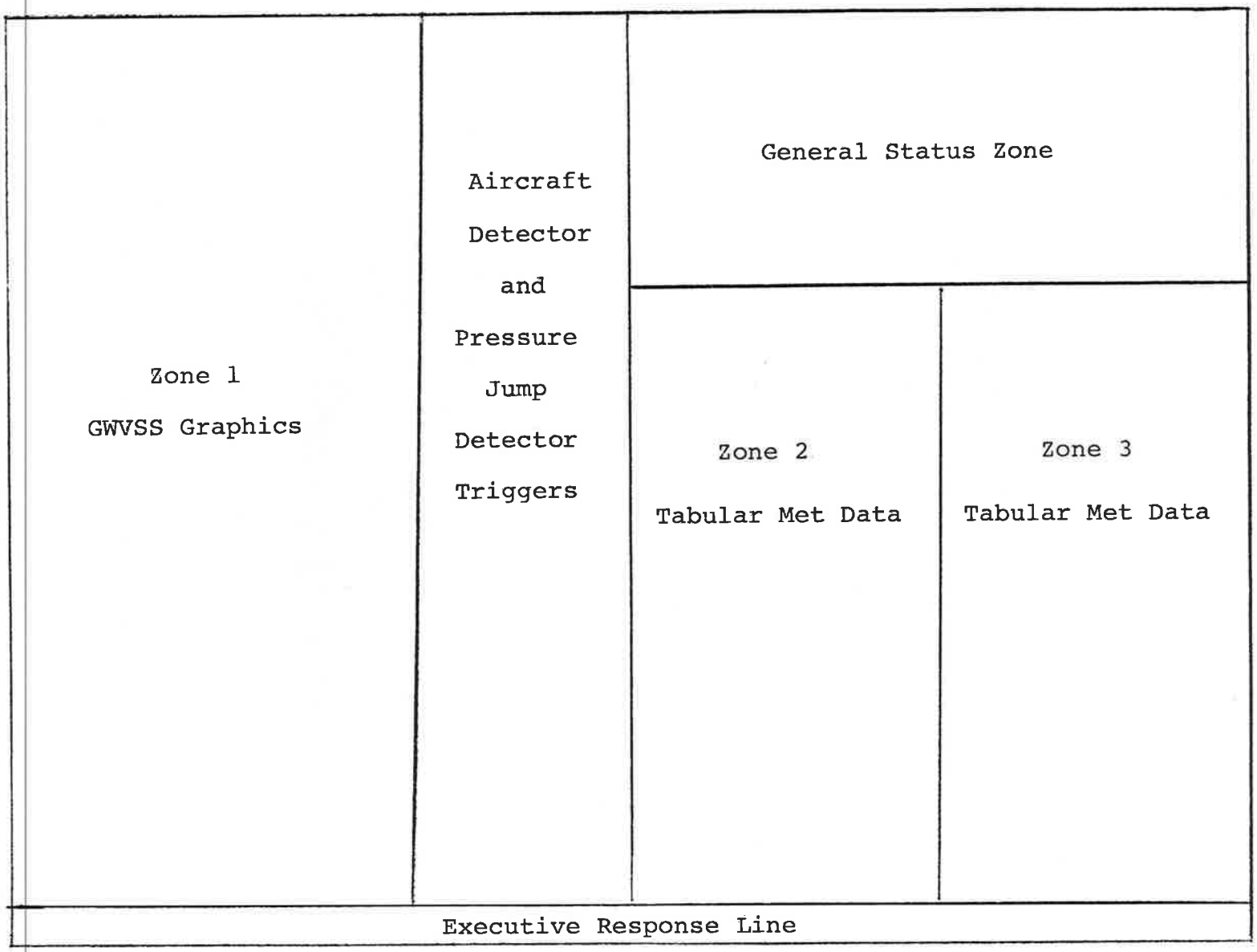

FIGURE 11. CATHODE-RAY TUBE DISPLAY ZONES

O'HARE INTERNATIONAL AIRPORT VORTEX TEST SITE

RUNWAY 27R ACTIVITY LOG

DATE: 18 MAR 77 SYSTEM STATUS:

WEATHER: C

TAPE NO: ORD18403187 7

Run No.	A/C Type	Time				Wind		Comments
		Day	Hour	Min.	Sec.	Dir.	Kts	
17	DC10	077	15	37	20	330	7	
18	DC8			38	42			U358 NOT AVAILABLE
19	DC9			40	35			
20	B737			42	06			
21	B727			43	58			
22	DC8			45	—			U343 NOT AVAILABLE
23	DC8			46	20			U200 213 000#
24	B707			47	56			A191 205 000#
25	B727			50	38			
26	SMALL PROP			52	19			DID NOT TRIGGER
27	DC8			53	41			U374 191 000# MISSED TRIGGER
28	B727			54	46			
29	DC10			56	06	330	06	
30	DC9			58	20			
31	B727			59	40			
32	SMALL PROP		16	01	07			

FIGURE 13. LOG SHEET

view of aircraft landing on runway 14R could be obtained. The aircraft type was identified by one of the site operators and transmitted to the main data collection facility by modem.

Data collection procedures at the 27R site were more cumbersome; since there were no cables available, the aircraft type had to be relayed to the main site by voice with walkie-talkies which tied up two operators for operations on one runway.

4.5 DATA RECORDING

The NOVA® minicomputer accepted the data from the GWVSS and meteorological systems and formatted them for recording on 9-track digital tape. Each meteorological and GWVSS data sample (GWVSS anemometer voltage, time code, aircraft ID code, etc.) was converted to a 16-bit word and scaled to engineering units. The NOVA assembled these words into frames and the data frames were grouped into records which consisted of an integral number of frames in a fixed record of 2048 words. If a new frame would result in a record exceeding 2048 words, the remainder of the current record was filled with zeros and the new frame was inserted at the start of the next record. This insured tape synchronization and error recovery capability in the data reduction process. Each tape was limited to a maximum of 4500 records to guarantee the proper double end-of-file (EOF) marks would be recorded on the tape. If the data collection was manually stopped, a single EOF was written on the tape. An optional ASCII message record could be written prior to the restart of data collection. Each tape was logically terminated with two consecutive EOFs.

The format of a typical data tape is shown in Figure 14. Each tape was prefaced with a fixed-format ASCII record identifying the site (ORD), the tape number, the date the tape was started, and the name of the site operator. This record was followed by optional ASCII message records (up to 80 characters each) through which pertinent information was passed to the data reduction and analysis systems (e.g., sensor failures).

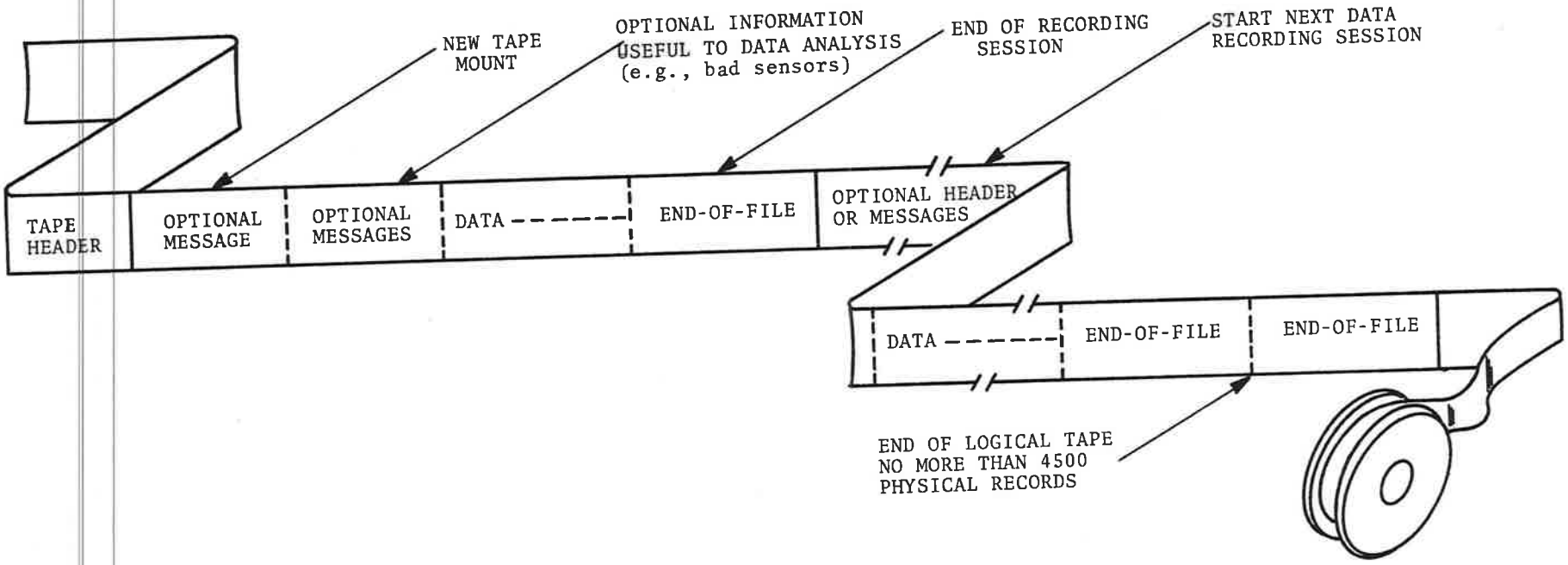

FIGURE 14. DIGITAL-TAPE FORMAT

The GWVSS data were collected at four frames per second from each active GWVSS line. The site operator would select the active sensor line(s) through switches on the computer. GWVSS data recording was independently initiated for each line by an aircraft detector trigger which would also set a 250-second count-down clock. Successive triggers would reset the clock. GWVSS data recording was terminated after 250 uninterrupted seconds. Experience from previous test sites (JFK, Denver, Heathrow) showed that 250 seconds was a very conservative upper limit for the collection of GWVSS data.

The meteorological data were nominally recorded 24 hours a day during the test period. Initially, and for special tests, the meteorological data were recorded from each tower every half second. After system verification, the nominal meteorological data collection rate was reduced to one frame per tower every 5.5 seconds.

5. DATA PROCESSING

The procedures used to reduce and process the GWVSS anemometer data and the meteorological data leading to their respective entries into the ORD data base were divided into four phases:

a) Reformatting
b) Digital and Analog Processing
c) Vortex Track Analysis and Meteorological Data Verification
d) ORD Data Base Development and Editing.

The individual tasks in this process are shown in Figure 15.

5.1 REFORMATTING

The reduction of the data was performed on the TSC XDS-9300 hybrid computer system which was primarily chosen for its relatively low cost, high availability, and on-line capabilities. The 7-track tape drives on this system required that the 9-track tapes generated at the test site be converted. This was accomplished on the TSC PDP-10 computer system.

ASCII data records were converted to BCD, and GWVSS and meteorological data were reformatted to be compatible with the XDS-9300 (24-bit word length). The data were repacked so that the number of 6-bit bytes recorded on the 7-track tape was no greater than the number of 8-bit bytes recorded on the 9-track tape, thereby preserving an approximate one-to-one match between the 9-track and 7-track data tapes.

5.2 DIGITAL AND ANALOG PROCESSING

The XDS-9300 data reduction program listed the meteorological data measured at the start of each aircraft run and generated a printer-plot of vortex location as a function of time. Punch cards were automatically produced which contained selected system parameters (e.g., time code, aircraft type, meteorological data, etc.) suitable for immediate entry into a data base.

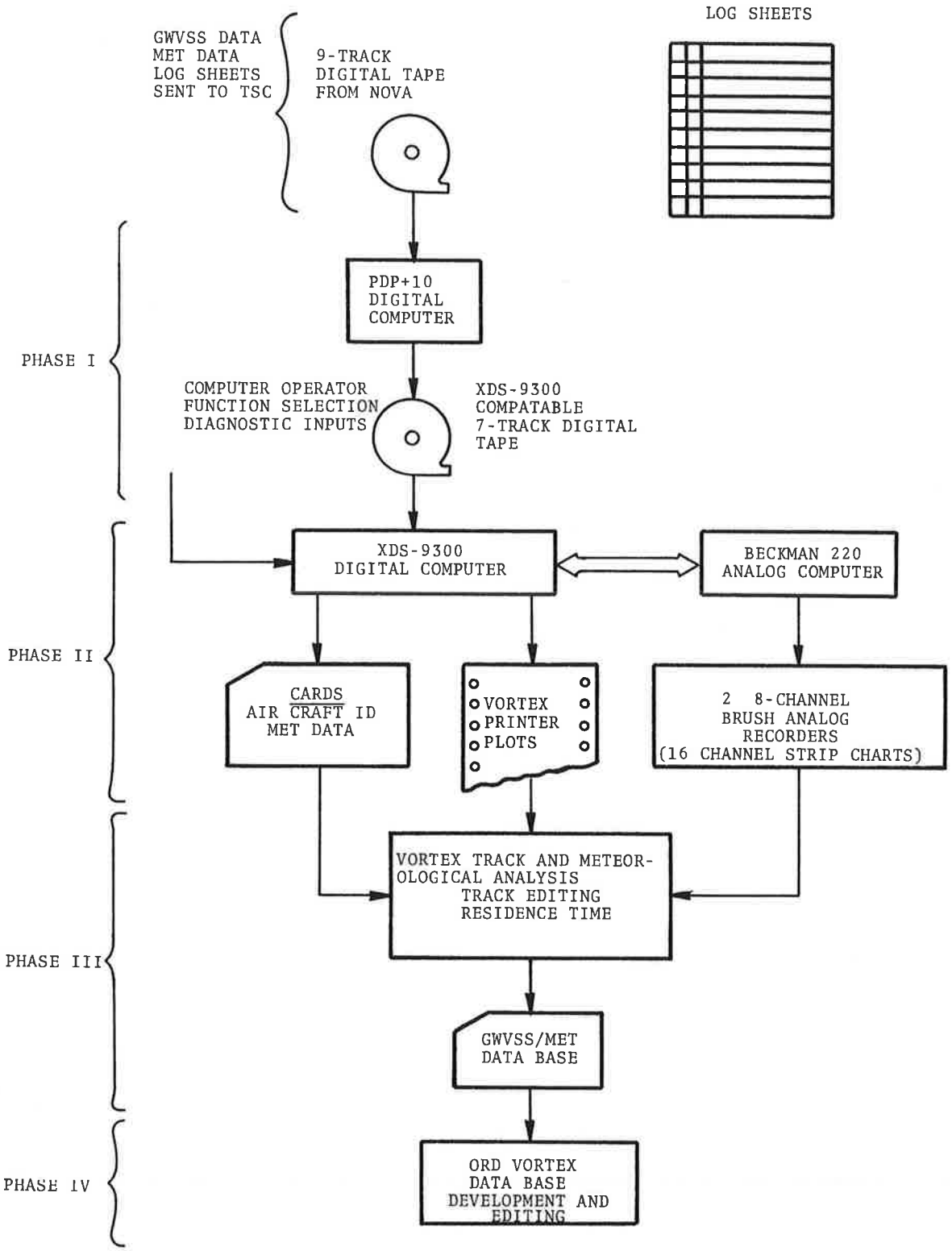

FIGURE 15. DIGITAL-TAPE PROCESSING SEQUENCE

The software was structured to allow interactive operator inputs from a teletype and/or sense switches to control the modes of data processing. Diagnosis of data reduction system performance and data systems malfunctions could be obtained through on-line requests for operator-selectable printouts of information in the digital input stream or analog stripchart recordings similar to Figure 4. Sixteen channels of operator-selectable data could be stripcharted from either the GWVSS or meteorological systems through an interface with a Beckman® 2200 analog computer.

The on-line capabilities of the XDS-9300 allowed for failed sensors to be detected, analyzed, and suppressed from further processing. GWVSS sensor failures nominally resulted in abnormally low or high voltages which were then erroneously interpreted by the processing software to be the location of one of the vortices. The data reduction system operator, having detected and analyzed a failed sensor, could eliminate it from further processing.

5.2.1 Meteorological Data Processing

At each start-of-run (SOR) initiated by an aircraft detector trigger, the first valid meteorological data frame associated with the active runway was extracted from the data stream and stored in a data base. Figure 16 shows a typical computer printout of vortex tracks for runway 14R. Since the data collection program was in support of the VAS development, it was desired to extract the meteorological conditions at the SOR and test the correlation of the VAS ellipse with these data.

Referring to Figure 16, the printed meteorological data are average wind magnitude (RB) in knots and direction (TB) in degrees; gust (G) in knots; sensors selected (R101, magnitude and direction sensors number 1 selected at this time); headwind (U positive toward the approaching aircraft) and crosswind (V, positive toward the right of the approaching aircraft) in knots; turbulence (TU) in $cm^{2/3}/sec$; atmospheric pressure (P) in millibars; temperature (T) in degrees centigrade; VAS status at the SOR (e.g., RRRR); number of VAS status changes since the last SOR (NΔG); and

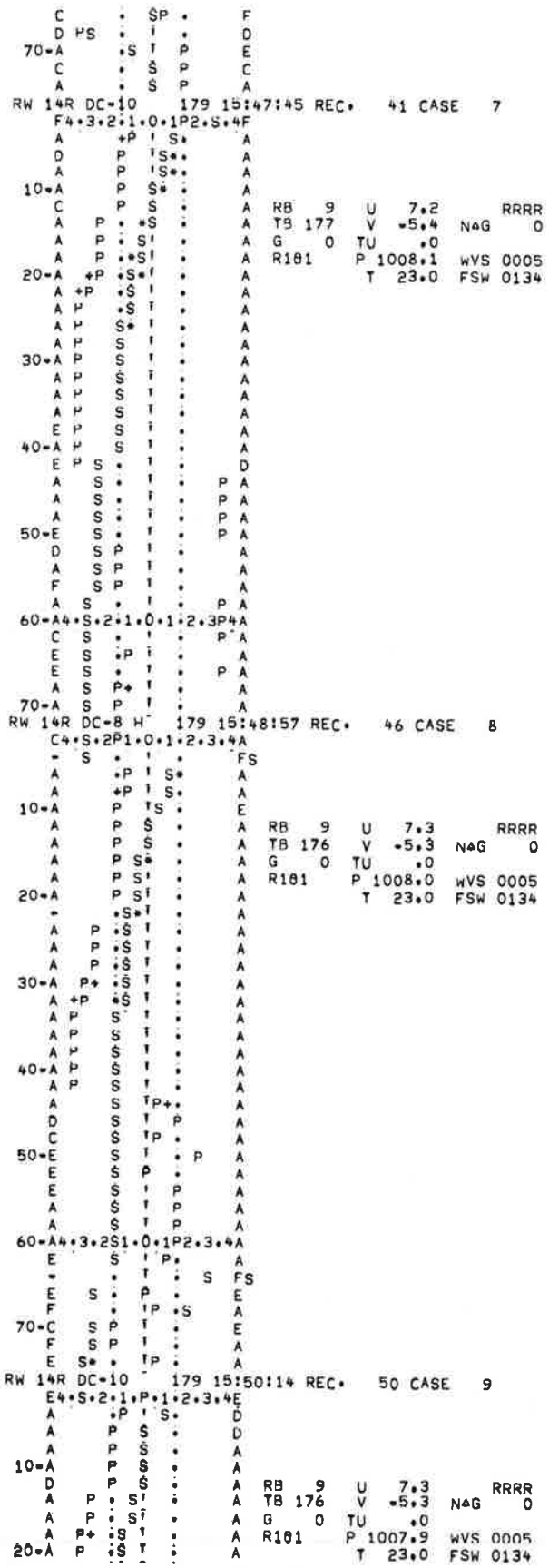

FIGURE 16. COMPUTER PRINTOUT OF VORTEX TRACKS

two words (WVS and FSW) whose individual bits describe the general status of the system at the SOR.

5.2.2 GWVSS Processing

The GWVSS processing algorithm had to be structured to handle data from three independent runways. Fortuitously, only 32L and 27R could be used simultaneously, since 14R is the other end of 32L. Since the SORs occur asyncronously on 32L and 27R and it was desired to display both runways simultaneously (Figure 17), a master clock was used for controlling the paper flow and secondary clocks were used for each active sensor line. The GWVSS data were processed such that 32L and 14R were always printed on the left side of the page, and 27R was always printed on the right side. Each line of print represents 2 seconds of data. In order to print continuously across the paperfolds without standard end-of-page skips, the XDS-9300 operating system was modified.

Referring to Figure 17, at each SOR a header line was printed identifying the runway (e.g., RW 27R), the aircraft type, the time code (day:hour:minute:second), the record number (e.g., REC. 1015) where the SOR may be found on the input tape, and the case (sequence) number for the respective runway. When two runways are operating simultaneously, the controlling clocks are adjusted so that the header line occupies a 2-second interval with respect to the other sensor line.

Immediately following each header line is a line of reference points (4.3.2.1, etc.) which is repeated every 60 seconds and is a reference for the sensor positions. The sensors are positioned at 50-foot intervals and each character position corresponds to one of the sensor positions. The integers correspond to the sensor positions in hundreds of feet about the runway centerline.

To avoid multiple triggers of the aircraft detectors, triggers occuring within 20 seconds of an SOR were suppressed. This feature created, as well as controlled, problems, especially on 27R. Aircraft preparing for takeoff on 32R would run up their

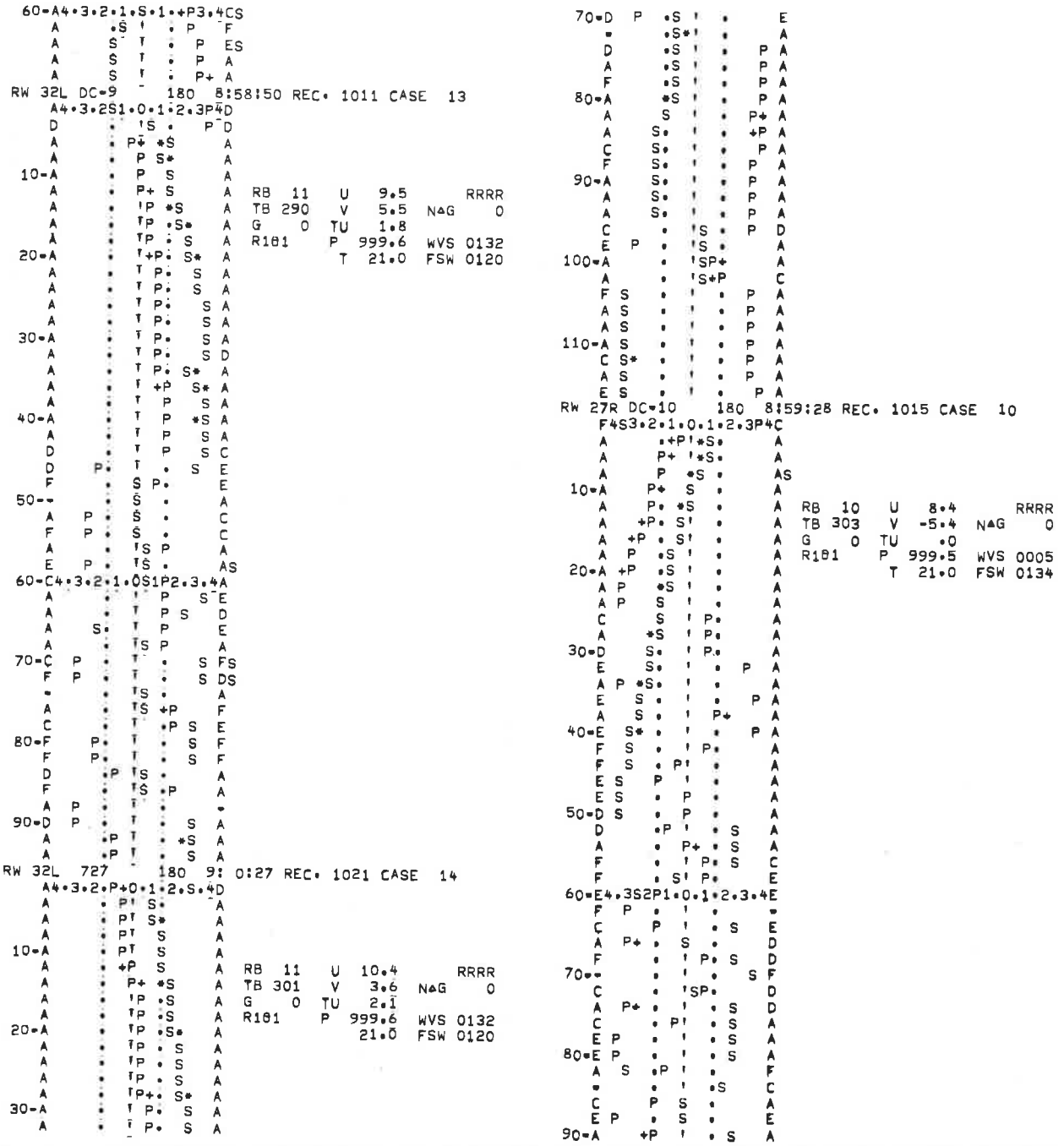

FIGURE 17. COMPUTER PRINTOUT OF VORTEX TRACKS ON TWO GROUND-WIND LINES

engines producing sufficient noise to trigger the aircraft detector and thereby either create false SORs or mask the true SOR of the aircraft landing within the 20-second interval.

The detection and tracking of the vortices were performed by comparing the voltage outputs of all the anemometers in a complete ground-wind line. The GWVSS location algorithm defined the position of the port (starboard) vortex to be at the location of the sensor with the lowest (highest) voltage output. The algorithm made the following assumptions: (1) when no vortices were present, the statistics of each anemometer were identical to every other anemometer on a sensor line, (2) random fluctuations of wind were uncorrelated from sensor to sensor, (3) local amplitude deviations of the winds were much faster than the variations of the local wind fields attributed to vortices, and (4) the vortex signatures while transporting through the sensor line were distinctive and limited only by the sample rate.

The data were processed in groups of eight frames or eight consecutive sets of anemometer outputs corresponding to two seconds of elapsed time. The location assigned to each vortex in a two-second interval was defined as the position of the sensor which was most frequently selected during the interval.

Each track is a time history of the port and starboard vortices as indicated by the vortex location algorithm. A time axis is listed at 10-second increments immediately to the left of each track. The apostrophes in the center of each track represent the location of the extended runway centerline. The dots to the left and right of the apostrophes represent a $\pm$ 150-foot safety corridor which is defined in Section 7.1. The vortex positions are printed at two-second increments with the port vortex assigned the character "P" and the starboard vortex the character "S". Whenever the indicated vortex location is distributed across two adjacent sensors, a "+" is associated with the port vortex and a "*" is associated with the starboard vortex.

The alphabetic characters (A,C,D, etc.) running down the page on both sides of the tracks correspond to a validity weighting assigned to the port (left column) and starboard (right column) vortex selected location. The number of times a particular location was chosen during the 2-second interval is an estimate of the confidence of the decision and was coded as follows:

Code	Number of Times a Location Chosen During A Two-Second Interval (Eight Samples)
A	8
C*	7
D	6
E	5
F	4
-	<4

When the chosen location contained less than four of the eight samples, a "-" code was listed and no vortex location was indicated. This validity weighting was used as an aid in the data analysis when a decision must be made as to whether the observed signals truly represented the existence of a vortex or were due to fluctuations in the ambient wind.

The column immediately to the right of each baseline is reserved for error flags. An "S" in this column indicates an error in data transmission was detected by the data acquisition system. When an error was detected, the entire frame for that sensor line was rejected.

The track for each active runway continued until the next SOR or 250 seconds had elapsed. In the latter case data collection for that particular runway was terminated.

*The algorithm was general purpose and based on the percentage of times chosen. "B" indicates between 90 and 99 percent; for an 8-sample system, B does not exist.

At the completion of the tape processing, a summary of aircraft parameters and meteorological data for each active runway was printed as shown in Figure 18. The summary was used by the data base editor to correlate with the site log sheets and correct or filter the automated processing. A column (RUN) was available to manually insert the test site run number (which may differ from the CASE number). The CODE column is a numerical code for the aircraft type which may also require editing. SEP. TIME is the interarrival aircraft separation time and RECORD is the location of the SOR on the data tape. The relatively high frequency of false aircraft detects on this runway (discussed in Section 5.2.2) may also be noted.

5.3 VORTEX TRACK ANALYSIS AND METEOROLOGICAL DATA VERIFICATION

A block diagram of the vortex track analysis and meteorological data verification process is given in Figure 19. The vortex track analysis consisted of identifying the times at which the vortices left a ± 150-foot corridor, or died on or within this corridor. This time was defined as the vortex residence time. Vortices which died on or within the corridor were additionally flagged. Analog stripchart outputs were obtained for the cases with residence times greater than or equal to 80 seconds and were analyzed in depth. In situations where the vortex tracks were not clearly discernable, the analyst considered the validity weighting factors (A, C, D, etc.) at the sides of the track, the meteorological parameters (headwind and crosswind), and the aircraft type. The residence times were transferred to data cards for entry into the data base.

The meteorological data were verified separately using a VAS Verification Program. If any errors in the meteorological data were detected, the data in the ORD vortex data base were edited. However, while the vortex analysis was being performed, the general correlation between vortex transport characteristics and the meteorological conditions were always considered and any suspect data were analyzed in depth.

RUN SUMMARY

7/7/77 BRD 0244 BIHARE INTNL RNWY 27R

R/W	CASE	RUN	ARR. TIME	A/C TYPE	CODE	SEP. TIME	RECORD	U	V
27R	1	180	8:49: 1	727	2	99:99:99	950	7.7	-6.4
27R	2	180	8:50:46	707	1	0: 1:45	961	8.9	-6.5
27R	3	180	8:52: 0		0	0: 1:14	969	10.0	-4.5
27R	4	180	8:53:19	PROP	13	0: 1:19	977	9.7	-2.6
27R	5	180	8:54:37	L1011	8	0: 1:18	985	9.8	-1.9
27R	6	180	8:55:27	727	2	0: 0:50	990	9.6	-2.9
27R	7	180	8:56: 1		0	0: 0:34	993	10.7	-2.5
27R	8	180	8:57: 3	747	4	0: 1: 2	1000	10.5	-3.4
27R	9	180	8:57:29		0	0: 0:26	1002	10.3	-3.9
27R	10	180	8:59:28	DC-10	7	0: 1:59	1015	8.4	-5.4
27R	11	180	9: 1:15		0	0: 1:47	1026	13.2	-4.8
27R	12	180	9: 1:50		0	0: 0:35	1029	14.0	-5.4
27R	13	180	9: 2:14		0	0: 0:24	1032	14.0	-5.4
27R	14	180	9: 3: 1	727	2	0: 0:47	1037	11.0	-4.9
27R	15	180	9: 4: 0		0	0: 0:59	1043	11.1	-6.7
27R	16	180	9: 4:22		0	0: 0:22	1045	10.3	-6.2
27R	17	180	9: 5:26	DC-10	7	0: 1: 4	1051	8.7	-5.0
27R	18	180	9: 7:46	727	2	0: 2:20	1066	11.2	-4.3
27R	19	180	9: 9:10	DC-9	6	0: 1:24	1075	14.6	-3.6
27R	20	180	9:10:53	727	2	0: 1:43	1085	12.5	-6.4
27R	21	180	9:12:17	DC-9	6	0: 1:24	1094	11.8	-5.5
27R	22	180	9:13:45	DC-9	6	0: 1:28	1103	13.5	-3.9
27R	23	180	9:15:48	727	2	0: 2: 3	1115	10.5	-3.4
27R	24	180	9:17:20	PROP	13	0: 1:32	1125	9.2	-3.9
27R	25	180	9:17:46		0	0: 0:26	1128	9.0	-4.4
27R	26	180	9:18:54	727	2	0: 1: 8	1135	10.0	-4.5
27R	27	180	9:21: 6	DC-9	6	0: 2:12	1148	10.1	-6.5
27R	28	180	9:22:38	727	2	0: 1:32	1158	13.9	-8.0
27R	29	180	9:24: 9	DC-10	7	0: 1:31	1167	11.2	-4.3
27R	30	180	9:25:50	DC-10	7	0: 1:41	1177	11.8	-5.5
27R	31	180	9:27:59	DC-8	5	0: 2: 9	1191	9.9	-4.8
27R	32	180	9:28:35		0	0: 0:36	1194	9.9	-4.8
27R	33	180	9:29:54	SM JET	14	0: 1:19	1202	10.5	-3.2
27R	34	180	9:31:38	PROP	13	0: 1:44	1208	11.0	-.2
27R	35	180	9:33:25		0	0: 1:47	1214	14.0	-.7
27R	36	180	9:36:21		0	0: 2:56	1224	17.4	-4.7
27R	37	180	9:37:23		0	0: 1: 2	1228	11.0	-4.7
27R	38	180	9:39:18		0	0: 1:55	1235	10.8	-7.3
27R	39	180	9:39:46		0	0: 0:28	1236	9.7	-7.1
27R	40	180	9:41:38	PROP	13	0: 1:52	1243	11.2	-8.4
27R	41	180	9:43:27	DC-9	6	0: 1:49	1249	11.8	-5.5
27R	42	180	9:45:47	DC-9	6	0: 2:20	1257	10.7	-2.7
27R	43	180	9:47:37	727	2	0: 1:50	1263	13.5	-3.6
27R	44	180	9:50:17	PROP	13	0: 2:40	1273	13.7	-2.9
27R	45	180	9:53:55		0	0: 3:38	1290	13.6	-3.1
27R	46	180	9:54:45		0	0: 0:50	1295	11.4	-3.7
27R	47	180	9:57:34	SM JET	14	0: 2:49	1309	14.6	-3.6

FIGURE 18. COMPUTER PRINTOUT OF PARAMETER SUMMARY

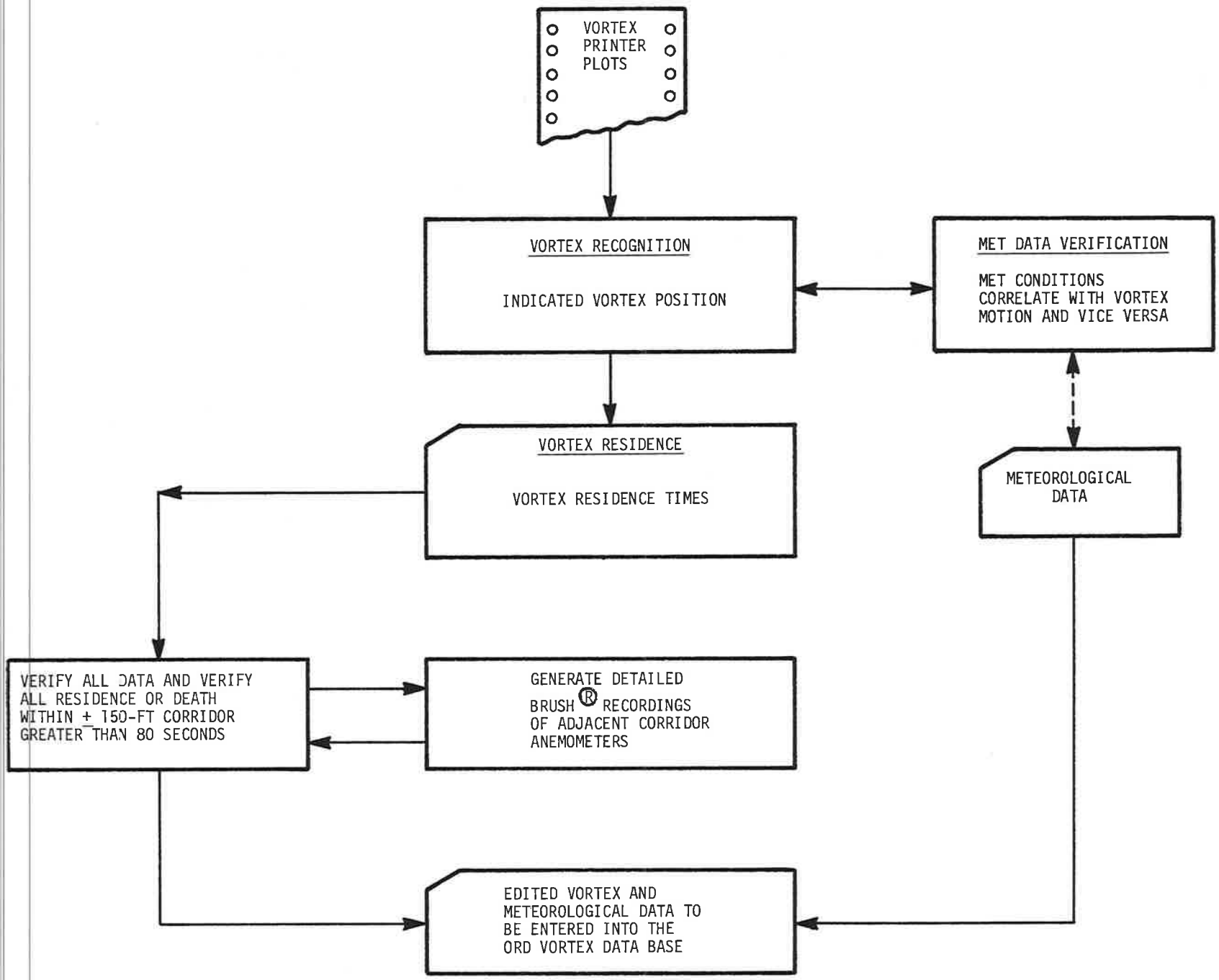

FIGURE 19. VORTEX TRACK ANALYSIS AND METEOROLOGICAL DATA VERIFICATION

5.4 ORD DATA BASE DEVELOPMENT AND EDITING

The GWVSS was the focal point for the ORD data base development. The data base is contained on two magnetic tapes and consists of the GWVSS data integrated with the MAVSS data (the MAVSS data and its analysis are discussed in Reference 11). Each case created by the GWVSS system became a potential entry in the data base. The correlation with the site log sheets added the run numbers, weather codes, and when available for B-707s and DC-8s, the airline, flight number, aircraft series, and landing weight. During data collection the site operators were asked to subjectively record the weather with codes such as S/1 (sunny with 10 percent cloud cover), C (cloudy), R (rain), etc., and this information was included in the data base.

Once the run numbers were integrated with the case numbers, those cases without run numbers (primarily due to false aircraft detector triggers) were deleted from the data base. In those instances where a false aircraft detector trigger masked the true SOR, a time correction factor derived from a clear vortex track was included to adjust the SOR time and the vortex residence times. On the next page is a list of GWVSS parameters contained in the ORD Data Base.

DATA	EXAMPLE
Site Designator	ORD
Tape Number	244
Day Number	180
Runway	32L (or 27R or 14R)
Runway Code (as defined in the VAS)	1 (or 3 or 6)
Case Number	19
Run Number	18
Aircraft Code	1
Aircraft Series Letter	(e.g., A corresponds to a B-707-120)
Aircraft Type	B-707
Time Code	Ø9:Ø9:37
Weather	S/Ø
Airline	AA
Flight Number	502
Weight (thousands of pounds)	163
Record Number	1077
U (headwind - knots)	11.4
V (crosswind - knots)	3.7
Turbulence	1.7
Temperature (°C)	21.0
Pressure (mb)	999.6
Fail Status Word (octal)	0120
Wake Vortex Status Word (octal)	0132
Tower Select	1
VAS Color at SOR	R
Port Residence/Death Time (sec.)	26
Port Corridor Death Flag	(* Inserted if vortex died in corridor)
Displacement Time Due to False SOR (sec.)	-6
Starboard Residence/Death Time (sec.)	14
Starboard Corridor Death Flag	(* Inserted if vortex died in corridor)
Indicator of Final Verification	K
Indicator of Long-Lived Vortex Verification	J

There are other parameters contained in the data base related to the development of the VAS (e.g., number of changes of VAS state during a run).

6. METEOROLOGY

Analysis of data collected at other test sites indicated that the ambient wind is the most important factor influencing wake vortex transport and decay characteristics. Although several meteorological parameters of the atmosphere could be, and in some cases were, measured (turbulence, solar flux, temperature inversion, etc.) this report deals only with the effects of the ambient wind.

6.1 WIND

To assign a single value to the wind components which represents the wind over the duration of the test run, a 60-second running average was used for the following reasons: (1) it is approximately the average lifetime of a vortex, (2) previous studies using Kennedy and Heathrow data (Refs. 1 and 5) have shown that the 60-second averages give consistent and reproducible characterization of vortices, and (3) the influence of wind gusts is minimized.

The distribution of the averaged longitudinal and cross winds are shown in Figs. 20 to 22. The winds are the 60-second averages recorded when a landing aircraft passed over the GWVSS array. Runways 32L and 27R were rarely used during tail wind conditions (5 and 3 percent, respectively). Runway 14R, however, was used a significant amount of time during tail wind conditions (28 percent) as compared to the results obtained at the Heathrow and Toronto test sites (16 and 18 percent, respectively). The cross winds were evenly distributed between positive and negative directions for the data from runway 27R; however, a significant trend to positive crosswinds (67 percent) was observed in the data from runway 32L and a substantial bias to negative cross winds (77 percent) was observed for the data from runway 14R. These data indicate a predominantly westerly wind at O'Hare; at least when these runways were used. The distribution of the total winds is

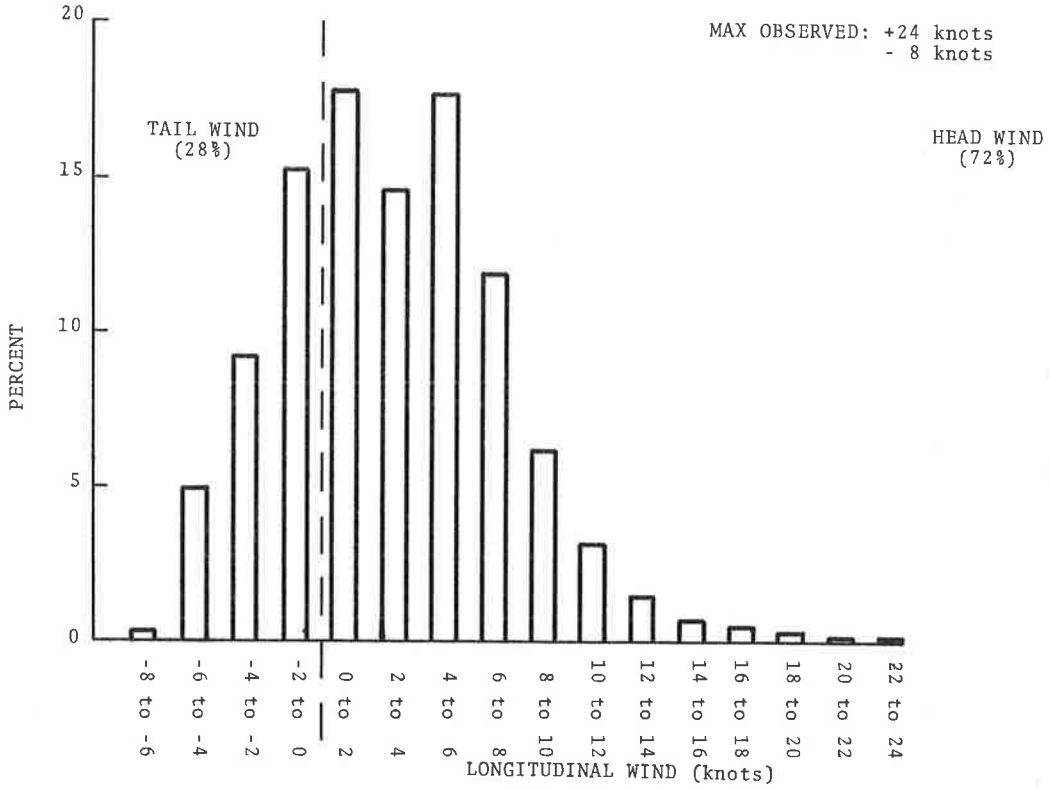

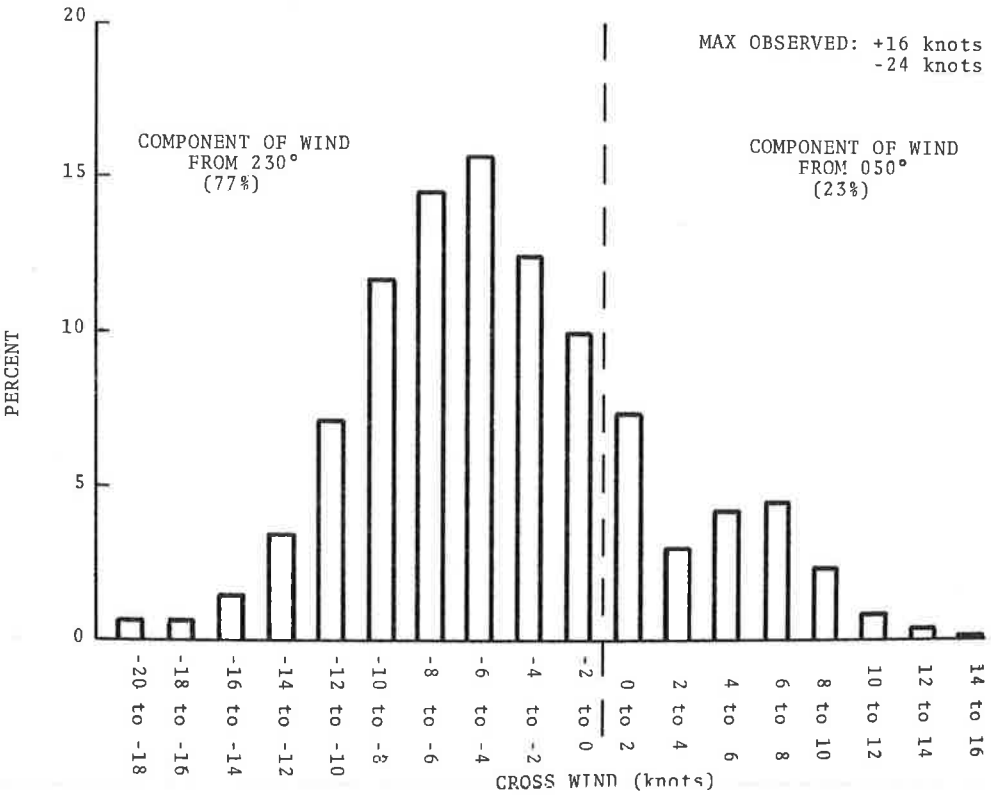

FIGURE 20. DISTRIBUTION OF ONE-MINUTE AVERAGED WINDS FOR RUNWAY 14R

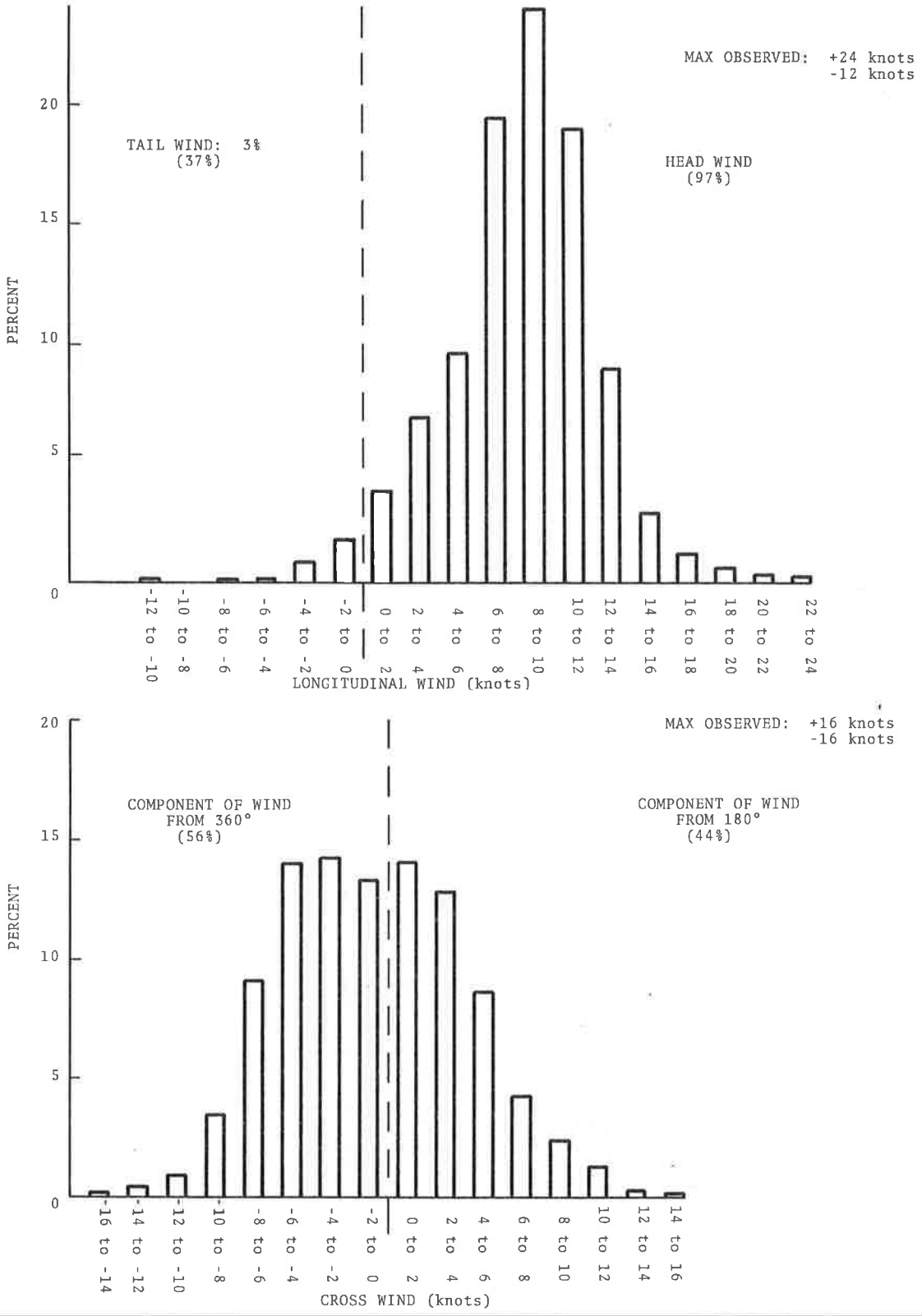

FIGURE 21. DISTRIBUTION OF ONE-MINUTE AVERAGED WINDS FOR RUNWAY 27R

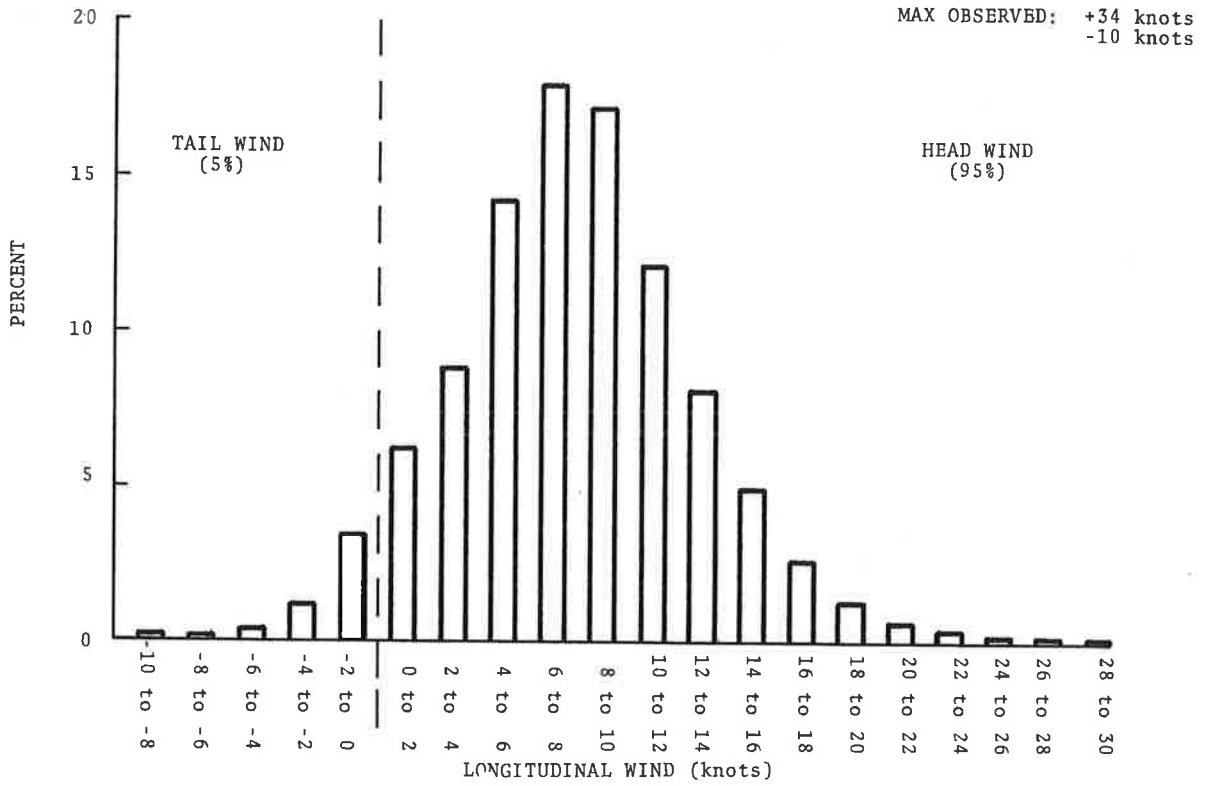

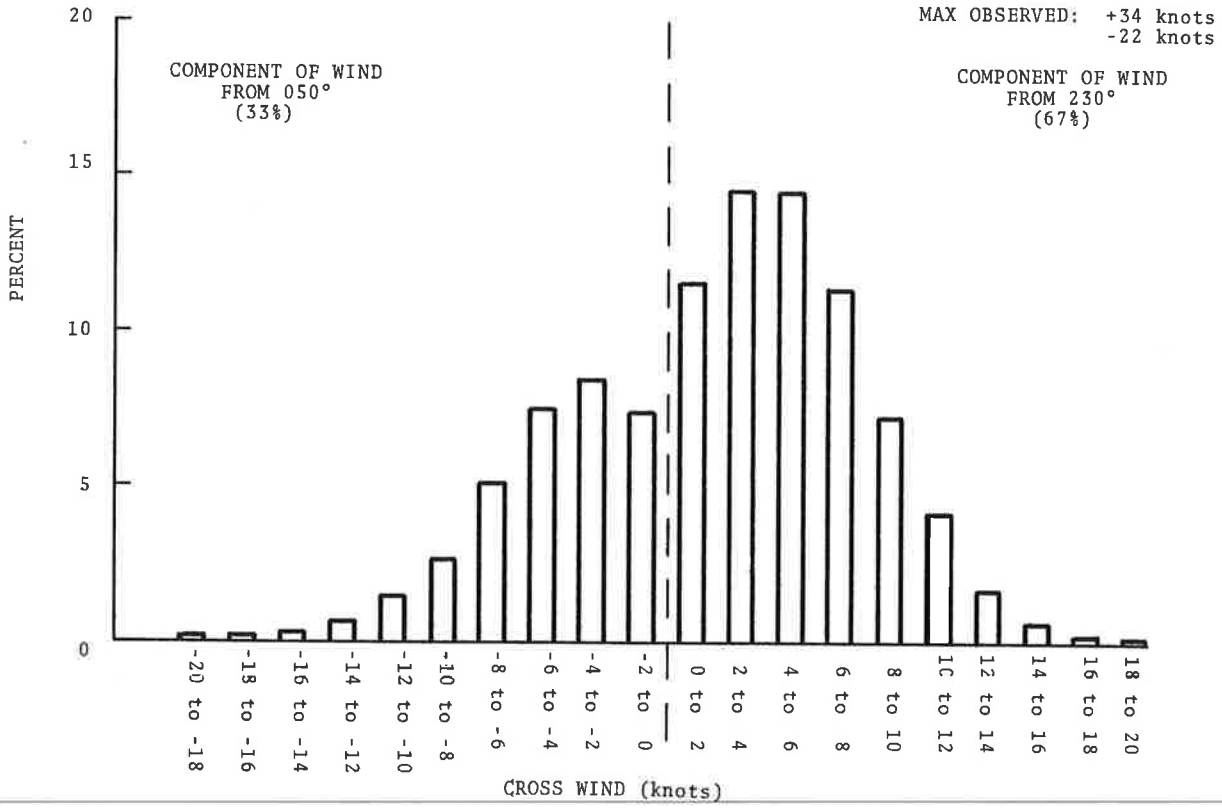

FIGURE 22. DISTRIBUTION OF ONE-MINUTE AVERAGED WINDS FOR RUNWAY 32L

shown in Figures 23 and 24. The winds recorded during the times of use of runway 14R were generally lower than those recorded during the times of use of runways 27R and 32L.

6.2 WIND VARIATIONS

The wind velocities used in this study are 60-second averaged values measured at the meteorological tower nearest the GWVSS (see Table 2). The VAS requires a meteorological tower in the vicinity of each landing runway (often one tower can service two or more runways); it was anticipated that the normal wind variations across an airport would be large enough to warrant the use of multiple towers not only for the VAS, but also for the correlation of vortex behavior with the winds. To study the situation, a data base was constructed consisting of wind velocities for one year (September 1976 through August 1977) from all six meteorological towers. The data base contained the computed 60-second running average of the winds updated every 5.5 seconds, and included data for the entire day and not just when vortex data were being collected.

Table 3 shows the maximum wind-magnitude differences (i.e., every 5.5 seconds the six wind magnitudes were examined and the difference between the largest and the smallest was labeled as ΔR, the maximum wind-magnitude difference). The mean value varied from a low of 3.5 knots (August) to a high of 5.0 knots (June). The mode or most probable value of ΔR was approximately 4 knots for each month.

The maximum wind-direction differences are shown in Table 4 (i.e., every 5.5 seconds the six wind directions were compared and the largest absolute difference in angle was labeled as $\Delta\Theta$). The mean value varied from 20.4 degrees (April) to 58.5 degrees (June). The mode was between 15 and 20 degrees for each month.

Table 5 shows the maximum vector differences (i.e., every 5.5 seconds the vector difference between pairs of the six wind velocities, a total of 15 combinations, was calculated and the largest vector difference was labeled $\overrightarrow{\Delta R}$). The maximum vector

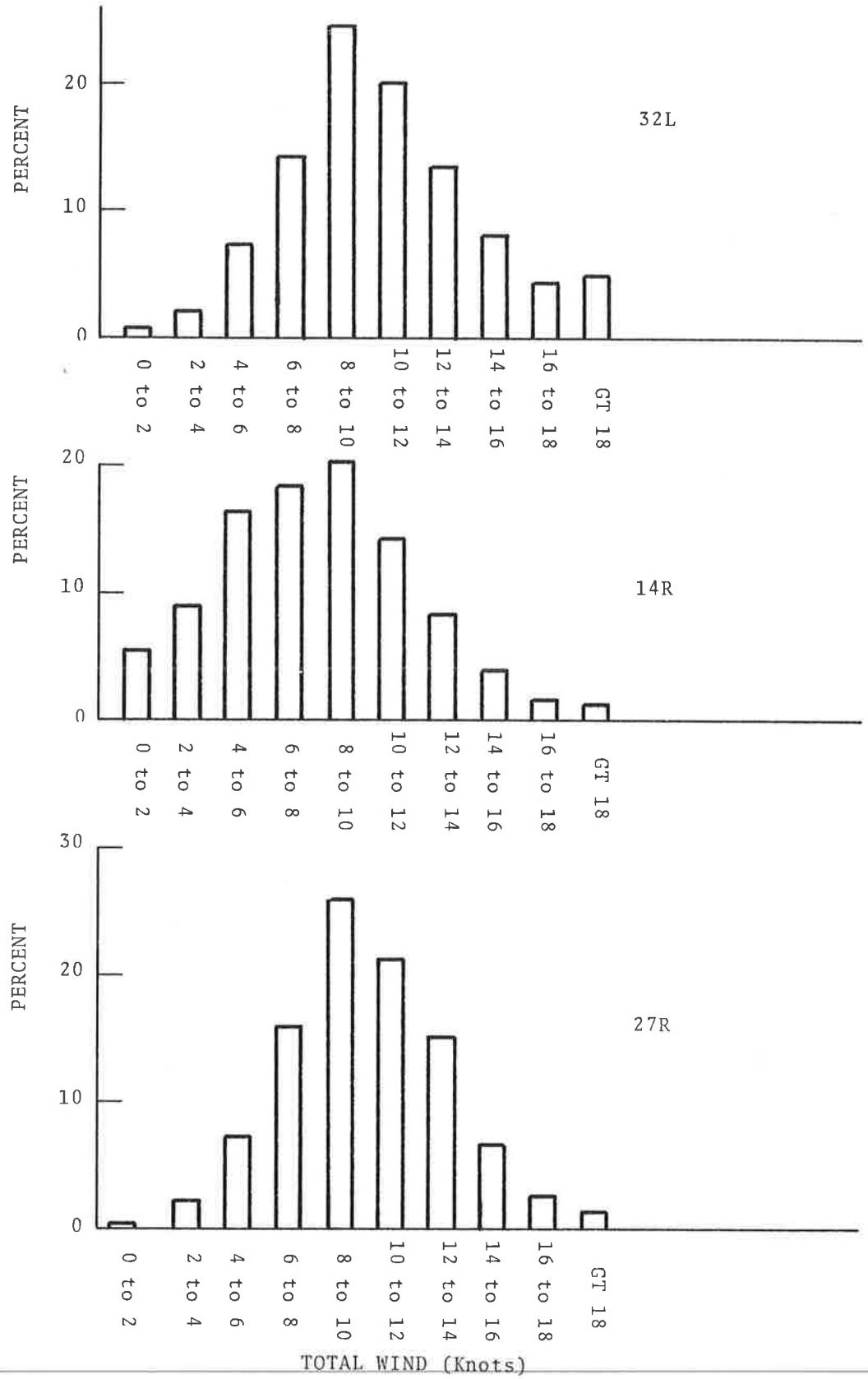

FIGURE 23. DISTRIBUTION OF TOTAL WINDS BY RUNWAY

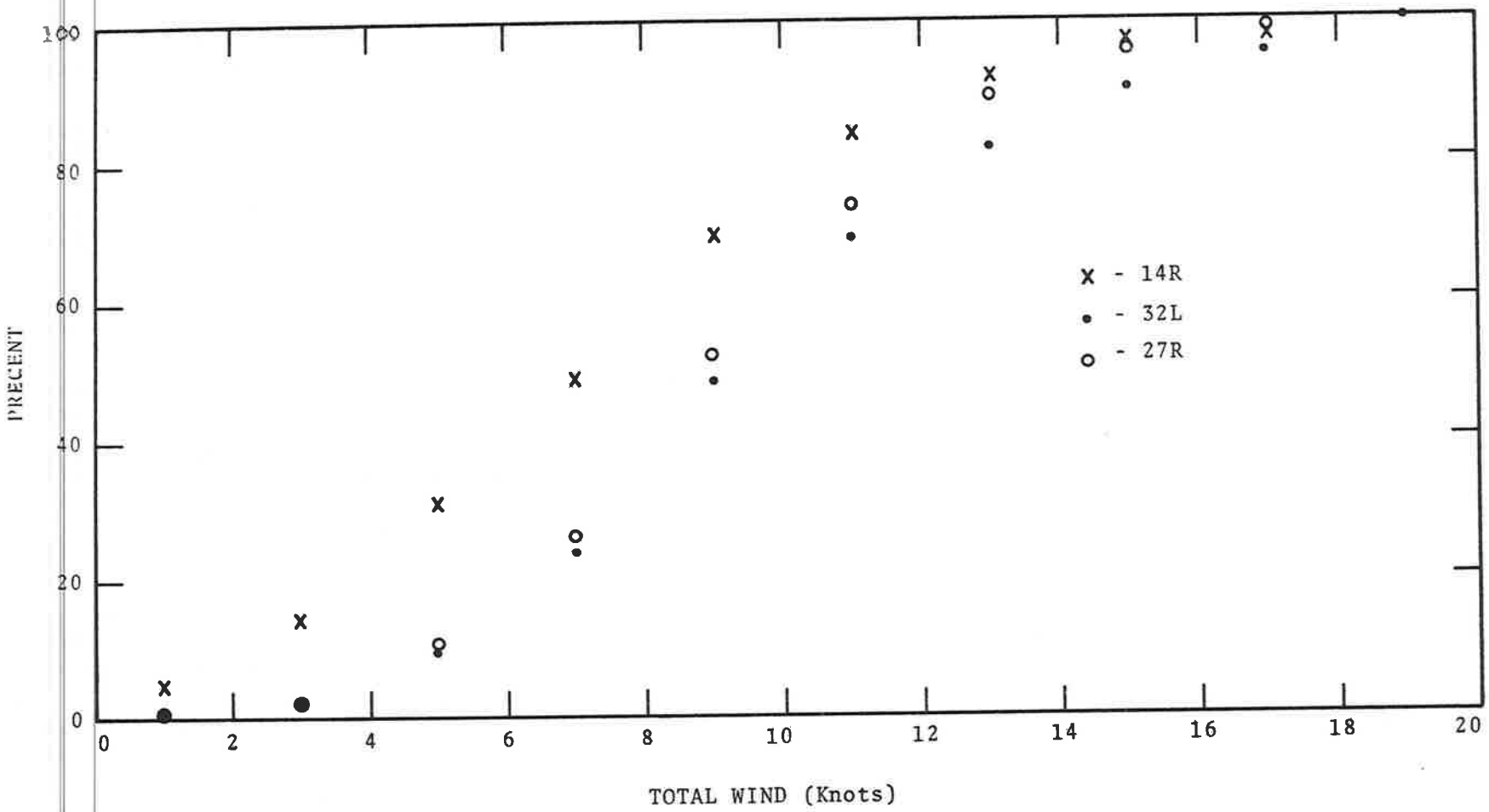

FIGURE 24. CUMULATIVE PERCENTAGE OF TOTAL WINDS BELOW ANY GIVEN WIND

TABLE 3. MAXIMUM WIND-MAGNITUDE DIFFERENCES

ΔR (knots)	PERCENTAGE FREQUENCY											
	Jan	Feb	Mar	Apr	May	Jun	Jul	Aug	Sep	Oct	Nov	Dec
0-2	3.573	3.163	3.858	6.104	11.240	1.737	4.383	9.855	3.567	3.958	3.028	3.215
2-4	36.037	33.398	30.404	28.134	39.118	25.904	25.786	45.971	35.792	27.074	34.360	30.030
4-6	36.413	35.405	33.084	33.653	29.456	36.348	35.788	30.373	36.158	36.876	39.482	37.075
6-8	16.294	18.418	17.984	19.874	13.049	22.320	23.231	10.661	17.055	21.951	17.183	19.354
8-10	5.185	6.584	8.291	8.728	5.008	8.852	8.084	2.489	5.905	7.302	4.77-	7.505
10-12	1.486	2.022	3.804	2.669	1.506	3.048	2.022	0.482	1.233	2.040	0.962	2.220
12-14	0.620	0.708	1.638	0.676	0.440	1.227	0.553	0.126	0.255	0.575	0.171	0.486
14-16	0.243	0.253	0.640	0.120	0.130	0.436	0.116	0.028	0.035	0.147	0.019	0.100
16-18	0.103	0.043	0.200	0.025	0.036	0.100	0.030	0.010	0.0	0.033	0.011	0.015
18-20	0.038	0.006	0.065	0.009	0.008	0.023	0.006	0.003	0.0	0.013	0.009	0.0
20--22	0.008	0.0	0.019	0.006	0.005	0.004	0.001	0.002	0.0	0.015	0.004	0.0
22-24	0.0	0.0	0.009	0.002	0.002	0.001	0.0	0.0	0.0	0.016	0.001	0.0
24-26	0.0	0.0	0.002	0.0	0.001	0.0	0.0	0.0	0.0	0.0	0.0	0.0
26-28	0.0	0.0	0.002	0.0	0.0	0.0	0.0	0.0	0.0	0.0	0.0	0.0

TABLE 4. MAXIMUM WIND-DIRECTION DIFFERENCES

Δθ (degrees)	PERCENTAGE FREQUENCY											
	Jan	Feb	Mar	Apr	May	Jun	Jul	Aug	Sep	Oct	Nov	Dec
0-10	9.126	6.442	8.016	6.105	6.254	2.312	3.462	6.148	2.856	3.286	5.937	6.627
10-20	53.111	45.499	45.036	43.122	27.920	20.450	29.307	34.594	26.132	28.798	48.895	50.736
20-30	23.330	25.879	26.645	26.022	24.927	21.907	23.539	24.734	26.406	24.689	28.276	25.054
30-40	7.505	10.378	10.272	10.927	15.090	13.302	11.984	13.645	16.608	14.131	10.387	9.131
40-50	3.114	4.246	4.522	5.617	7.922	9.734	6.219	7.171	8.528	8.226	3.998	3.501
50-60	1.251	2.131	1.972	2.835	5.300	5.591	4.537	3.837	5.249	4.319	1.597	1.645
60-70	0.565	1.248	1.099	1.360	3.704	4.024	3.422	2.881	3.456	2.824	0.551	0.976
70-80	0.440	0.948	0.761	0.733	1.783	3.125	1.739	1.446	1.951	2.003	0.187	0.587
80-90	0.232	0.725	0.464	0.413	1.230	3.160	1.412	1.078	1.564	1.600	0.096	0.431
90-100	0.274	0.690	0.320	0.385	1.107	2.826	1.691	0.727	1.085	1.455	0.035	0.285
100-110	0.264	0.589	0.280	0.256	0.829	1.457	1.624	0.562	0.879	1.289	0.019	0.160
110-120	0.179	0.264	0.172	0.193	0.726	1.116	1.885	0.565	0.803	0.914	0.009	0.144
120-130	0.116	0.169	0.125	0.208	0.590	1.072	1.871	0.436	0.784	0.756	0.006	0.105
130-140	0.113	0.214	0.085	0.202	0.571	1.343	1.821	0.353	0.661	0.803	0.002	0.074
140-150	0.125	0.224	0.090	0.249	0.469	1.538	1.676	0.496	0.710	0.851	0.001	0.071
150-160	0.112	0.176	0.050	0.437	0.511	1.804	1.508	0.512	0.650	0.976	0.002	0.099
160-170	0.068	0.103	0.054	0.464	0.665	2.380	1.449	0.417	0.801	1.394	0.002	0.157
170-180	0.075	0.075	0.037	0.472	0.402	1.860	0.854	0.398	0.868	1.686	0.0	0.217

TABLE 5. MAXIMUM WIND-VECTOR DIFFERENCES

$\vec{\Delta R}$ (knots)	PERCENTAGE FREQUENCY											
	Jan	Feb	Mar	Apr	May	Jun	Jul	Aug	Sep	Oct	Nov	Dec
13-14	0.298	0.335	0.851	0.250	0.216	0.511	0.278	0.052	0.152	0.330	0.076	0.191
14-15	0.218	0.233	0.553	0.156	0.156	0.355	0.131	0.030	0.701	0.200	0.028	0.104
15-16	0.167	0.115	0.379	0.093	0.082	0.226	0.061	0.011	0.022	0.114	0.010	0.046
16-17	0.096	0.051	0.226	0.052	0.061	0.125	0.026	0.009	0.007	0.025	0.009	0.018
17-18	0.054	0.020	0.136	01038	0.045	0.078	0.016	0.007	0.010	0.105	0.004	0.009
18-19	0.039	0.009	0.085	0.009	0.025	0.051	0.012	0.006	0.011	0.015	0.007	0.001
19-20	0.020	0.002	0.061	0.007	0.015	0.024	0.005	0.005	0.002	0.013	0.003	0.0
20-21	0.009	0.0	0.031	0.007	0.008	0.010	0.006	0.003	0.002	0.007	0.002	0.0
21-22	0.003	0.0	0.020	0.007	0.002	0.003	0.006	0.002	0.0	0.009	0.0	0.0
22-23	0.0	0.0	0.014	0.007	0.001	0.003	0.005	0.002	0.0	0.008	0.0	0.0
23-24	0.0	0.0	0.011	0.007	0.001	0.001	0.003	0.001	0.0	0.008	0.001	0.0
24-25	0.0	0.0	0.006	0.006	0.004	0.002	0.001	0.002	0.0	0.0	0.0	0.0
25-26	0.0	0.0	0.005	0.004	0.003	0.003	0.0	0.002	0.0	0.0	0.0	0.0
26-27	0.0	0.0	0.009	0.002	0.002	0.0	0.0	0.001	0.0	0.0	0.0	0.0
27-28	0.0	0.0	0.007	0.002	0.002	0.0	0.0	0.0	0.0	0.0	0.0	0.0
28-29	0.0	0.0	0.006	0.002	0.001	0.0	0.0	0.0	0.0	0.0	0.0	0.0
29-30	0.0	0.0	0.001	0.001	0.001	0.0	0.0	0.0	0.0	0.0	0.0	0.0
30-31	0.0	0.0	0.002	0.0	0.002	0.0	0.0	0.0	0.0	0.0	0.0	0.0
31-32	0.0	0.0	0.002	0.0	0.001	0.0	0.0	0.0	0.0	0.0	0.0	0.0

magnitude was greater than or equal to 13 knots only 0.133 percent of the month of August (0.99 hours) but 2.406 percent of the month of March (17.90 hours). The vector differences were caused by large ΔR's and small $\Delta\Theta$'s about one third of the time, small ΔR's and large $\Delta\Theta$'s about one third of the time, and moderate values of both ΔR and $\Delta\Theta$ the remaining one third of the time.

Because of the computer cost, vector differences were calculated only when at least two of the six wind magnitudes exceeded 6.5 knots, and were printed only when at least one pair gave a vector difference of at least 10 knots. The length of time that at least one tower pair gave a vector difference of at least 13 knots, 14 knots, 15 knots, etc. was determined. The time intervals for consecutive 5.5-second vector differences of at least 13 knots varied from the minimum 5.5 seconds to 759 seconds (a storm in March which closed O'Hare for a short time).

Figure 25 shows the cumulative probability for the vector magnitude to equal or exceed 13 knots. Four months are shown; the others cluster about the curves for February and December. The curves are bounded by $e^{-(R/c)}$ and $e^{-(R/c)^2}$, where c is a scale factor with units of speed. A bivariate normal distribution gives a good fit to the data in the range shown. Extrapolating the data to 100 percent cumulative probability yields vector differences between 3 and 7 knots.

When the vector difference exceeded 15 knots, it usually existed between two neighboring towers, not across the entire airport. The event occurred when one sensor either measured a much higher wind speed than all the others or, more frequently, when one sensor measured a much lower wind speed than at the rest of the towers.

The variations indicated in Tables 3 to 5 are large enough to justify the use of multiple meteorological towers in the VAS as well as for the data collection. At a typical airport the runway thresholds can be as much as two miles apart; the wind, particularly a 60-second average wind, should be expected to be

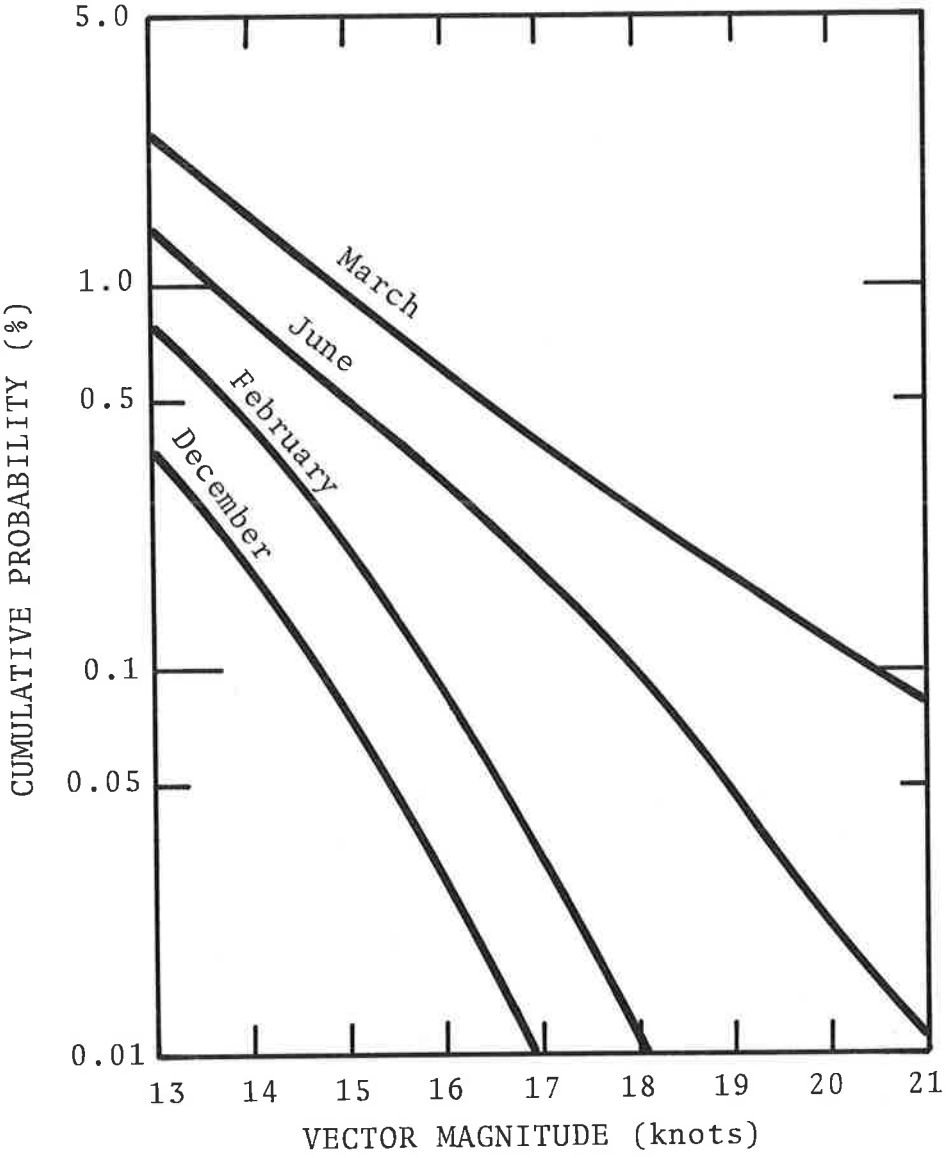

FIGURE 25. CUMULATIVE PROBABILITY FOR THE MAXIMUM WIND-VECTOR MAGNITUDE

different across two miles -- with a 10-knot wind it will take in excess of 10 minutes for a parcel of wind or gust to travel from one side of the airport to the other.

7. DATA ANALYSIS

Final Approach represents the most dangerous region when considering the wake vortex hazard to an aircraft. Historically, the major portion of vortex-related accidents have occurred with one aircraft landing behind another on the same runway, according to National Transportation Safety Board records. During a ten-year observation period (1964-1973) over 83 percent of the vortex-related accidents took place when the encountering aircraft was between the middle marker and the runway threshold (Ref. 12).

The motion of a vortex is controlled primarily by two forces, the ambient wind and mutual induction. Each vortex is influenced by the velocity field of the other vortex and/or interaction with its image vortex near the ground (Ref. 1). In general, the mutual induction forces cause the vortices to descend initially at a rate of about 4 knots. Thus, for one aircraft landing behind another and following essentially the same flight path, the vortices for the lead aircraft will descend or transport out of the path of the following aircraft and present no hazard. However, on the Final Approach at aircraft altitudes of less than 150 feet, vortex descent is arrested by interaction with the ground. The combination of ground effect and the effect of the ambient wind lead to the possibility of producing conditions for vortex stalling (i.e., the vortex remaining near the extended runway centerline). Recognizing this as the most probable region for observing a hazardous vortex, the GWVSS were installed where aircraft altitudes were approximately 150 feet.

7.1 SAFETY ZONE

The safety zone is defined as the region where the presence of a vortex might present a hazard to a following aircraft under normal operating conditions. If both vortices from a lead aircraft have exited the safety zone, either by moving out or by dissipating, a following aircraft will not be affected by the vortices of the lead aircraft.

The boundaries on the safety zone depend on the distance from the runway threshold and are deliberately chosen to be conservative. In the region from the middle marker to touchdown the safety zone has no vertical boundary. The width was determined from two criteria. First, as part of the TSC vortex data collection at Denver's Stapleton International Airport (Refs. 1 to 3) it was determined from photographs that 3σ or 99.74 percent of landing aircraft were within 50 feet of the extended runway centerline from the middle marker region to touchdown. Most of the aircraft involved in these tests were conducting visual approaches during clear weather; instrument approaches should be much closer (Ref. 13). Second, six-degree-of-freedom aircraft-vortex encounter simulations done at TSC and elsewhere (Refs. 1 and 14) have indicated that if the fuselage of any aircraft is at least 100 feet from the center of any vortex, the aircraft will not experience an unacceptable disturbance. This claim is supported by limited flight test data. The 100-foot figure is conservative and represents the most dangerous case of a light general aviation aircraft approaching a vortex formed by a widebody jet. The exact figure depends on the characteristics of the vortex-generating/encountering-aircraft pair. Thus, the safety zone was selected to extend 50 + 100 or 150 feet on both sides of the extended runway centerline.

The detection of a vortex in the safety zone is defined as a potentially hazardous situation. This is a very conservative approach as close inspection of selected cases has shown that the GWVSS will continue to indicate the presence of a vortex after it has decayed to a level which would not pose a hazard to a following aircraft. Additionally, the aircraft and the vortex can be separated by as much as 200 feet and yet both be within the safety zone. Furthermore, the vortex may have been generated by an aircraft whose vortices will not affect the following aircraft; e.g., a DC-9 followed by a B-747. Thus, the existence of a vortex within the safety zone when a following aircraft arrives does not mean that a hazardous condition exists; it is a necessary but not a sufficient condition.

7.2 AIRCRAFT TYPES

A total of 21,193 landings were monitored during these tests. A distribution of the aircraft types observed on the three runways is given in Table 6. Fifteen percent of the aircraft observed were in the Heavy class, seventy-three percent were in the Large class, and twelve percent were in the Small class.

7.3 VORTEX RESIDENCE TIMES

The "residence" time is defined as the time required for both vortices to exit the safety zone. The vortices may exit by one of two mechanisms: transporting out of the safety zone or decaying below a detectable level inside the safety zone. In most cases detection of a vortex is determined from the computer printout vortex tracks as discussed in Section 5. However, all cases where the vortex apparently remained in the safety zone for at least 80 seconds were given special attention by analyzing the analog anemometer stripchart outputs to supplement the normal computer track data. This resulted in identifying many cases where the signals were very weak and the vortex was determined to have dissipated, whereas the computer algorithm continued to indicate the existence of a vortex track.

The data were analyzed to determine the probability of finding a vortex in the safety zone as the vortex ages. Using the total data base of all aircraft, all runways, and all winds combined, the results are plotted in Figure 26. As an example, the probability of finding a vortex in the safety zone for times longer than 100 seconds is approximately 10^{-2}. Thus, statistically speaking, one out of every 100 aircraft vortices will remain in the safety corridor for a time longer than 100 seconds. The special attention given to the select group of vortices which remained in the corridor longer than 80 seconds resulted in a slight bias in the data toward shorter residence times at the 80-second mark and can be seen as a subtle discontinuity in plotted data for the probability of a vortex remaining in the corridor as shown in Figure 26.

TABLE 6. AIRCRAFT DISTRIBUTION

AIRCRAFT TYPE	COUNT				PERCENTAGE*			
	14R	27R	32L	ALL	14R	27R	32L	ALL
B-707	535	237	730	1502	6	6	8	7
B-727	3347	1420	3850	8617	41	39	41	41
B-737	351	228	553	1132	4	6	6	5
B-747	281	121	246	648	3	3	3	3
DC-8	348	251	249	848	4	7	3	4
DC-9	1474	343	1810	3627	18	9	19	17
DC-10	643	341	497	1481	8	9	5	7
L-1011	116	45	181	342	1	1	2	2
B-707H	49	19	86	154	1	1	1	1
DC-8H	196	49	112	357	2	1	1	2
Small Prop	703	497	877	2077	9	14	9	10
Small Jet	117	85	175	377	1	2	2	2
Other	6	6	19	31	0	0	0	0
Total	8166	3642	9385	21193				

TOTAL AIRCRAFT - 21193

*NOTE: Roundoff errors will result in this total not adding to 100 percent

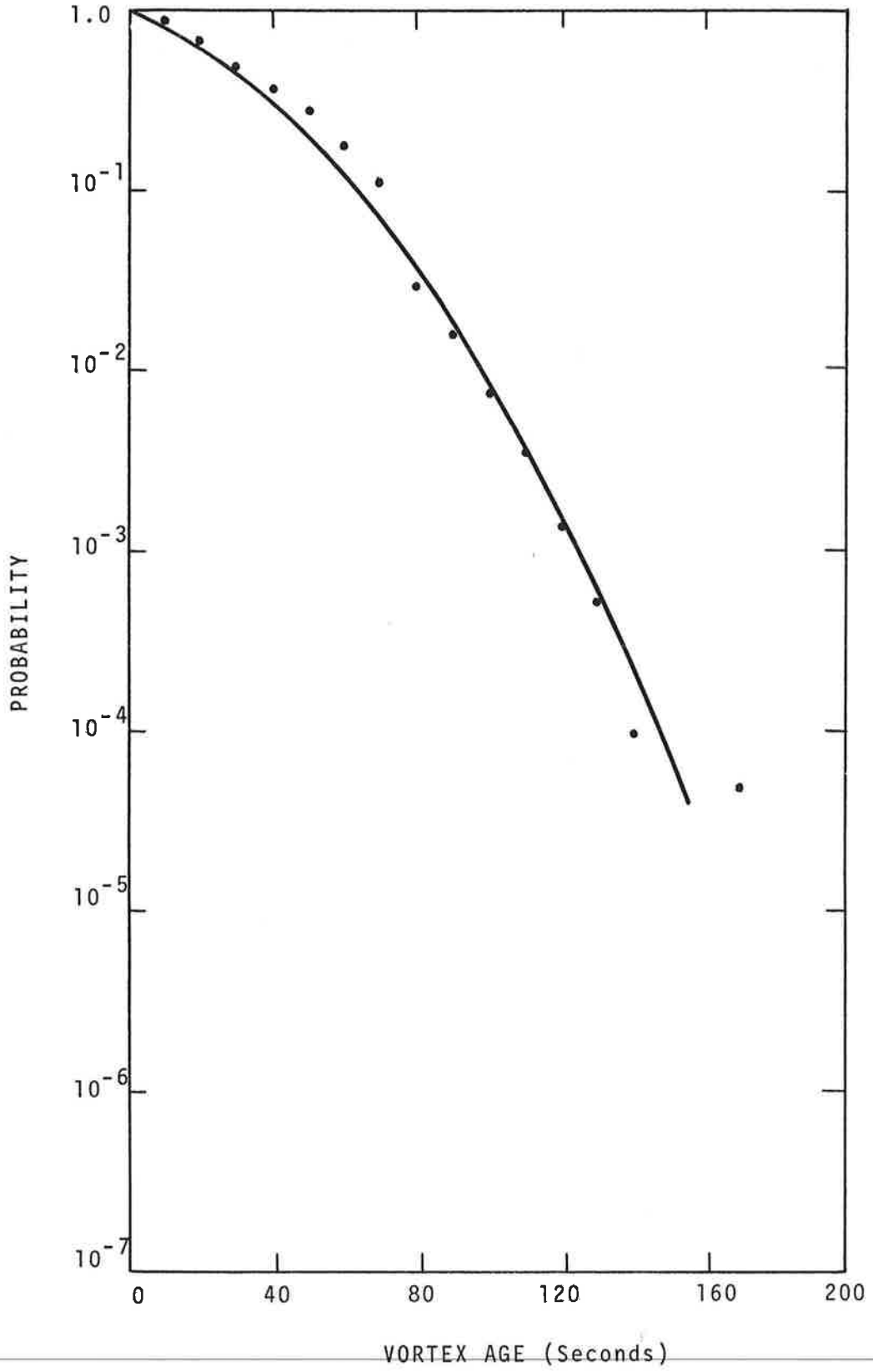

FIGURE 26. PROBABILITY FOR A VORTEX TO REMAIN IN SAFETY ZONE LONGER THAN A GIVEN TIME

The O'Hare residence data are compared to the Heathrow residence data (Ref. 5) in Figure 27. The data for the Heathrow inner baseline compare very favorably with the O'Hare data. This is to be expected since the O'Hare sensor lines are approximately the same distance from the runway threshold as the Heathrow inner sensor line.

7.3.1 Residence Times by Runway

The data on Figure 26 can be disaggregated by runway and is shown in Figure 28. There is very little difference in the data from the three runways for vortex ages in excess of 80 seconds. However, at earlier times the probability of finding a vortex in the safety zone is noticeably highest in the data from runway 27R and lowest in the data from runway 14R. This appears at first to be the opposite of what one would expect when considering air traffic operations at O'Hare. Runway 27R is often used on sunny days with relatively high winds which are the conditions which one would expect to yield relatively short-lived vortices. Runway 14R, on the other hand, is often used on cloudy days with relatively low winds which are the conditions which one would expect to yield relatively long-lived vortices. Figures 23 and 24 confirm that runway 14R is used during lower wind conditions than runway 27R. However, Figures 20 and 22 show that the distribution of the winds into their component parts is quite different for these two runways. Runway 14R is used more frequently with higher crosswinds than runway 27R. The percentage of the time the runways are used with crosswinds greater than 6 knots are 47 percent for runway 14R and 23 percent for runway 27R. This observation leads to the conclusion that the higher residence times for runway 27R are contributed by vortices tending to stall and eventually decaying in the safety zone rather than transporting out of the zone. The correlation between the residence time and the number of vortices that decayed in the safety zone is given in Figure 29. The higher crosswinds for runway 14R result in vortices transporting out of the safety zone relatively quickly compared to runway 27R;

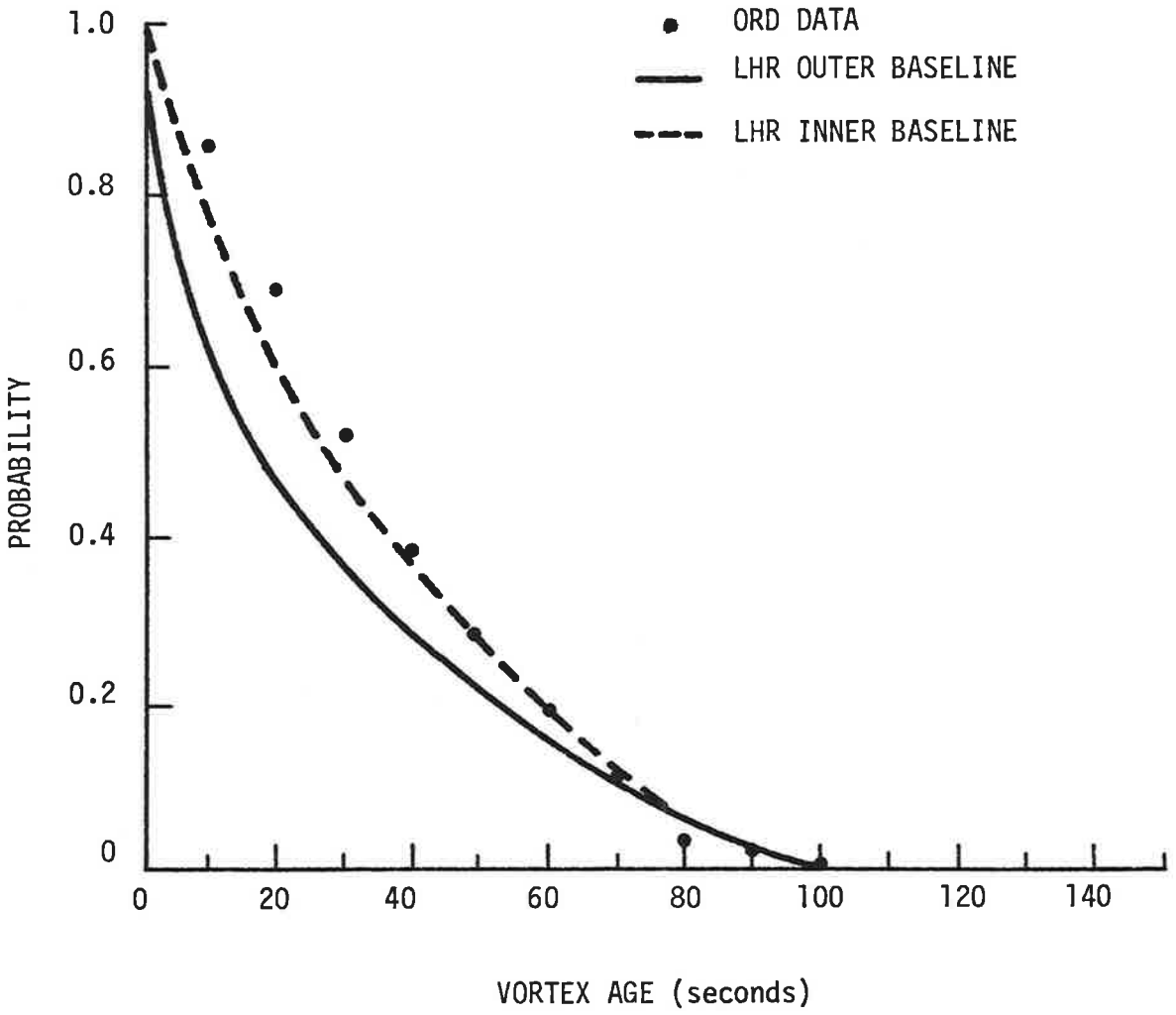

FIGURE 27. PROBABILITY FOR A VORTEX TO REMAIN IN SAFETY ZONE LONGER THAN A GIVEN TIME, COMPARISON OF HEATHROW AND O'HARE DATA

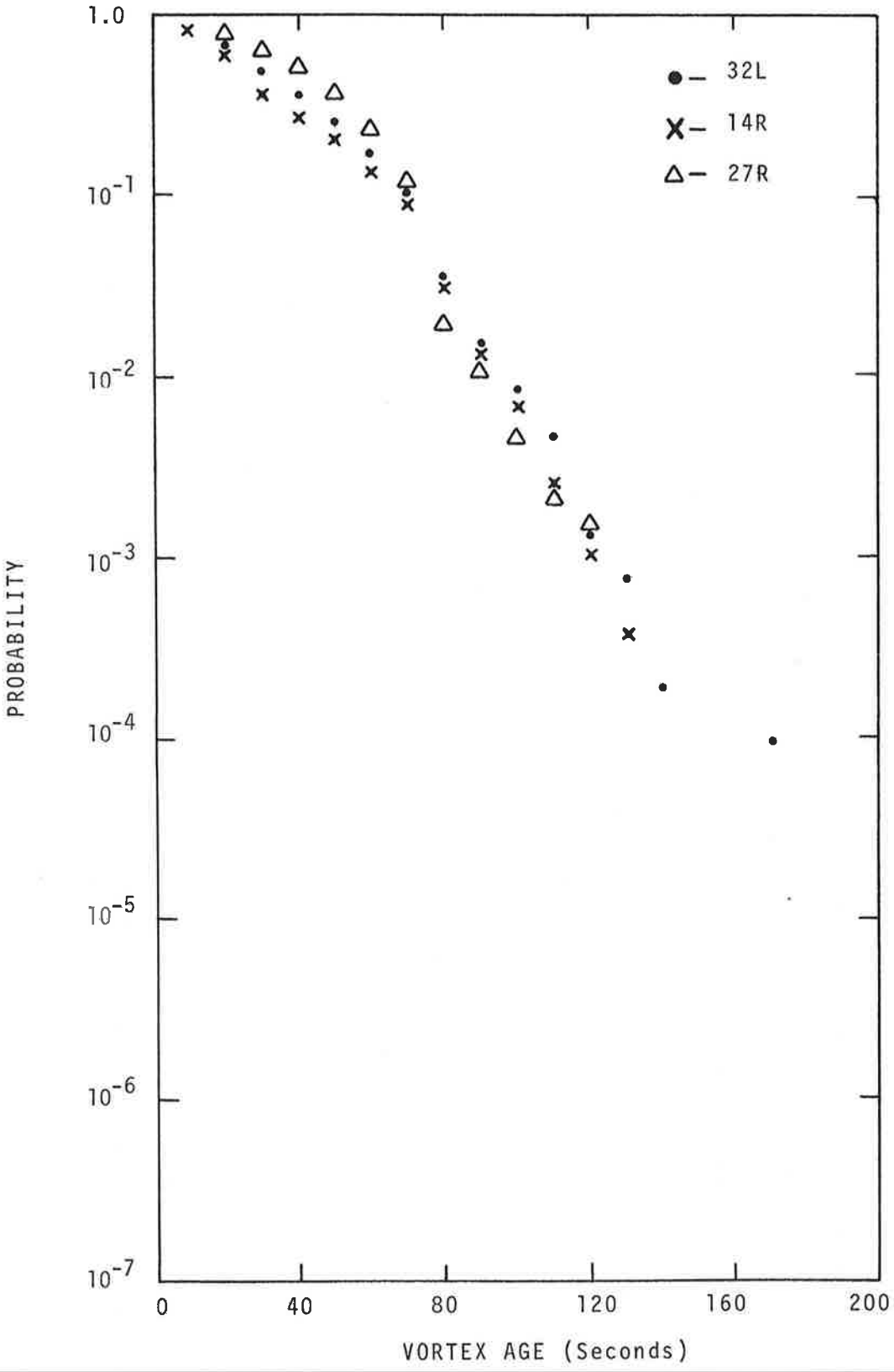

FIGURE 28. PROBABILITY FOR A VORTEX TO REMAIN IN THE SAFETY ZONE LONGER THAN A GIVEN TIME, COMPARISON BY RUNWAY

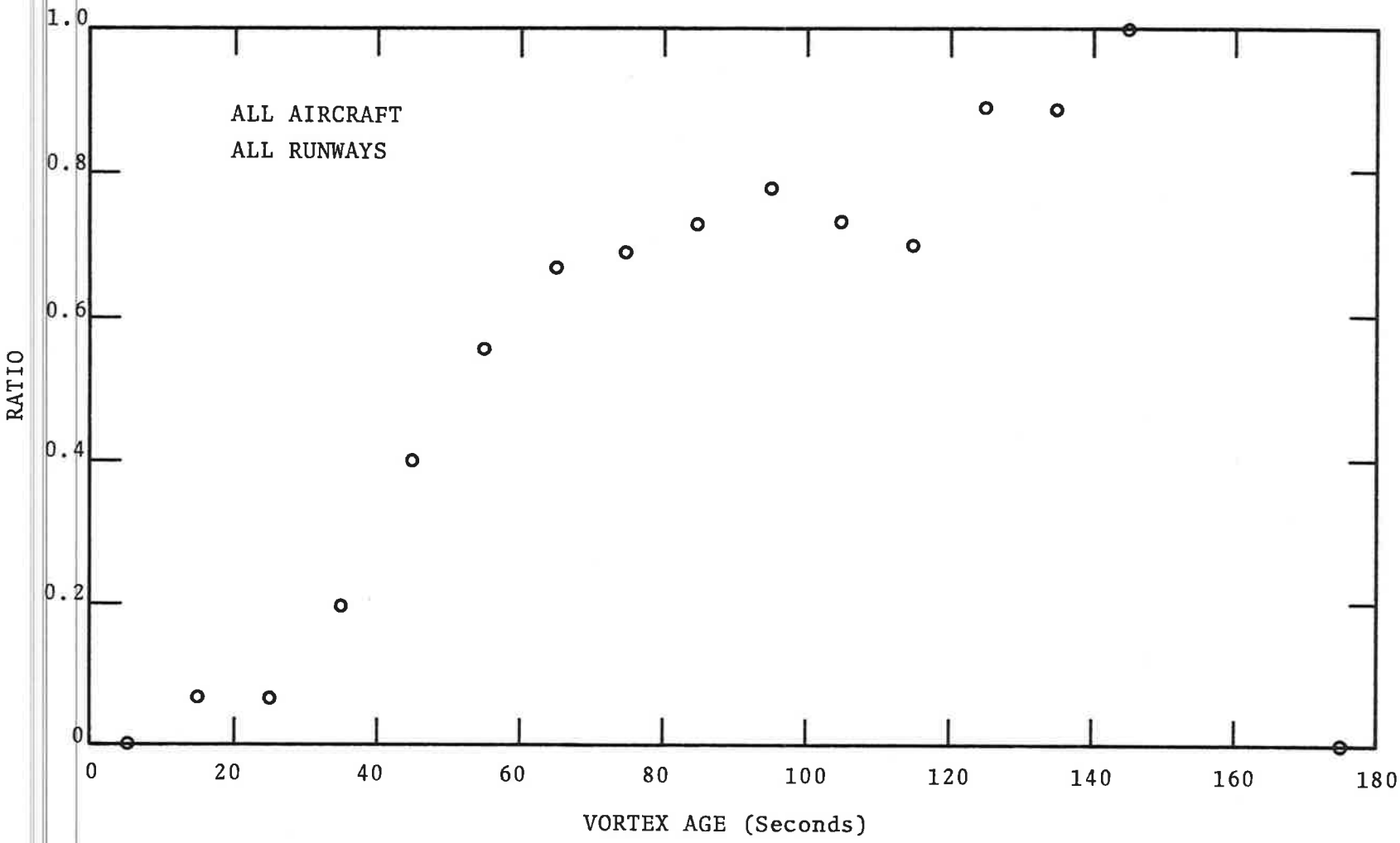

FIGURE 29. RATIO OF NUMBER OF VORTICES WHOSE RESIDENCE TIME DUE TO DECAY IN SAFETY ZONE TO TOTAL NUMBER OF VORTICES OBSERVED

although the winds are generally higher on runway 27R, they are almost pure headwind and therefore the vortices remain in the safety zone for longer times.

7.3.2 Residence Times by Aircraft Type

The disaggregation of the residence time statistics by aircraft type produced no surprises. The jumbo aircraft yielded higher probabilities of long-lived vortices as shown in Figure 30. Several other combinations of aircraft types of interest (B-707H vs. B-707, DC-8H vs. DC-8, DC-8H vs. B-707, L-1011 vs. DC-10) are compared in Figures 31 to 34. Appendix A gives distributions of residence time data by aircraft type.

There is obviously a significant difference in the residence times of the B-747 vortices as compared to the residence times of the B-727 vortices as could be expected. However, the data for the remaining combinations are surprisingly similar. It might have been expected that the vortices of B-707Hs and DC-8Hs would have longer residence times than those of the Large B-707 and DC-8s, respectively. However, the data show no marked differences as shown in Figures 31 and 32. There also is no significant difference in the residence statistics of the B-707H and DC-8H as shown in Figure 33 and for the DC-10 and L-1011 as shown in Figure 34.

The residence data for a few selected aircraft for the O'Hare tests are compared to the residence data for the Heathrow tests in Figures 35 through 39. In general, the comparisons are excellent. Since there was very little difference in the residence statistics of the B-707 and B-707H, their data are combined in these plots. The same situation holds for the DC-8 and DC-8H.

7.3.3 Wind Effects on Residence Times

Cross-wind magnitude is the most important parameter affecting the vortex residence time statistics. The percentage of vortices that remained resident in the corridor segregated by cross-wind component is shown in Figure 40. As expected, the

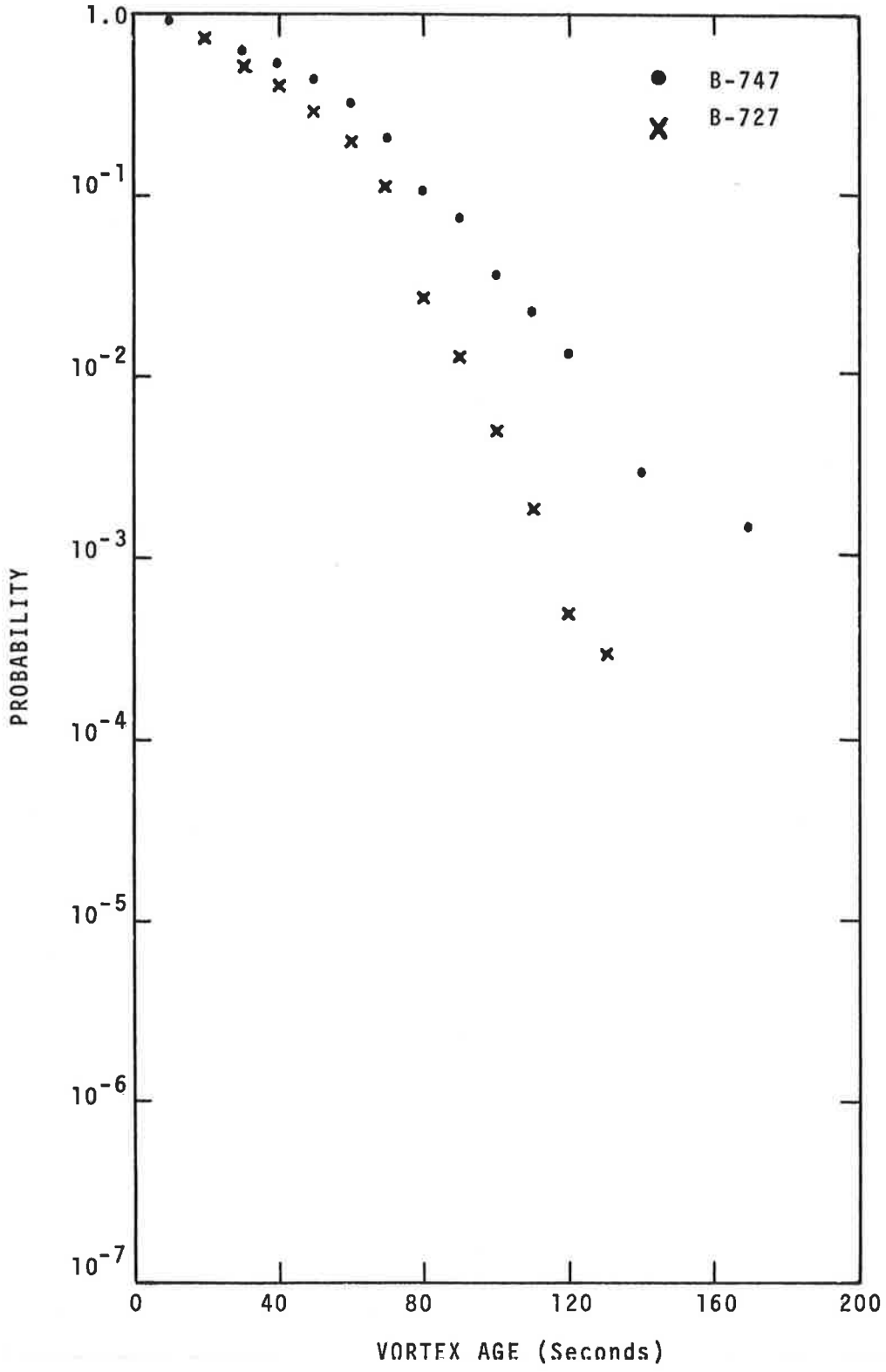

FIGURE 30. PROBABABILITY FOR A VORTEX TO REMAIN IN THE SAFETY ZONE LONGER THAN A GIVEN TIME FOR B-747 AND B-727 AIRCRAFT

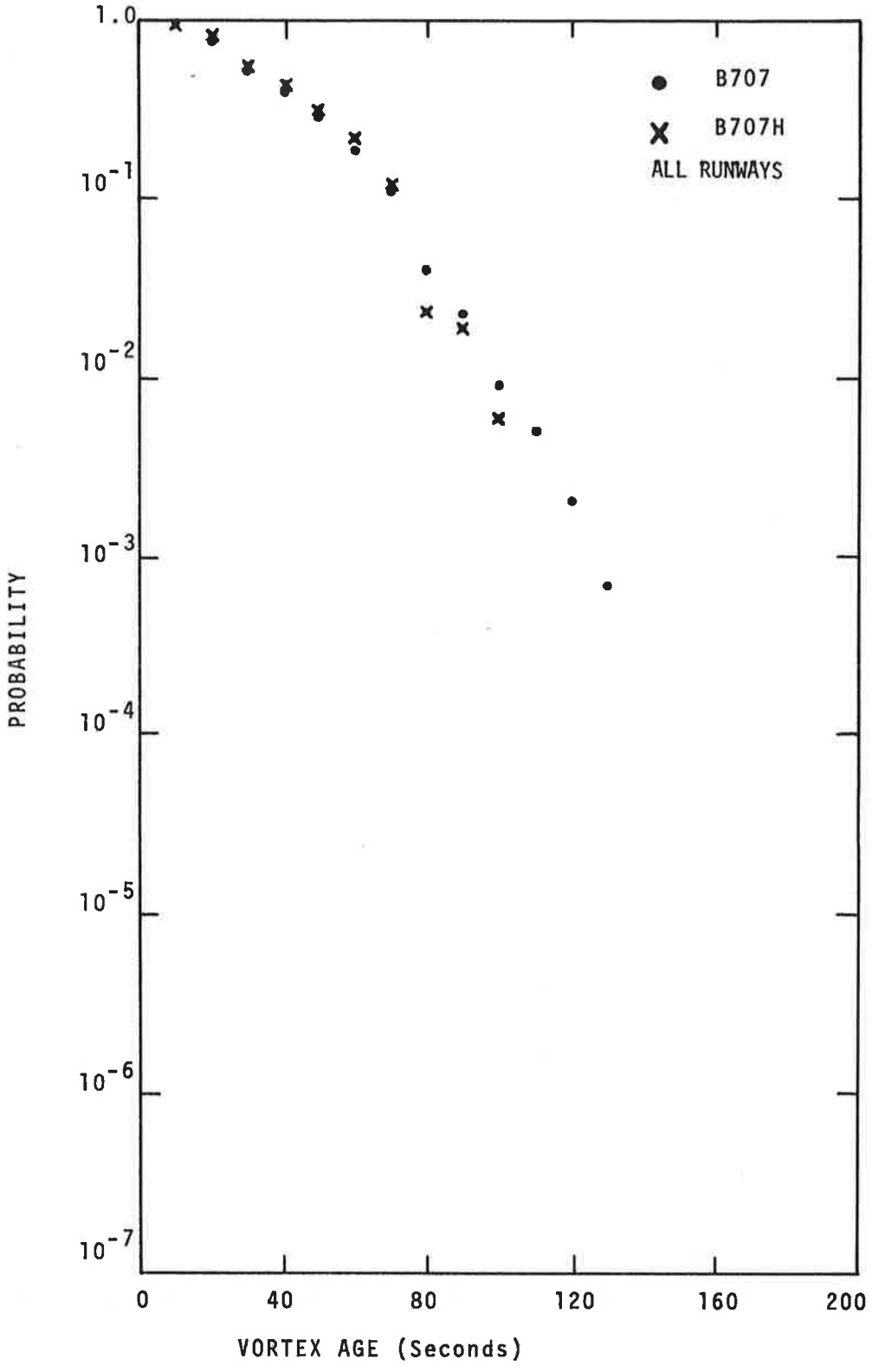

FIGURE 31. PROBABILITY FOR A VORTEX TO REMAIN IN THE SAFETY ZONE LONGER THAN A GIVEN TIME FOR B-707 AND B-707H AIRCRAFT

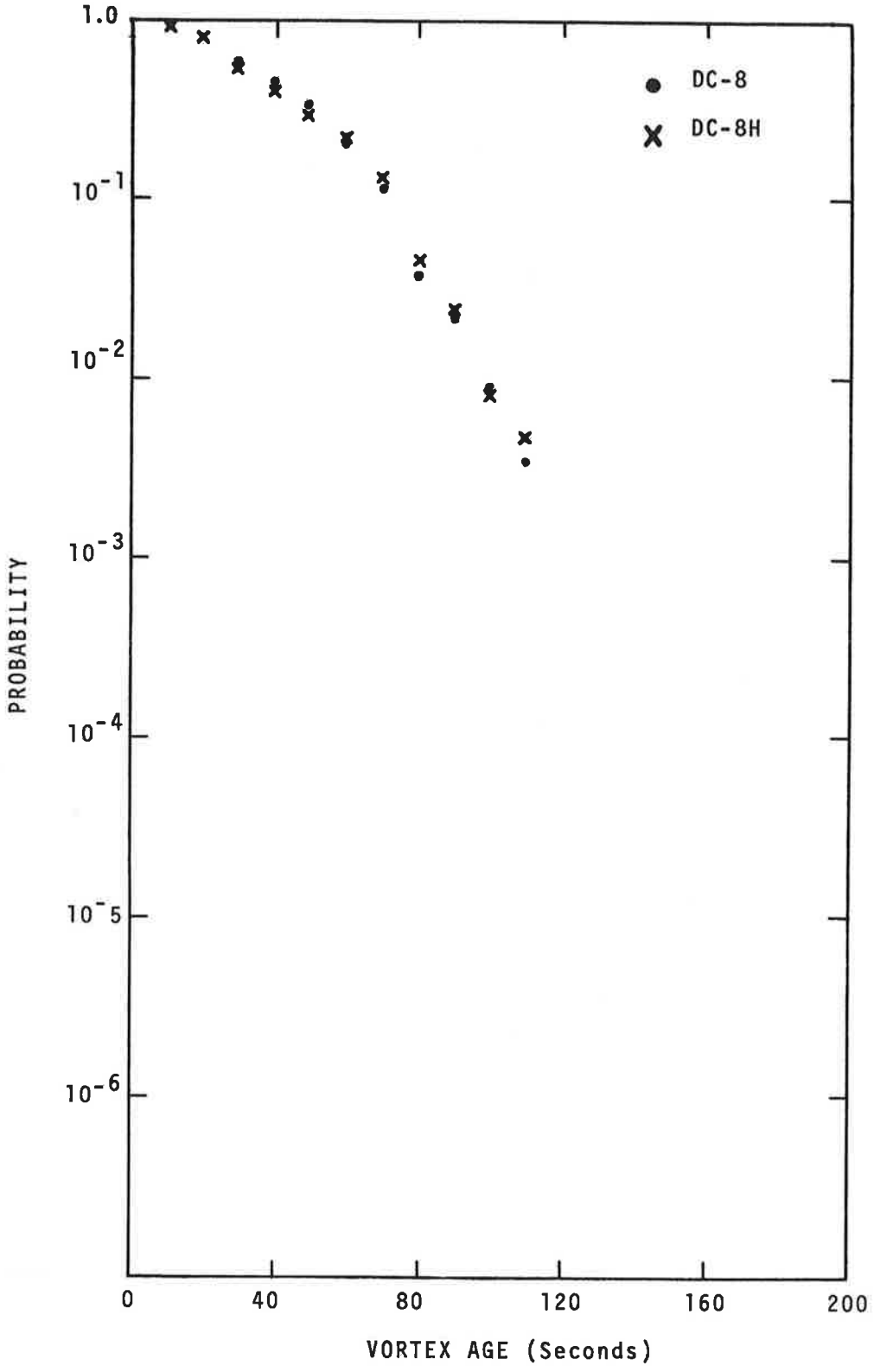

FIGURE 32. PROBABILITY FOR A VORTEX TO REMAIN IN THE SAFETY ZONE LONGER THAN A GIVEN TIME FOR DC-8 AND DC-8H AIRCRAFT

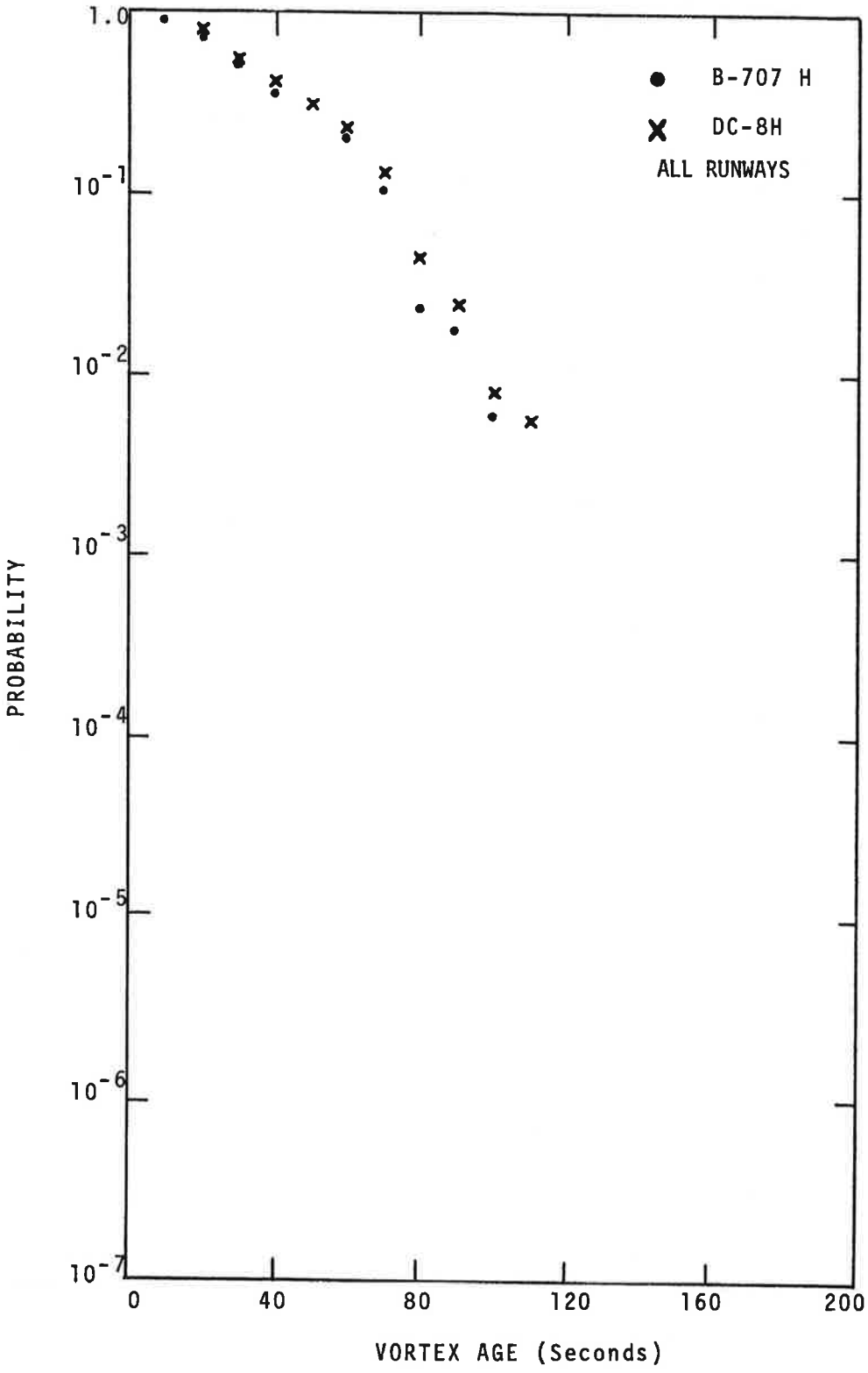

FIGURE 33. PROBABILITY FOR A VORTEX TO REMAIN IN THE SAFETY ZONE LONGER THAN A GIVEN TIME FOR B-707H AND DC-8H AIRCRAFT

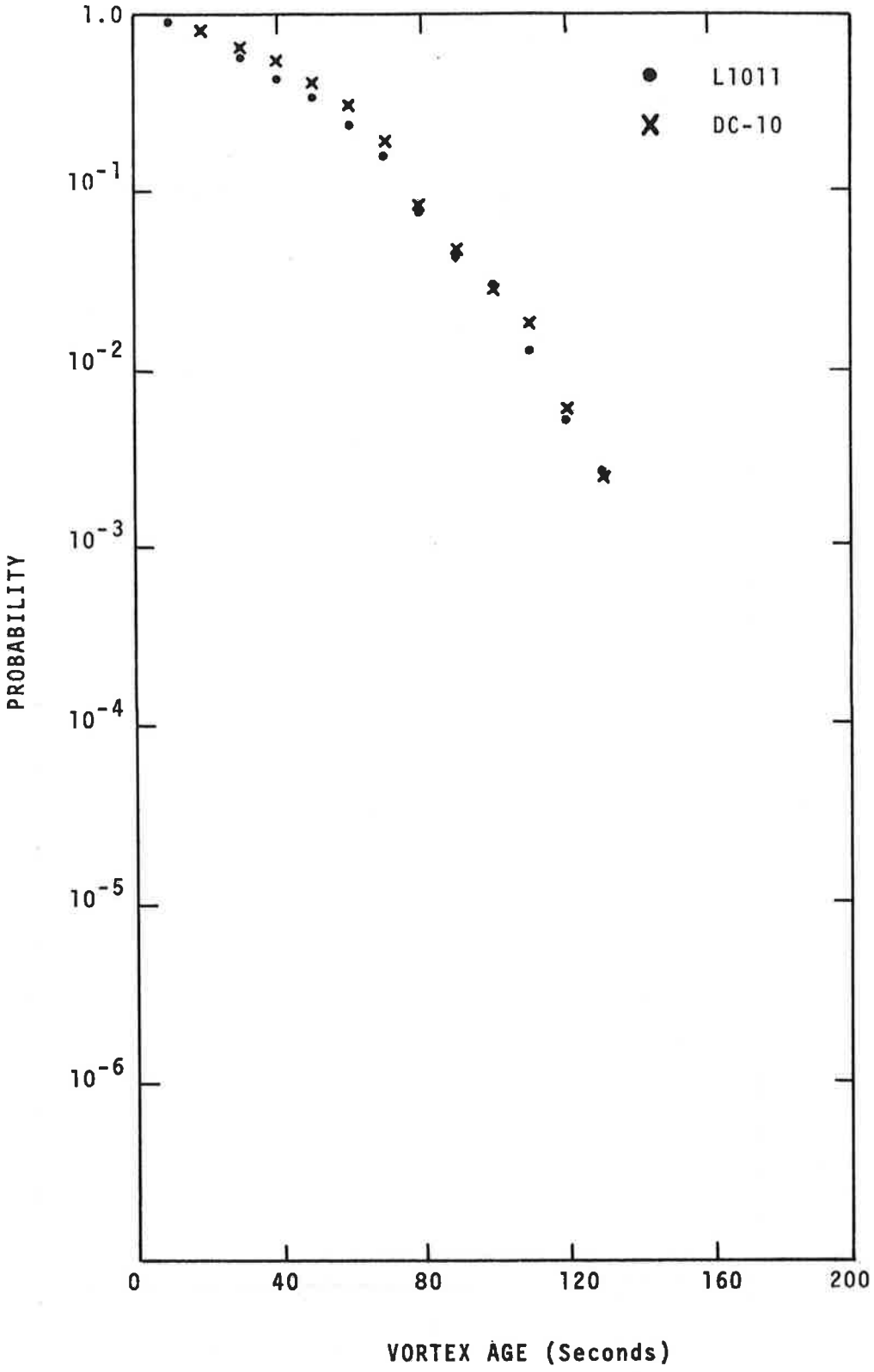

FIGURE 34. PROBABILITY FOR A VORTEX TO REMAIN IN THE SAFETY ZONE LONGER THAN A GIVEN TIME FOR L-1011 AND DC-10 AIRCRAFT

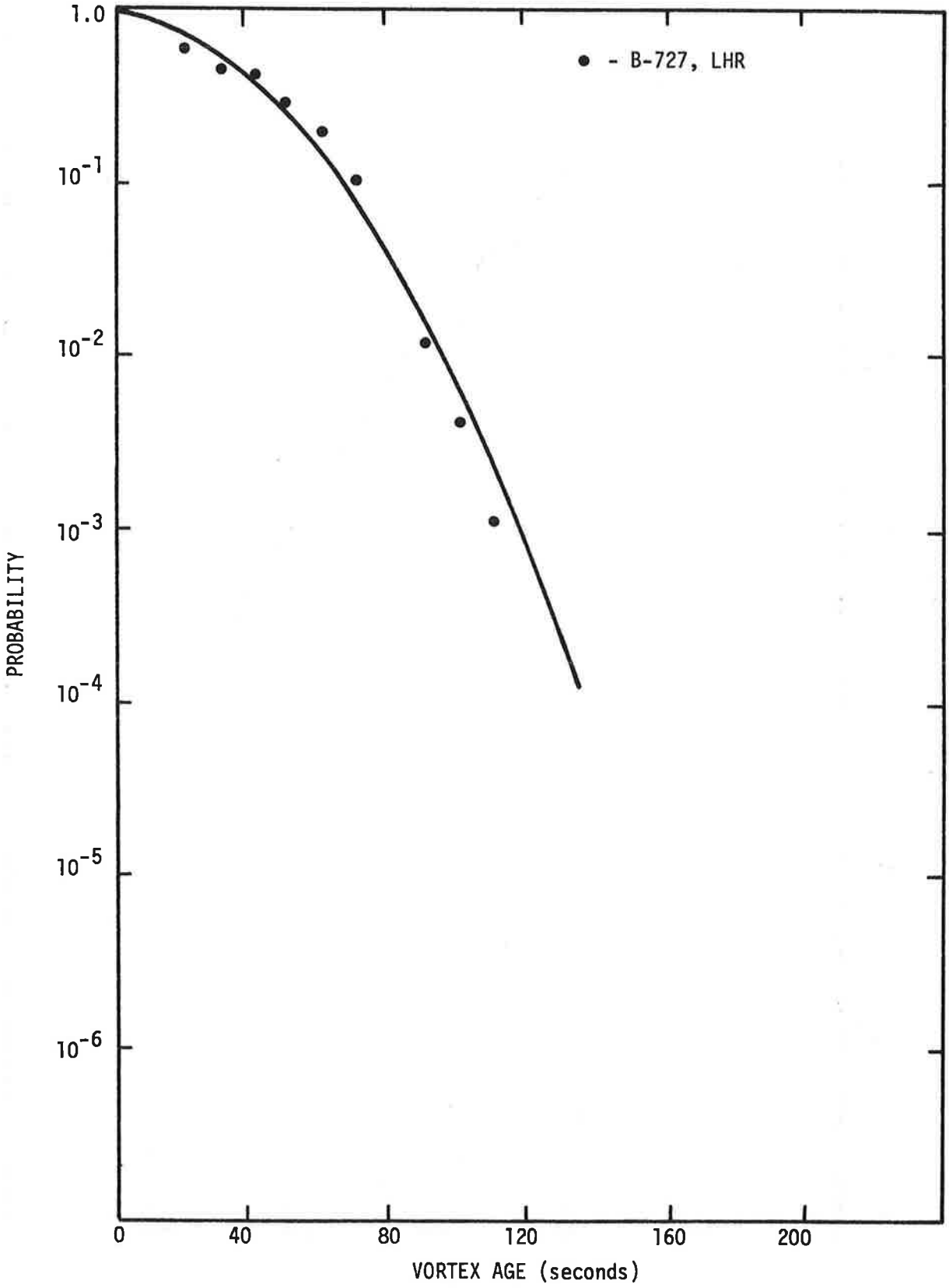

FIGURE 35. COMPARISON OF O'HARE AND HEATHROW RESIDENCE TIME DATA, B-727

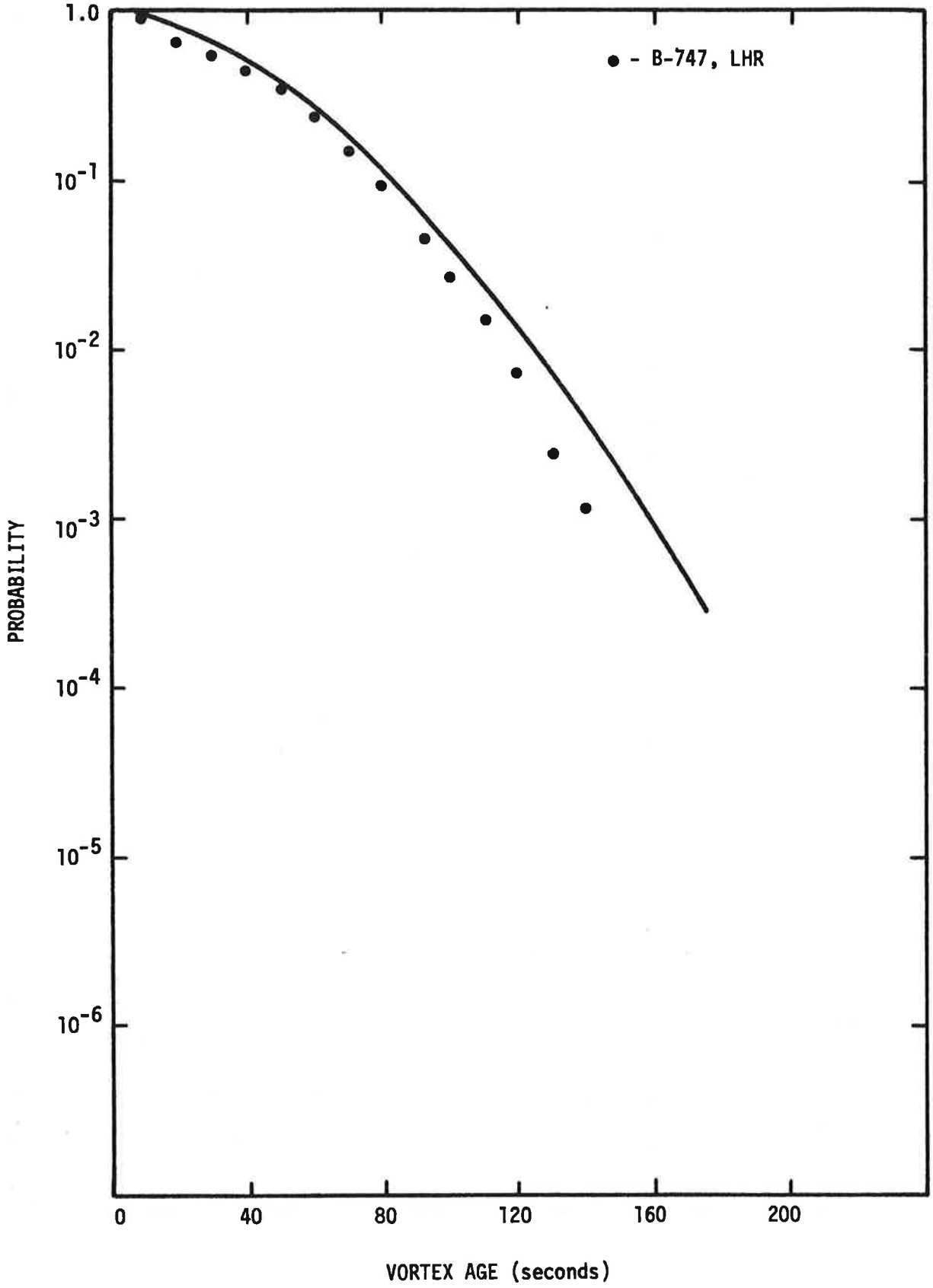

FIGURE 36. COMPARISON OF O'HARE WITH HEATHROW RESIDENCE TIME DATA, B-747

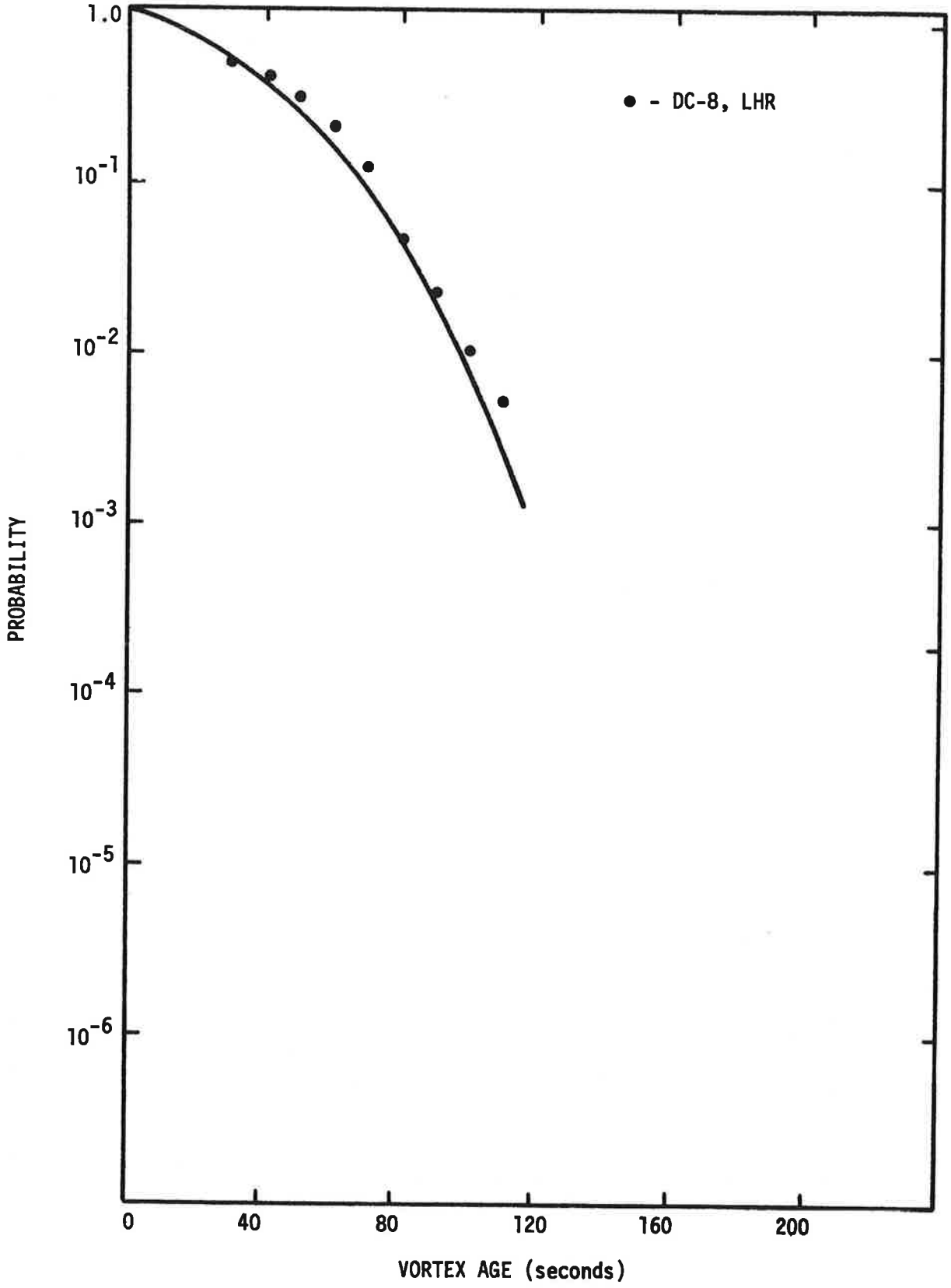

FIGURE 37. COMPARISON OF O'HARE WITH HEATHROW RESIDENCE TIME DATA, DC-8

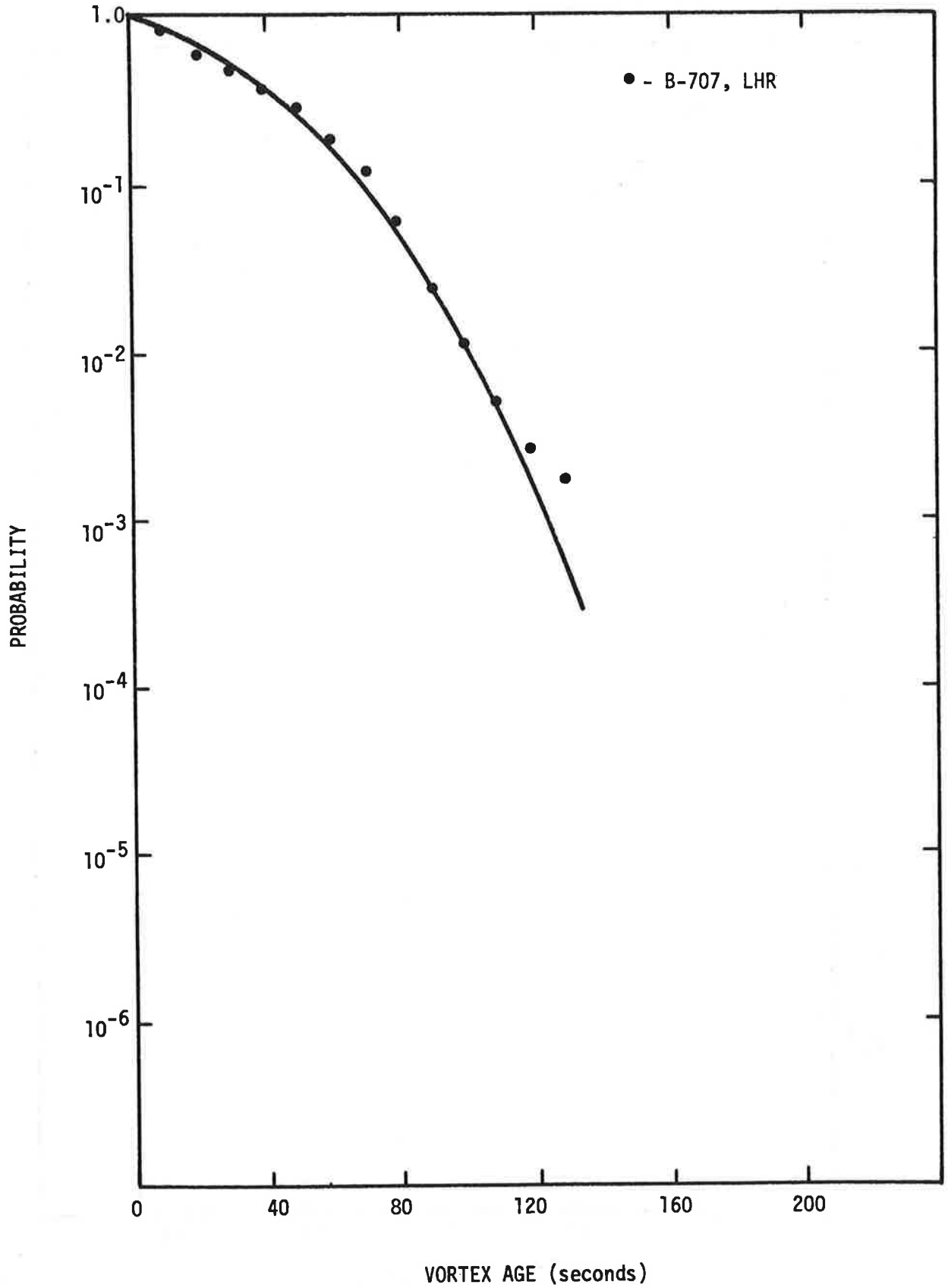

FIGURE 38. COMPARISON OF O'HARE WITH HEATHROW RESIDENCE TIME DATA, B-707

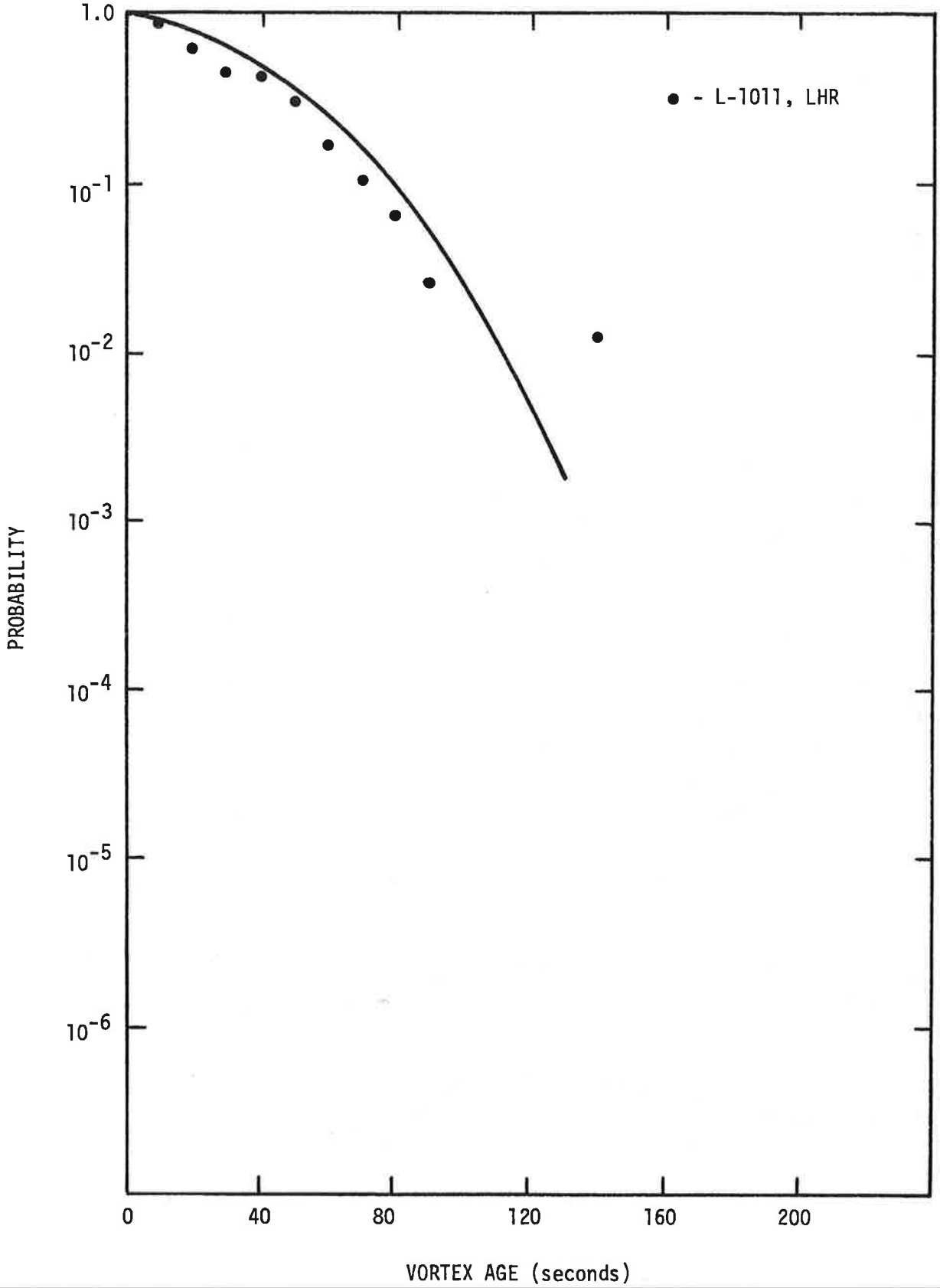

FIGURE 39. COMPARISON OF O'HARE WITH HEATHROW RESIDENCE TIME DATA, L-1011

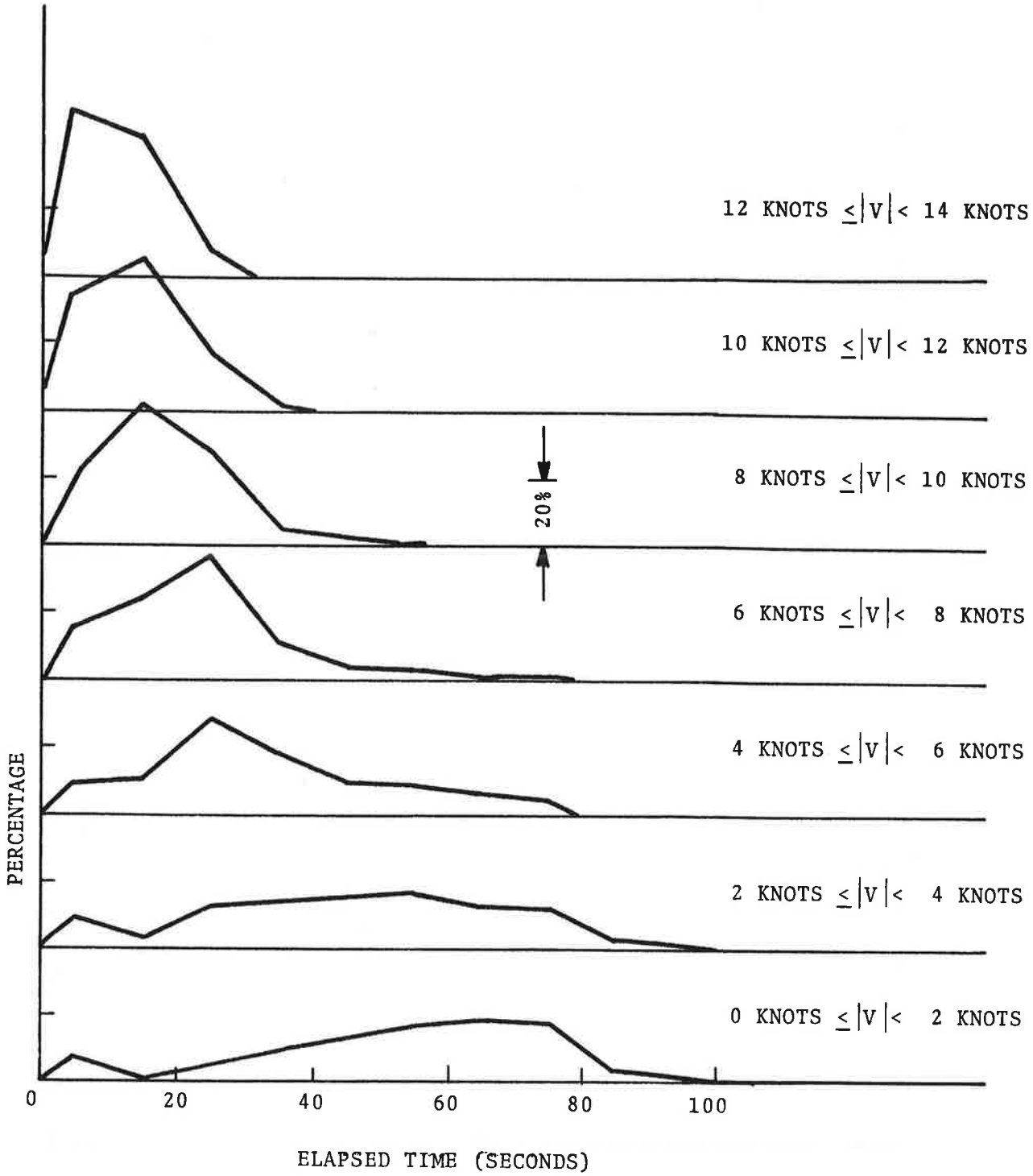

FIGURE 40. PERCENTAGE OF VORTICES THAT REMAINED IN SAFETY CORRIDOR AS FUNCTION OF CROSSWIND

mean of the curve tends toward zero as the crosswind is increased. It is significant to note the absence of cases with long residence times for the higher crosswinds. Thus a condition for short residence times is a relatively high crosswind. The data are further segregated to show the difference in these characteristics as a function of the aircraft type. The data for the B-747 and B-727 are plotted in Figures 41 and 42, respectively. A similar trend is noted in each of these plots with the mean vortex residence time for the B-747 being higher as would be expected.

The vortex residence times have similar trends when displayed as a function of headwind component and total wind. The data are parameterized as a function of the total wind, R, in Figure 43. A similar trend with the mean residence time decreasing as the total wind is increased is also observed; however, it is important to note that even when the total wind gets very large a number of longer residence times were recorded. Thus, total wind alone is not a promising parameter for correlating with short residence times.

The data are parameterized as a function of the headwind component, H, in Figure 44. In general, the distributions are much flatter with no outstanding trends. There may even be a reverse effect where the shorter mean residence times occur for the lower headwinds. This effect can be attributed to the correlation of higher crosswinds with lower headwinds which can be seen in Figures 45 and 46. Under conditions of high headwinds at O'Hare, the crosswinds were relatively small. This is consistent with airport operations where the stronger the wind, the greater the effort to operate with the runway which aligns most directly with the wind. Since it was shown that a higher crosswind will transport the vortex out of the safety zone more quickly, it is consistent that the apparent reverse trend be observed in the headwind residence data.

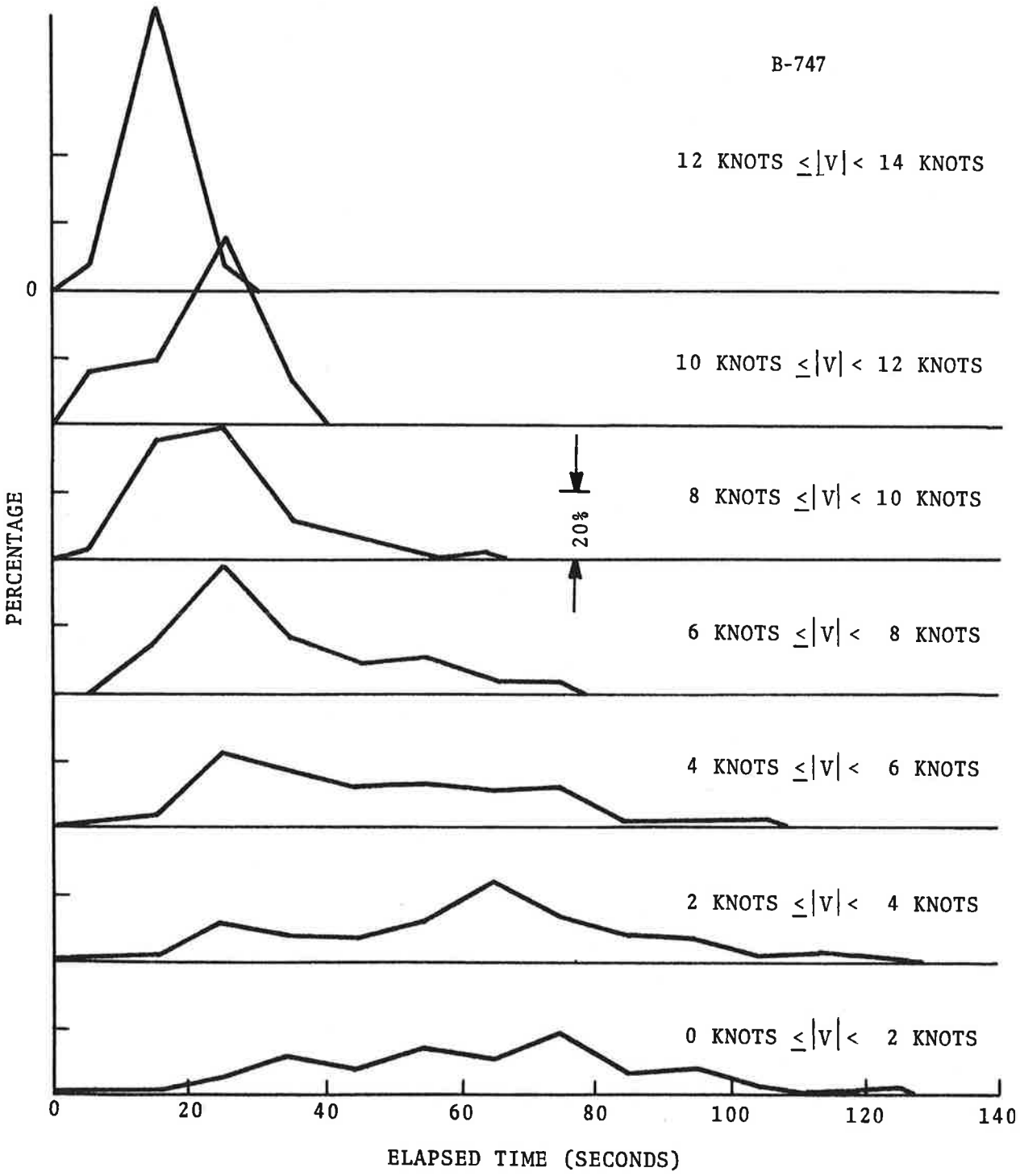

FIGURE 41. PERCENTAGE OF B-747 VORTICES THAT REMAINED IN SAFETY CORRIDOR AS A FUNCTION OF CROSSWIND

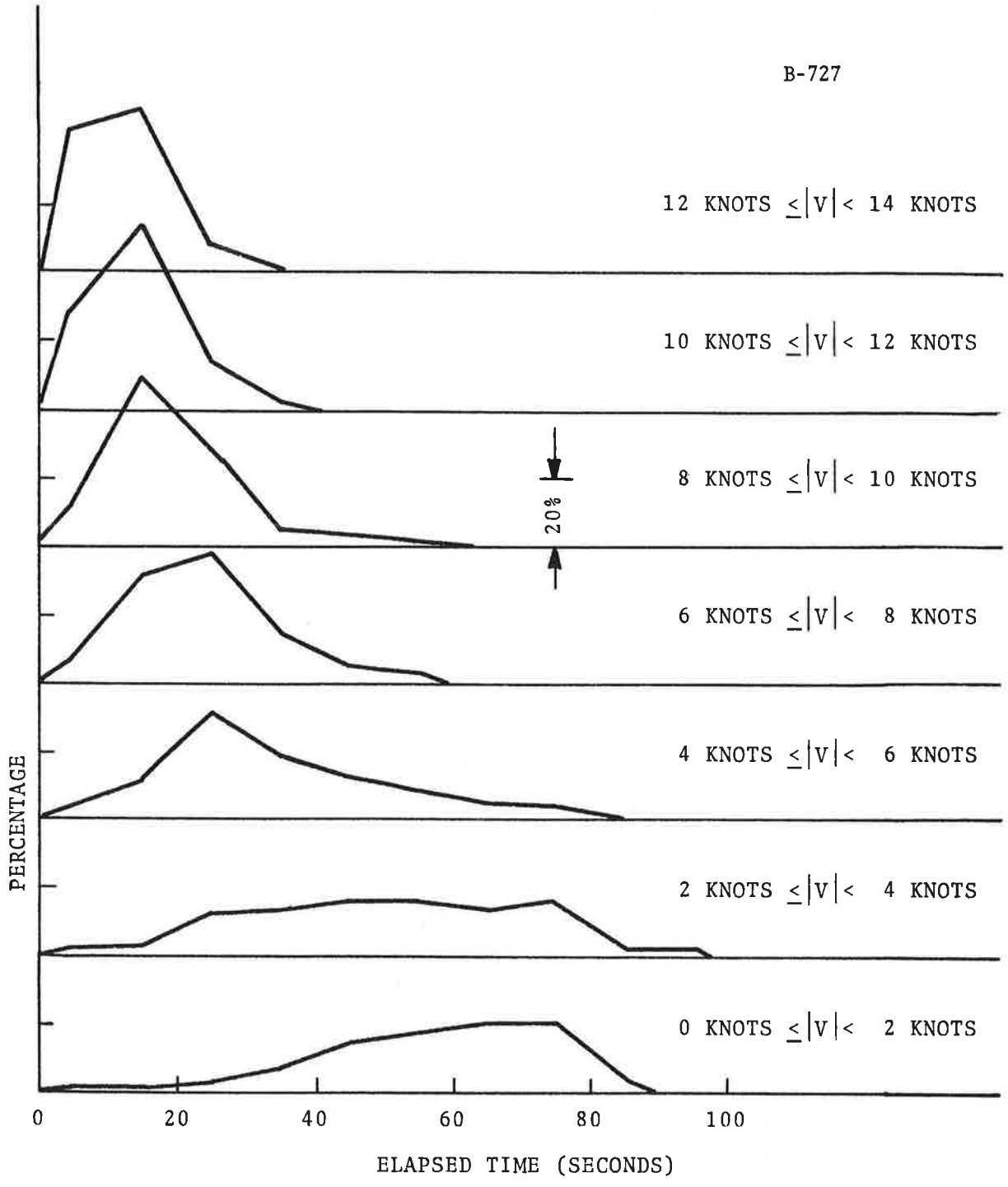

FIGURE 42. PERCENTAGE OF B-727 VORTICES THAT REMAINED IN SAFETY CORRIDOR AS A FUNCTION OF CROSSWIND

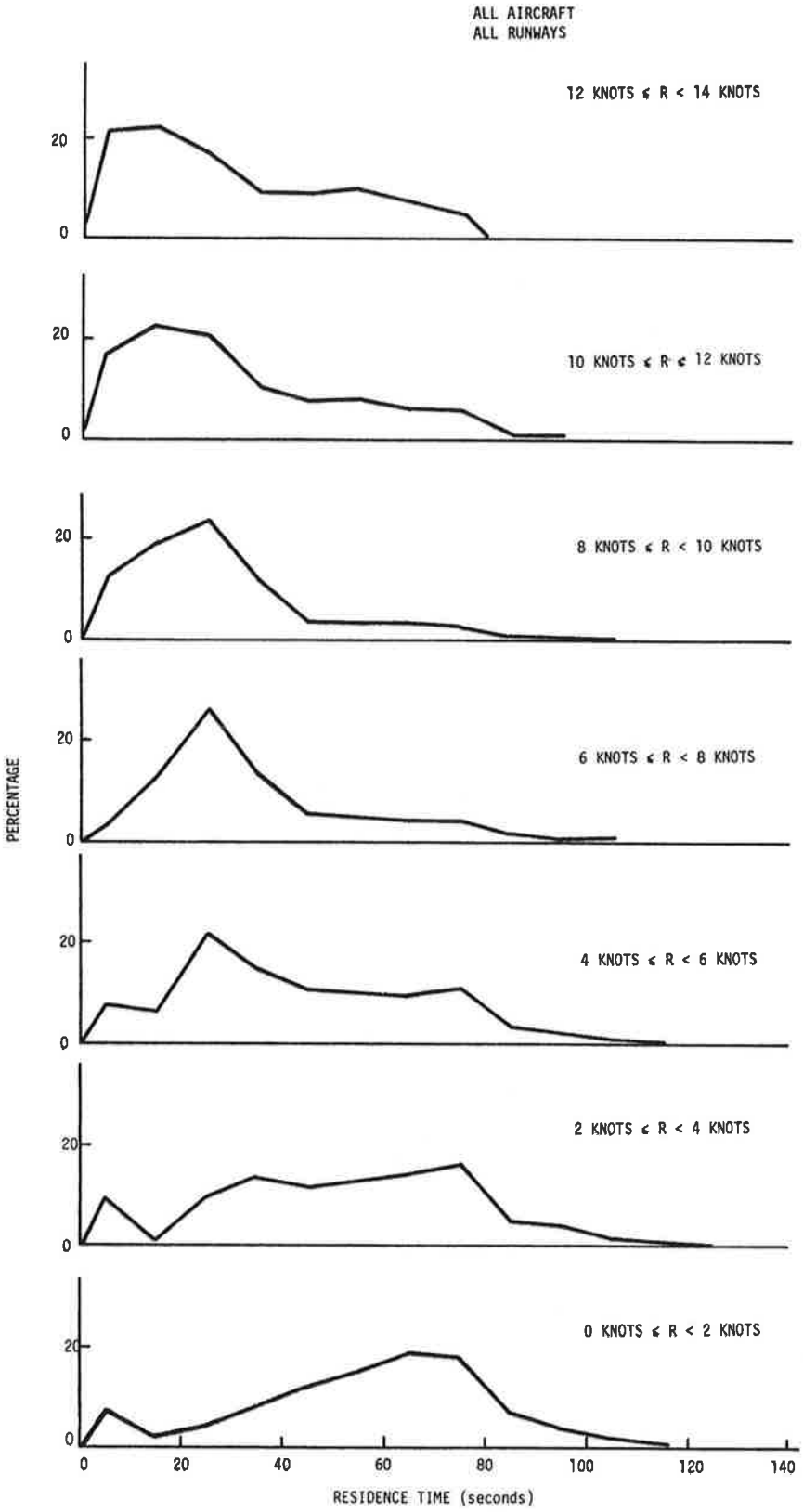

FIGURE 43. PERCENTAGE OF VORTICES THAT REMAINED IN SAFETY CORRIDOR AS A FUNCTION OF TOTAL WIND

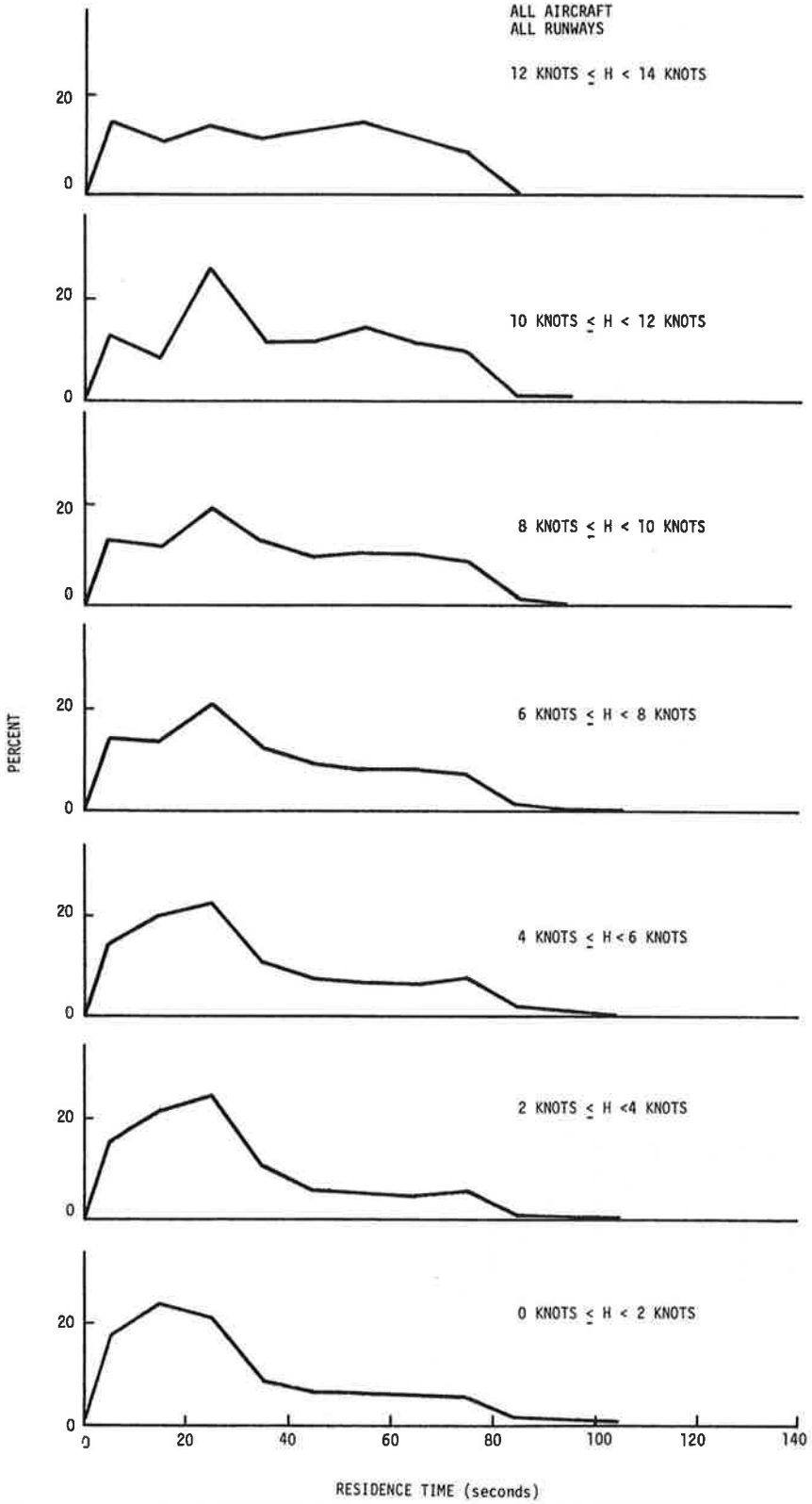

FIGURE 44. PERCENTAGE OF VORTICES THAT REMAINED IN SAFETY CORRIDOR AS A FUNCTION OF HEADWIND COMPONENT

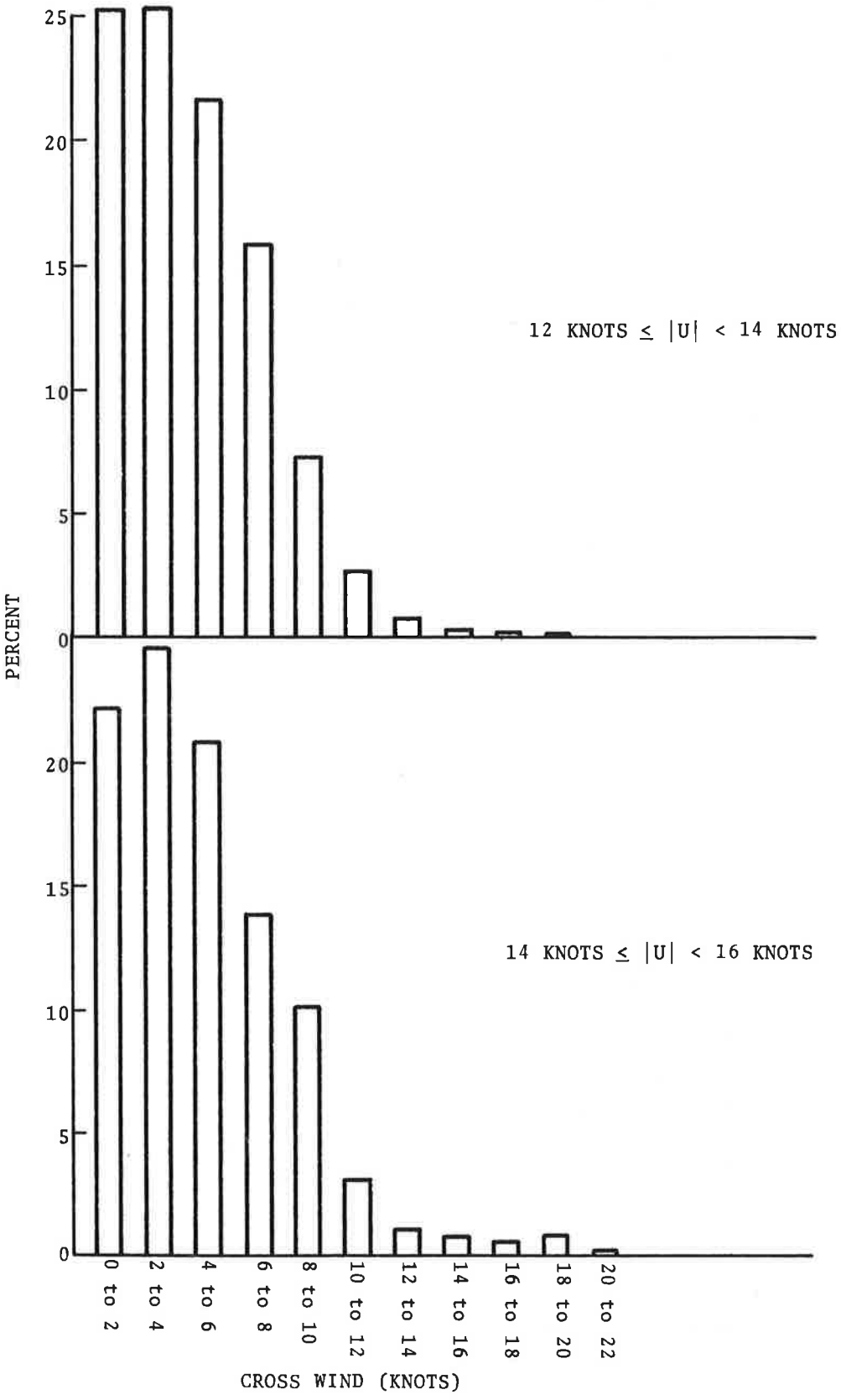

FIGURE 45. DISTRIBUTIONS OF CROSSWIND MAGNITUDE FOR HEAD WIND COMPONENTS BETWEEN 12 and 16 KNOTS

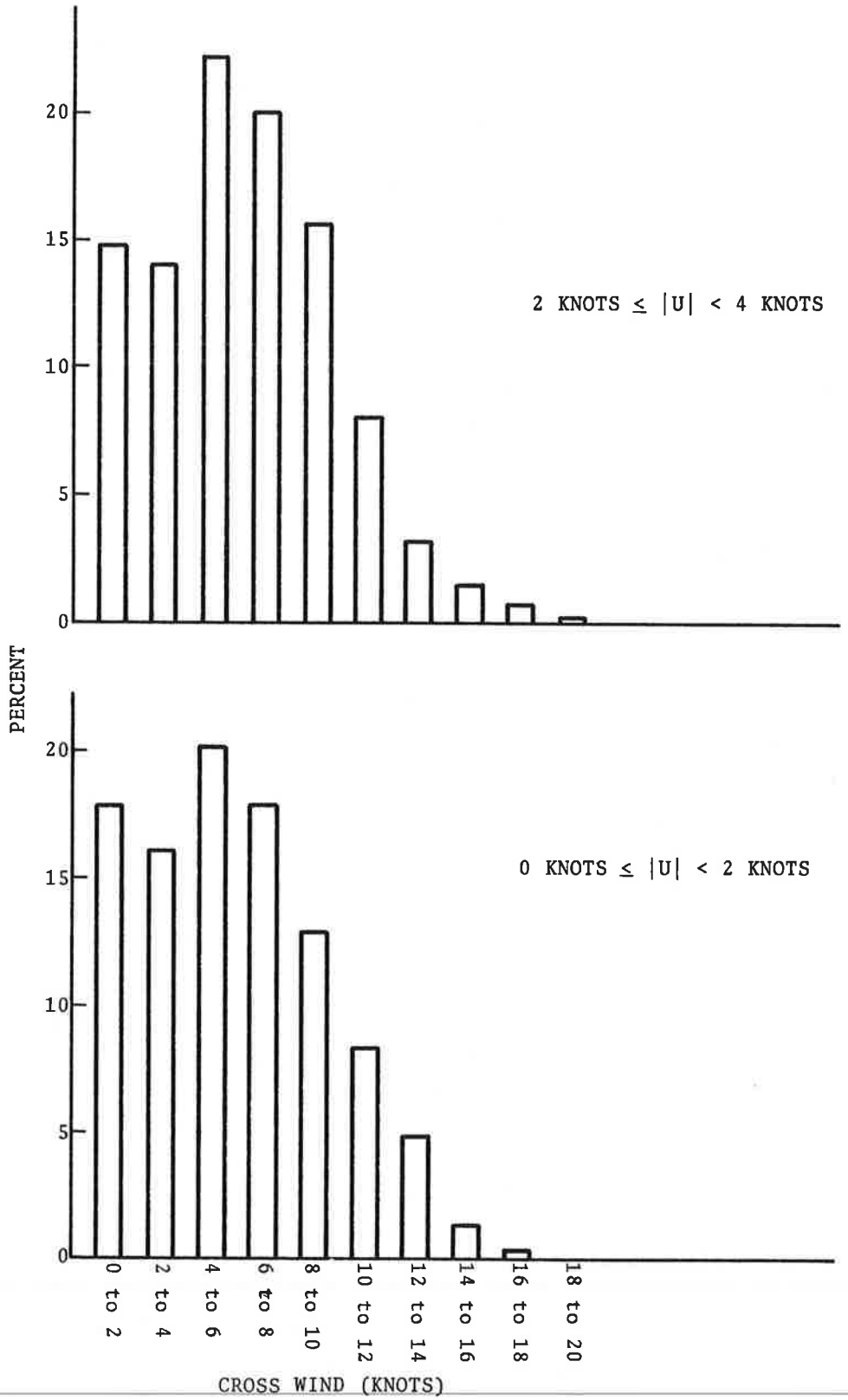

FIGURE 46. DISTRIBUTION OF CROSSWIND MAGNITUDE FOR HEAD WIND COMPONENTS BETWEEN 0 AND 4 KNOTS

7.4 VORTEX LIFETIME

McGowan (Ref. 15) devised a curve which bounded the maximum observed lifetime of a vortex as a function of the total wind. He obtained the relationship by fairing a curve to all the known (in 1970) vortex lifetime data in such a manner that all the data were included under the curve. McGowan's curve has been widely used in the literature. Most of the data that McGowan had available came from tower tests where smoke from canisters on a tower became imbedded in the vortex, and the decay was assessed visually. By necessity this type of data involved mainly a cross-wind component since a cross wind was required to translate the vortex to and past the tower. The Heathrow data added data which included winds along the direction of the vortex and revised the McGowan curve as shown in Fig. 47.

The data from the O'Hare test site provided records of vortices which exceeded the boundaries of these curves. These cases are plotted in Figure 48 and a curve is drawn to enclose them. It should be noted, however, that vortex lifetime in this figure has various definitions. McGowan defined lifetime as meaning when smoke no longer was entrained in a vortex. The Heathrow and O'Hare data define lifetime as the time at which the vortex signal detected by the GWVSS blends with the ambient wind signal. Neither of these definitions have been related to what constitutes a hazard to a vortex-encountering aircraft. The GWVSS certainly overestimates the hazard lifetime; the presence or absence of smoke in a vortex has been found to be a poor indicator of hazard lifetime (Ref. 16).

7.5 PREDICTIVE CAPABILITY AND SYSTEMS

One of the primary reasons for performing the tests at O'Hare was to provide additional data for the development of the predictive wind algorithm of the Vortex Advisory System (VAS). In the Heathrow tests (Refs. 4 and 5) an elliptical wind criterion was developed which encompassed the wind conditions where the vortices of Heavy aircraft were observed to remain in the safety corridor

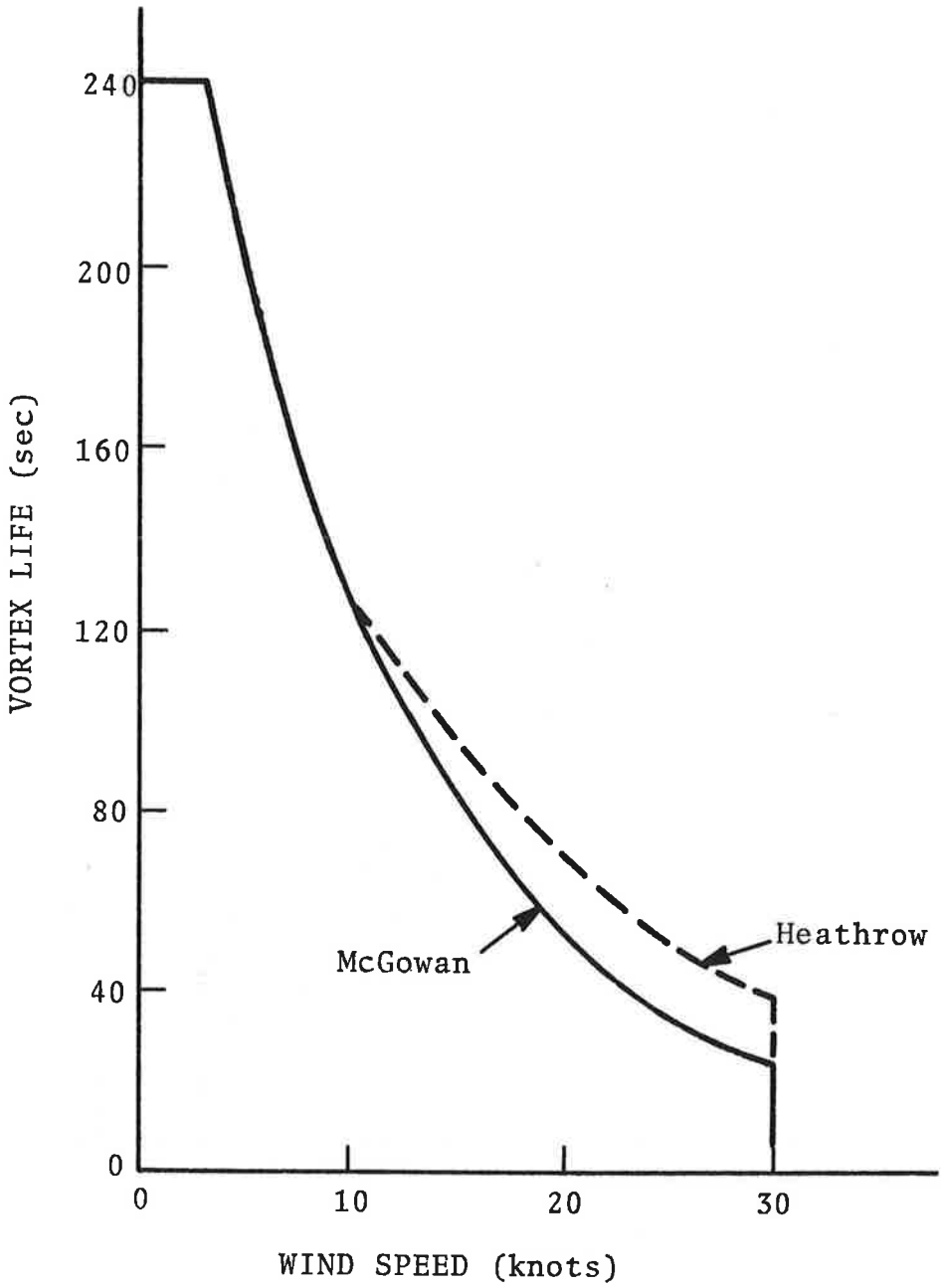

FIGURE 47. MCGOWAN CURVE OF MAXIMUM OBSERVED VORTEX LIFETIMES AS FUNCTION OF WIND SPEED

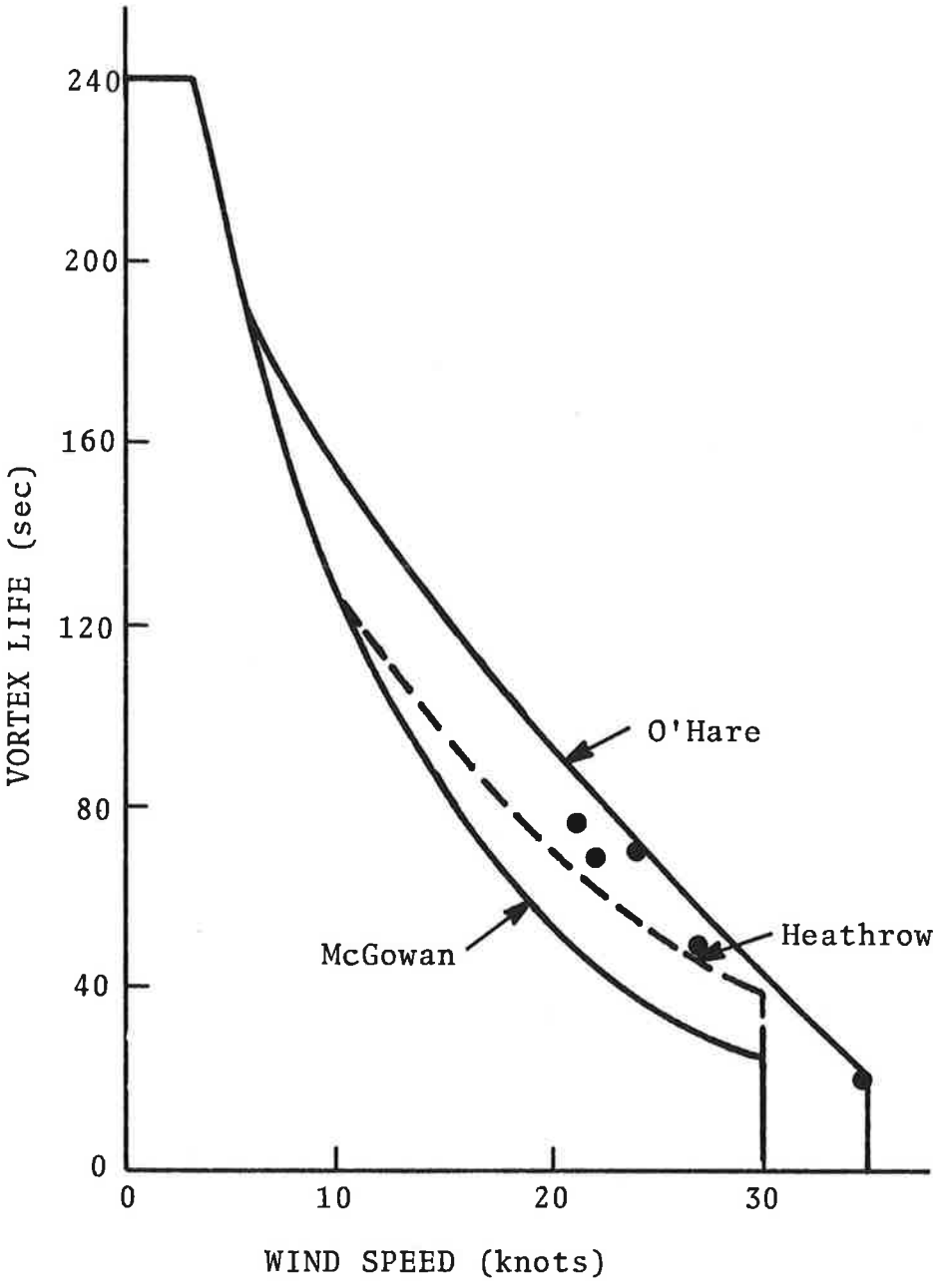

FIGURE 48. MCGOWAN CURVE OF MAXIMUM OBSERVED VORTEX LIFETIMES AS FUNCTION OF WIND SPEED REVISED TO INCLUDE O'HARE DATA

for at least 80 seconds. For normal aircraft approach speeds, 80 seconds represents a three-nautical-mile inter-aircraft spacing. The VAS is based on the idea that, for wind conditions which fall outside this elliptical criterion the vortices from Heavy aircraft would not be found in the safety zone at times longer than 80 seconds and hence it would be safe to allow a reduction in inter-arrival spacing to a uniform three nautical miles for all classes of aircraft. The elliptical wind criterion developed in the Heathrow report (Refs. 4 and 5) had a semi-major axis of 12 knots and a semi-minor axis of 5.5 knots. This ellipse also included the long-lived cases from previous tests at both Stapleton International Airport, Denver, Colorado, and John F. Kennedy International Airport, New York (Refs. 1-3).

An elliptical wind criterion was also generated from the data collected from the O'Hare test site. The winds which led to residence times of at least 80 seconds for vortices from Heavy aircraft are plotted in Figure 49. An ellipse is drawn to enclose these points and has a semi-major axis of 12.5 knots and a semi-minor axis of 5.5 knots. This ellipse, slightly larger than the Heathrow ellipse in the headwind direction, is used as the wind criterion in the Vortex Advisory System. The data of Figure 49 were segregated to show the cases whose residence times fell into 10-second intervals between 80 and 120 seconds and residence times greater than 120 seconds and are plotted in Figures 50 through 54. There appears to be no significant trend in the distribution of data points as the residence times vary.

The cases whose residence times were between 70 and 80 seconds are plotted in Figure 55. In the Heathrow report this subset of data indicated a possible pattern which led to the hypothesis that the interarrival aircraft spacing might be further reduced to almost two nautical miles if a pure crosswind criterion were used in place of the ellipse. The data from the O'Hare tests do not show this simple trend.

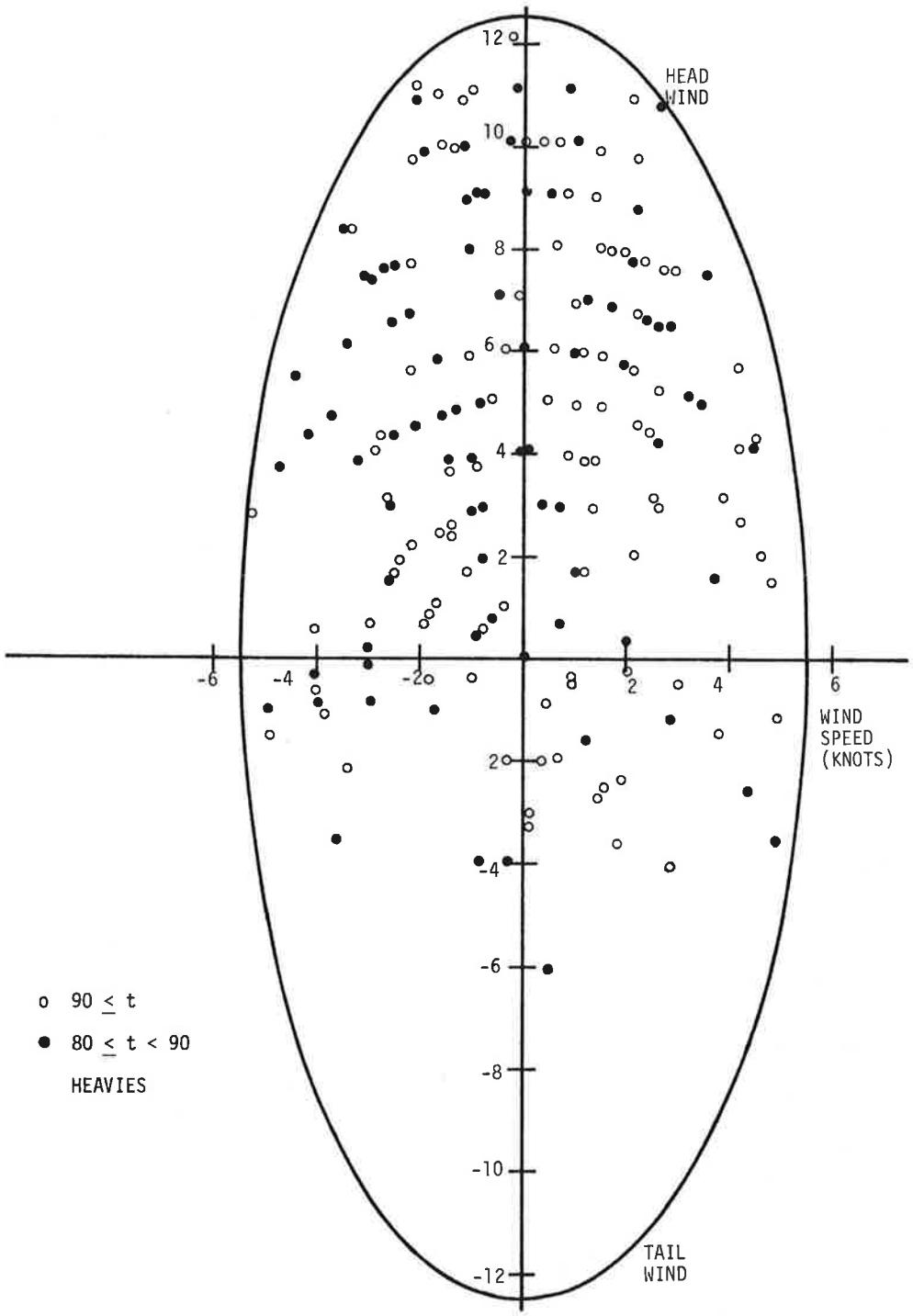

FIGURE 49. WIND CONDITIONS (IN KNOTS) WHICH LED TO RESIDENCE TIMES IN EXCESS OF 80 SECONDS FOR HEAVY CATEGORY AIRCRAFT

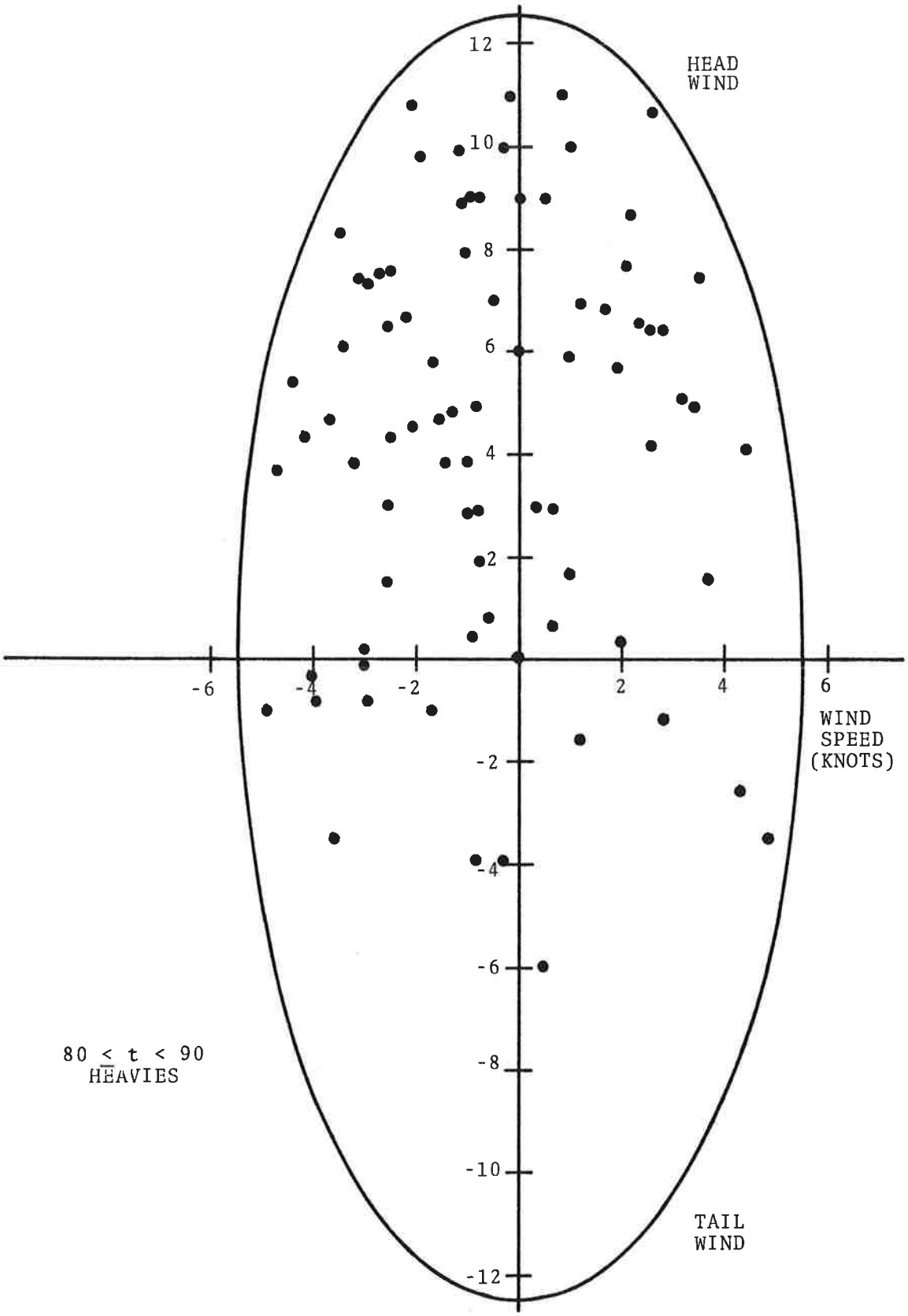

FIGURE 50. WIND CONDITIONS (IN KNOTS) WHICH LED TO RESIDENCE TIMES BETWEEN 80 AND 89 SECONDS

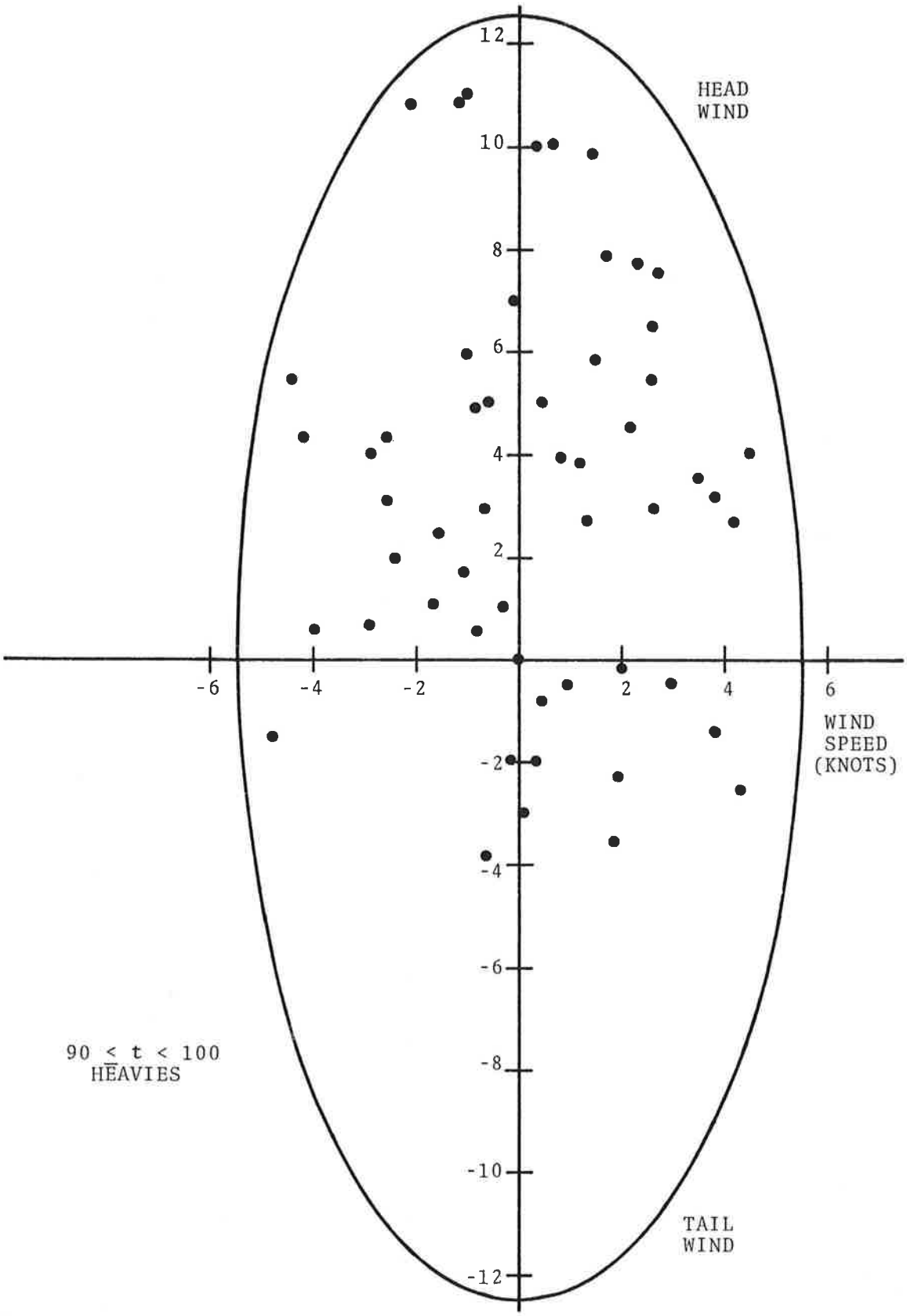

FIGURE 51. WIND CONDITIONS (IN KNOTS) WHICH LED TO RESIDENCE TIMES BETWEEN 90 AND 99 SECONDS

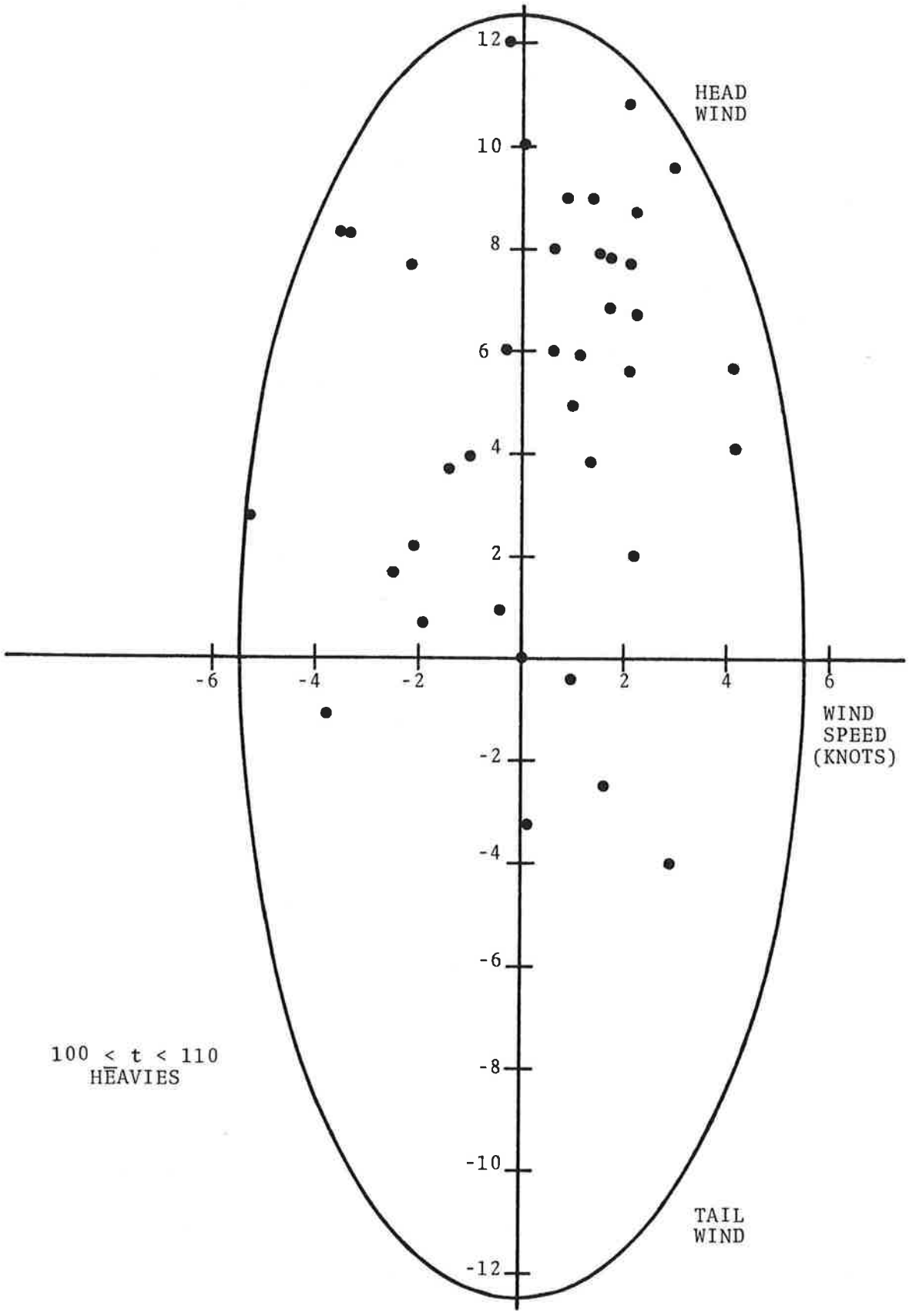

FIGURE 52. WIND CONDITIONS (IN KNOTS) WHICH LED TO RESIDENCE TIMES BETWEEN 100 AND 109 SECONDS

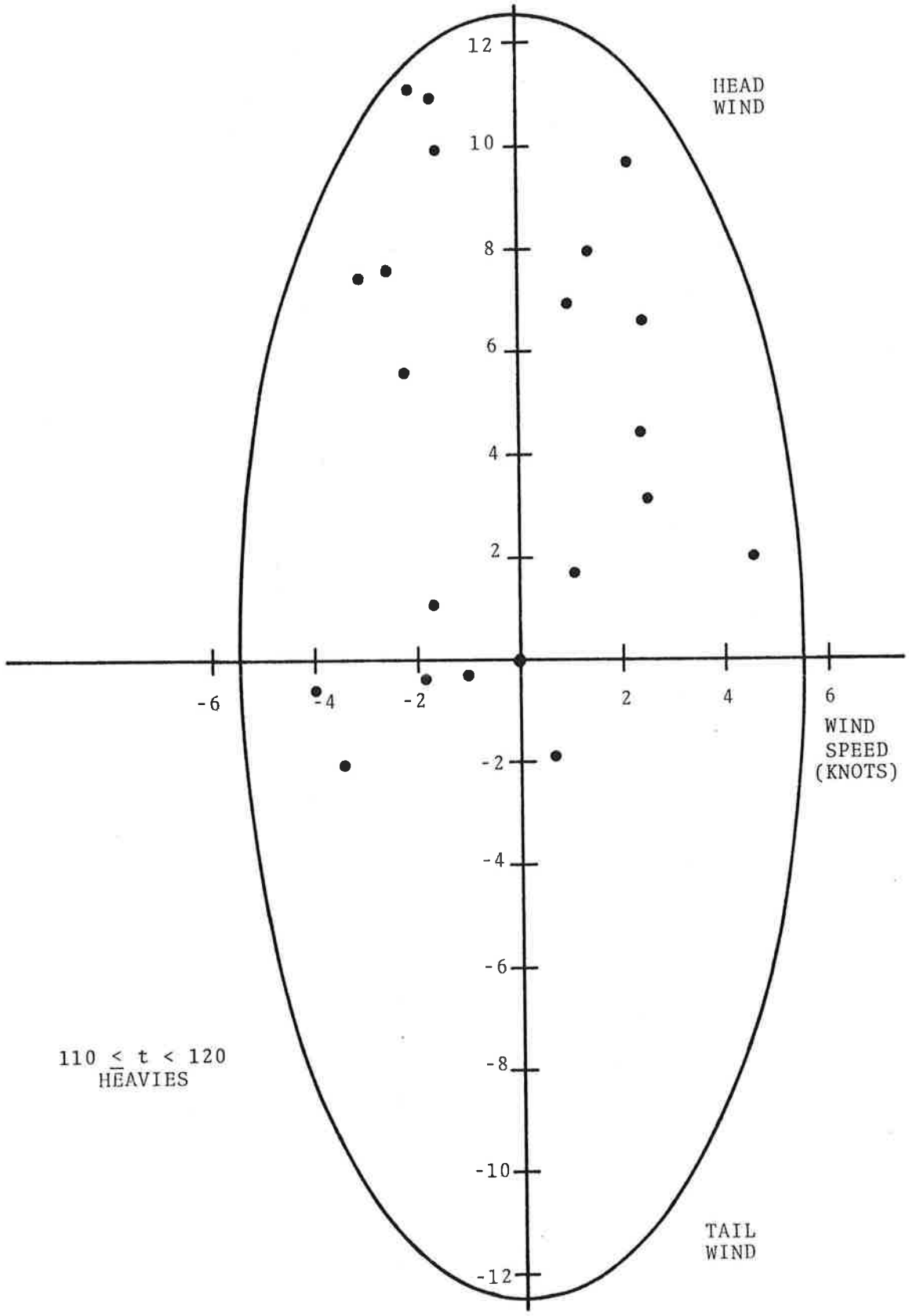

FIGURE 53. WIND CONDITIONS (IN KNOTS) WHICH LED TO RESIDENCE TIMES BETWEEN 110 AND 119 SECONDS

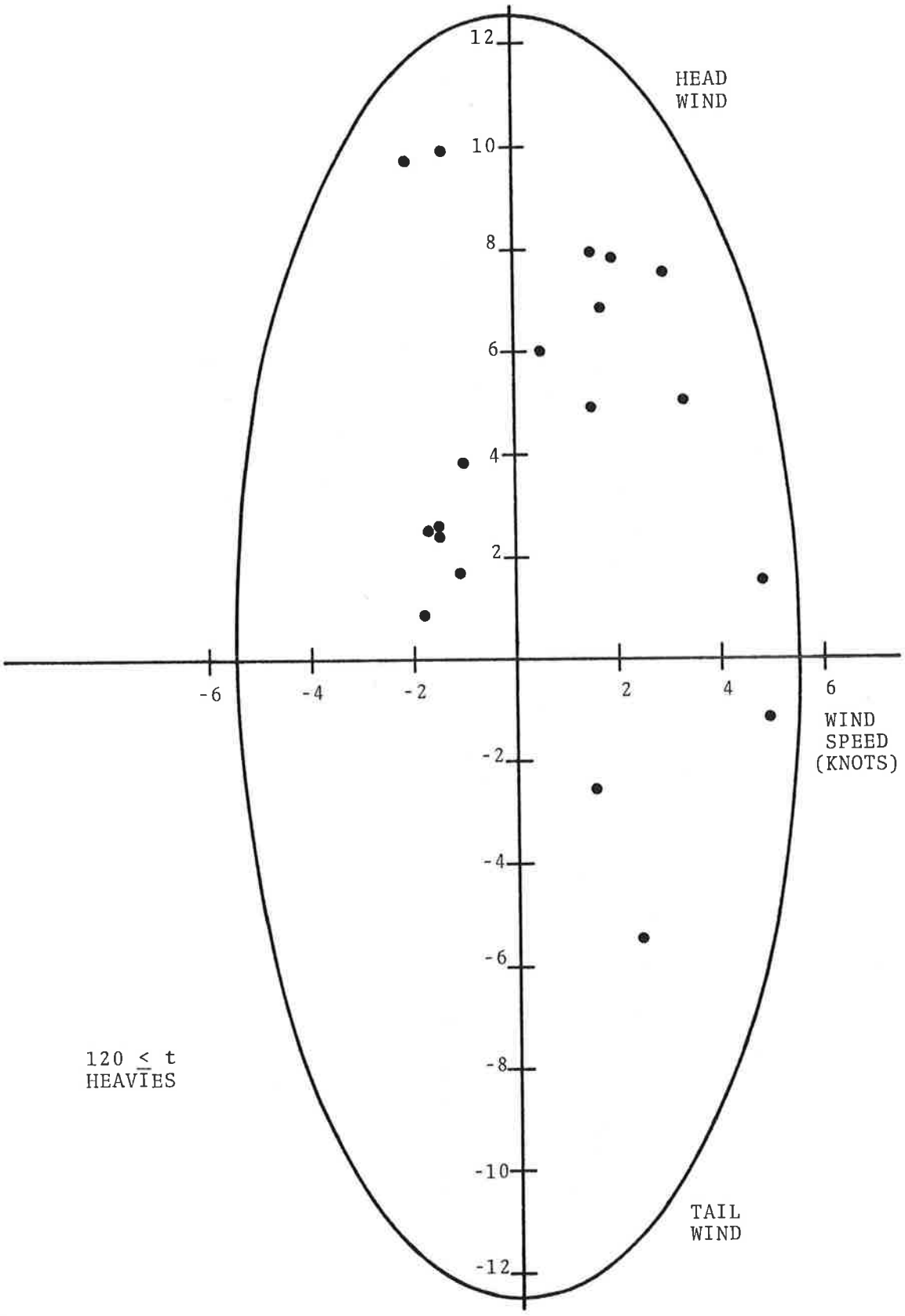

FIGURE 54. WIND CONDITIONS (IN KNOTS) WHICH LED TO RESIDENCE TIMES OF 120 SECONDS OR GREATER

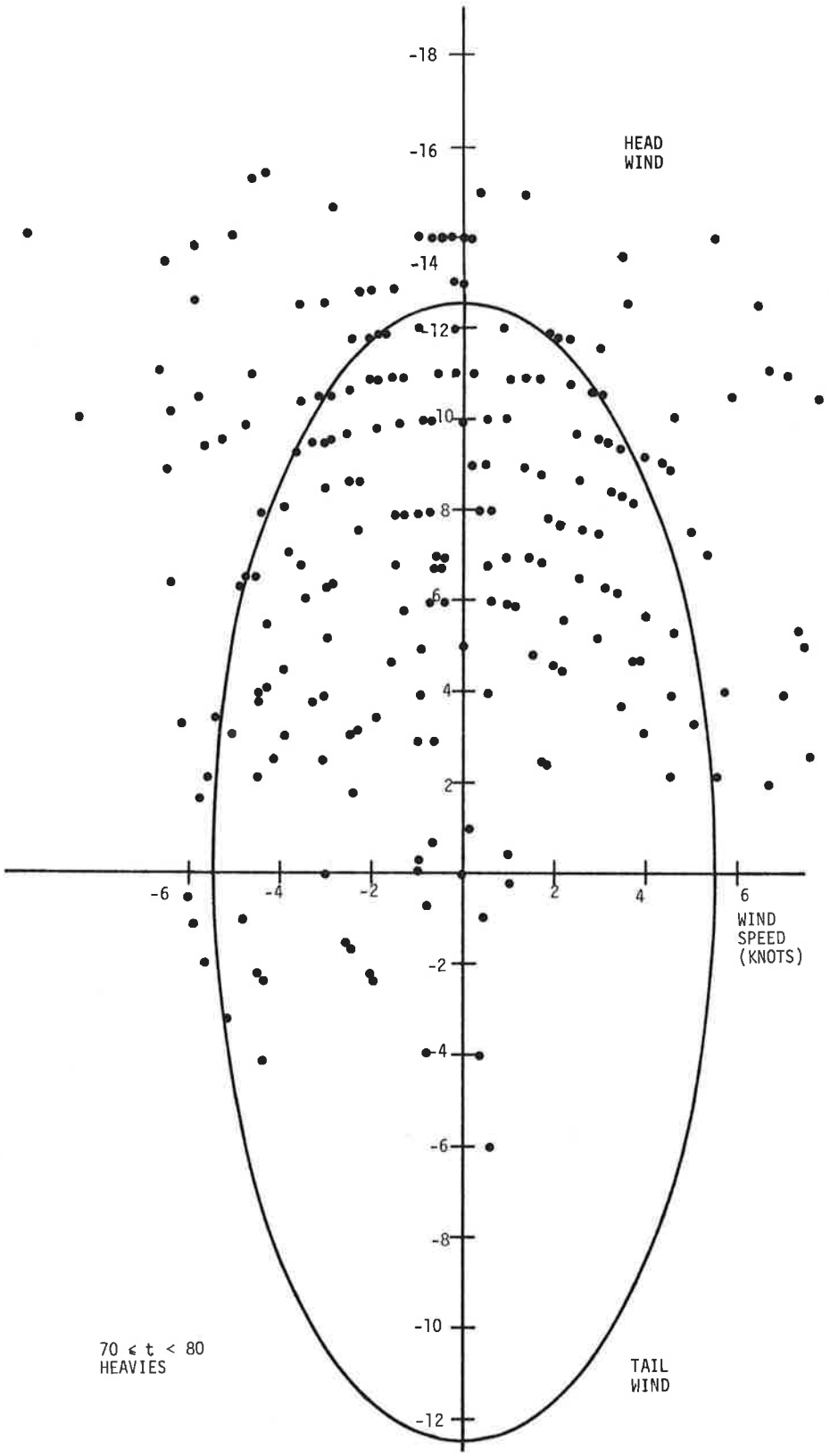

FIGURE 55. WIND CONDITIONS (IN KNOTS) WHICH LED TO RESIDENCE TIMES BETWEEN 70 AND 79 SECONDS

8. SUMMARY

Between July 1976 and September 1977, vortex tracks from over 21,000 landing aircraft were recorded at O'Hare. Vortex behavior was recorded using three sensor systems; the propeller anemometer Ground-Wind Vortex Sensing System (GWVSS) data are discussed herein. Data collected using the Monostatic Acoustic Vortex Sensing System (MAVSS) are discussed in Reference 11, and data collected using the Laser Doppler Velocimeter (LDV) are discussed in Reference 17.

The keystone of the VAS concept is the elliptical wind criterion. The O'Hare data collection furthered the Heathrow effort and established the ellipse now used in the VAS. The validity of the ellipse is based on finding no violations of the criterion among the 35,000 vortex tracks collected at Stapleton, Kennedy, and Heathrow; the 21,000 cases examined herein; nor the 14,000 cases collected at O'Hare for the system tests.

9. REFERENCES

1. Hallock, J.N. and Eberle, W.R. (editors), "Aircraft Wake Vortices: A State-of-the-Art Review of the United States R&D Program," FAA-RD-77-23, Feb. 1977, Transportation Systems Center, Cambridge, MA.

2. Hallock, J.N., "Monitoring the Movement of Wake Vortices at Kennedy and Stapleton Airports," Proceedings of the 5th Annual Symposium of the Society of Flight Test Engineers, SFTE, Anaheim, CA, 1974, p. 4/7-4/12.

3. Hallock, J.N., Wood, W.D., and Spitzer, E.A., "The Motion of Wake Vortices in the Terminal Environment," Proceedings of the 6th Conf. on Aerospace and Aeronautical Meteorology, Amer. Met. Soc., El Paso, TX, 1974, p. 393-398.

4. Hallock, J.N. and Wood, W.D., "Joint US/UK Vortex Tracking Program at Heathrow International Airport, Vol. I: Executive Summary," FAA-RD-76-58.I, Mar. 1976, Transportation Systems Center, Cambridge, MA.

5. Hallock, J.N., Winston, B.P., Sullivan, T.E., Burnham, D.C., McWilliams, I.G., and Wood, W.D., "Joint US/UK Vortex Tracking Program at Heathrow International Airport; Vol. II, Data Analysis," FAA-RD-76-58.II, Sep. 1977, Transportation Systems Center, Cambridge, MA.

6. Spitzer, E.A., "Operational System Guidelines for the Vortex Advisory System," FAA-RD-79-20, Apr. 1979, Transportation Systems Center, Cambridge, MA.

7. Hallock, J.N., Wood, W.D., and Spitzer, E.A., "Vortex Advisory System," Proceedings of the 7th Conf. on Aerospace and Aeronautical Meteorology, Amer. Met. Soc., Melbourne, FL, 1976, p. 162-166.

8. Hallock, J.N., "Vortex Advisory System Safety Analysis; Vol. I: Analytical Model," FAA-RD-78-68.I, Sep. 1978, Transportation Systems Center, Cambridge, MA.

9. Spitzer, E.A., Hallock, J.N., and Wood, W.D., "Status of the Vortex Advisory System," In: Proceedings of the Aircraft Wake Vortex Conf., FAA-RD-77-68, June 1977, p. 326-334.

10. Burnham, D.C., "Chicago Monostatic Acoustic Vortex Sensing System, Vol. I: Data Collection and Reduction," FAA-RD-79-103,I, Oct. 1979, Transportation Systems Center, Cambridge, MA.

11. Burnham, D.C. and Hallock, J.N., "Chicago Monostatic Acoustic Vortex Sensing System, Vol. II: Decay of B-707 and DC-8 Vortices," FAA-RD-79-103,II, to be published.

12. Gupta, V., "Vortex-Related Accidents over the Ten-Year Period 1964-1973," FAA-EM-75-76, Apr. 1975, Mitre Corp., McLean, VA.

13. Clay, L.E., DeLong, R.C., and Rockafellow, R.I., "ILS Flight and Ground Data from Unusual Events Recording System in a Commercial 737 Aircraft," FAA-RD-72-113, Nov. 1972, Technology Inc., Dayton, OH.

14. Harlan, R.B. and Madden, S.J., "A Hazard Definition for Wake Turbulence Encounter During Terminal Area Operations," RE-81, Mar. 1973, MIT, Cambridge, MA.

15. McGowan, W.A., "Aircraft Wake Turbulence Avoidance," Paper 72/6, 12th Anglo-American Aeronautical Conference, July 1971, Calgary, SK, Canada.

16. Burnham, D.C., Hallock, J.N., Tombach, I.H., Brashears, M.R., and Barber, M.R., "Ground-Based Measurements of the Wake Vortex Characteristics of a B-747 Aircraft in Various Configurations," FAA-RD-78-146, Dec. 1978, Transportation Systems Center, Cambridge, MA.

17. Hallock, J.N., "Vortex Advisory System Safety Analysis, Vol. III: Summary of Laser Data Collection and Analysis," FAA-RD-78-68,III, Aug. 1979, Transportation Systems Center, Cambridge, MA.

APPENDIX

RESIDENCE TIME DATA SUMMARY

The residence time data segregated by aircraft type are presented in Figures 56 through 62. The residence time is separated into 10-second intervals where, for example, the 30 entries represent residence times greater than or equal to 20 seconds but less than 30 seconds. The shaded portion of the column represents the portion of the cases where the vortices decayed in the corridor rather than transporting out of the corridor. The numbers above the column represent the number of cases observed for the corresponding time interval. The TOTAL indicates the total number of cases observed.

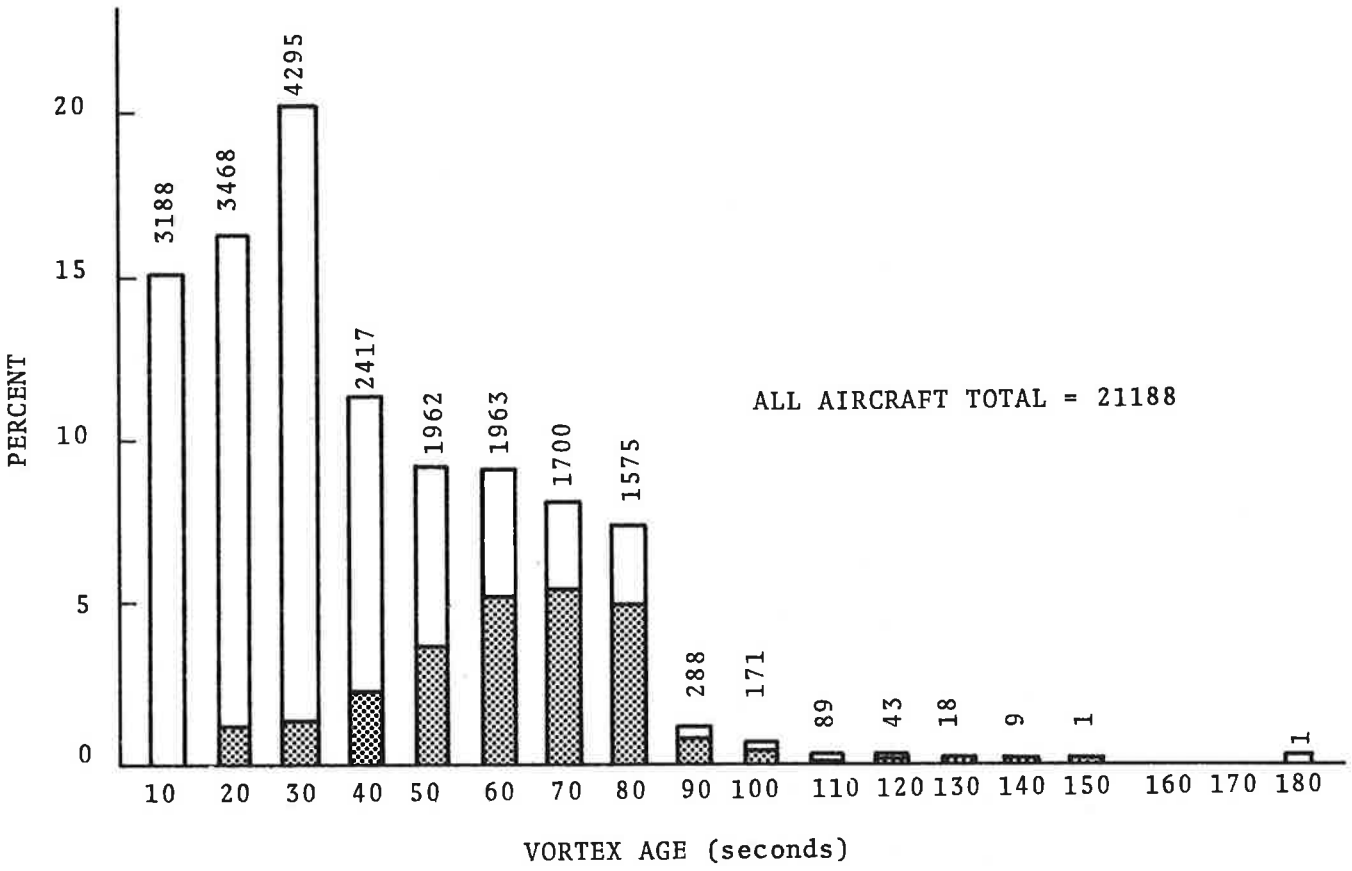

FIGURE 56. RESIDENCE TIME DATA FOR ALL AIRCRAFT

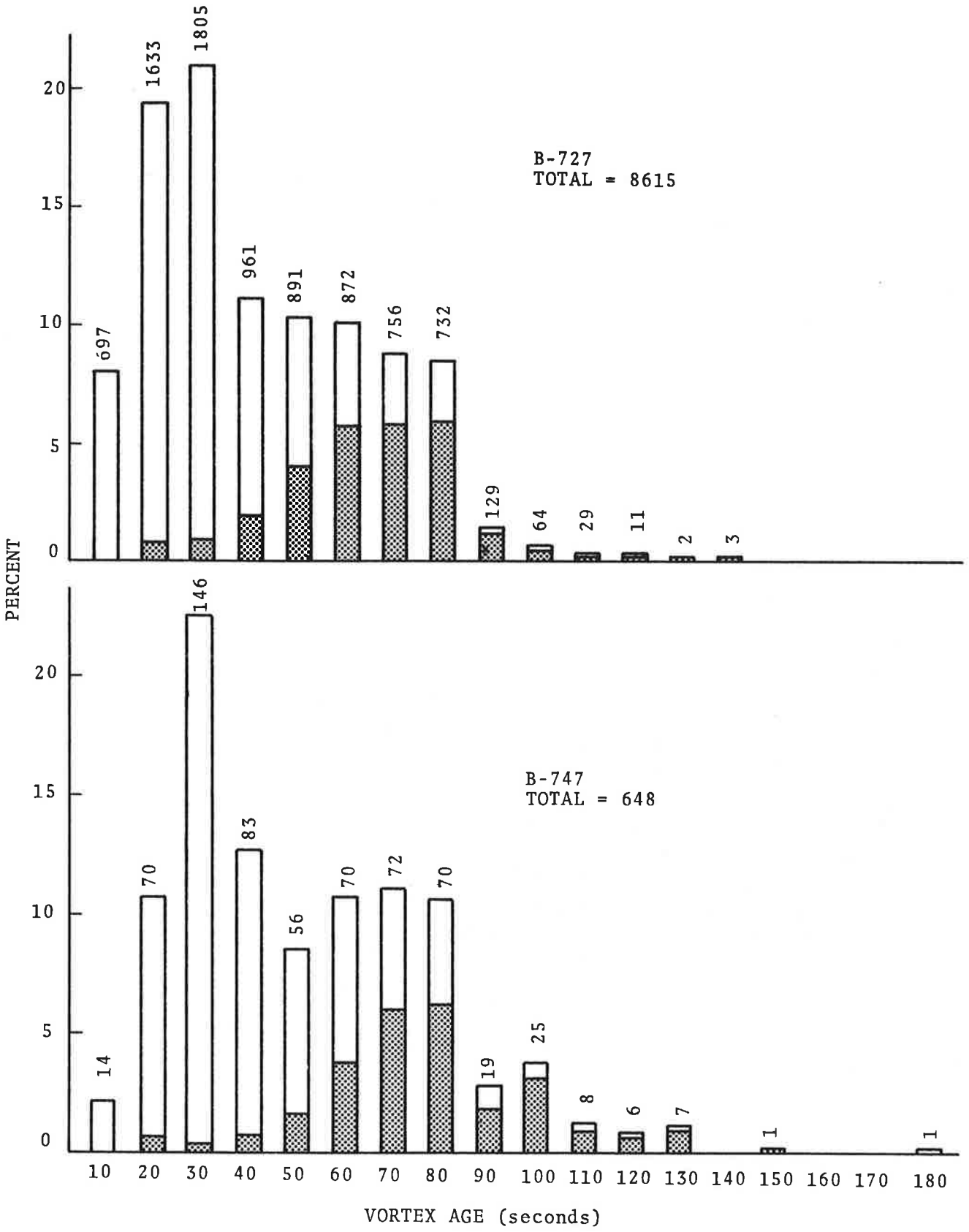

FIGURE 57. RESIDENCE TIME DATA FOR B-727 (TOP) AND B-747 (BOTTOM) AIRCRAFT

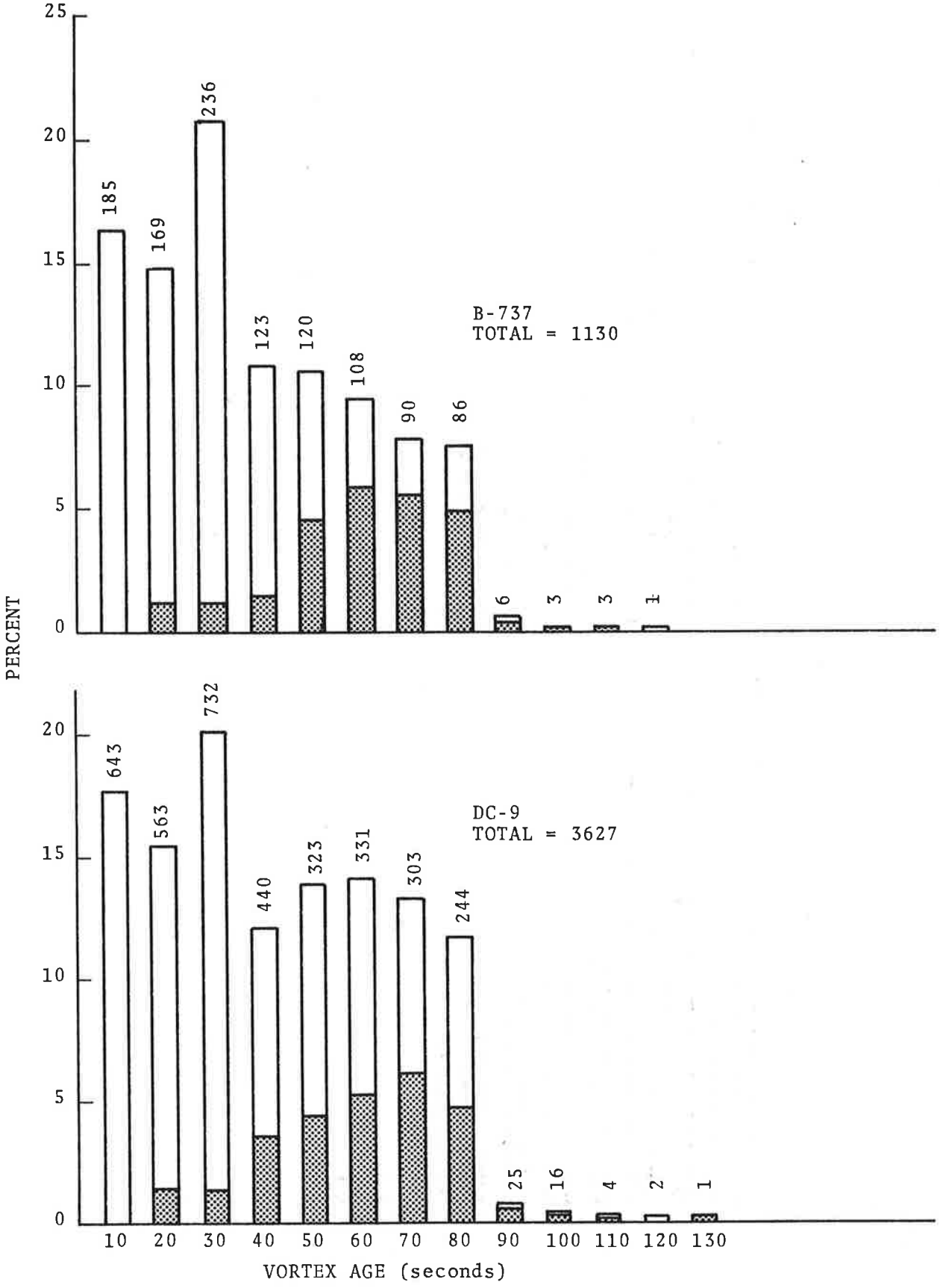

FIGURE 58. RESIDENCE TIME DATA FOR B-737 (TOP) AND DC-9 (BOTTOM) AIRCRAFT

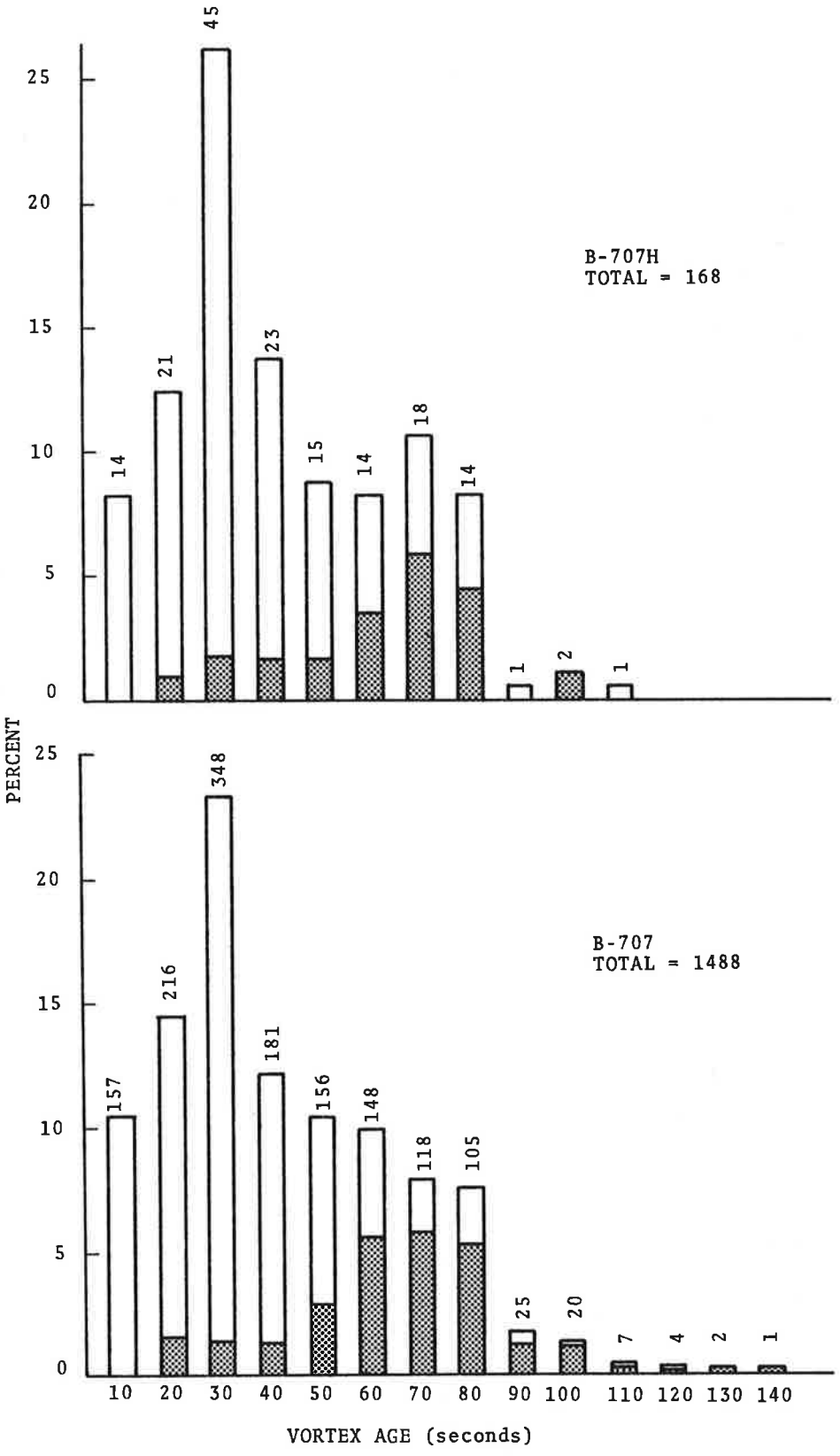

FIGURE 59. RESIDENCE TIME DATA FOR B-707H (TOP) AND B-707 (BOTTOM) AIRCRAFT

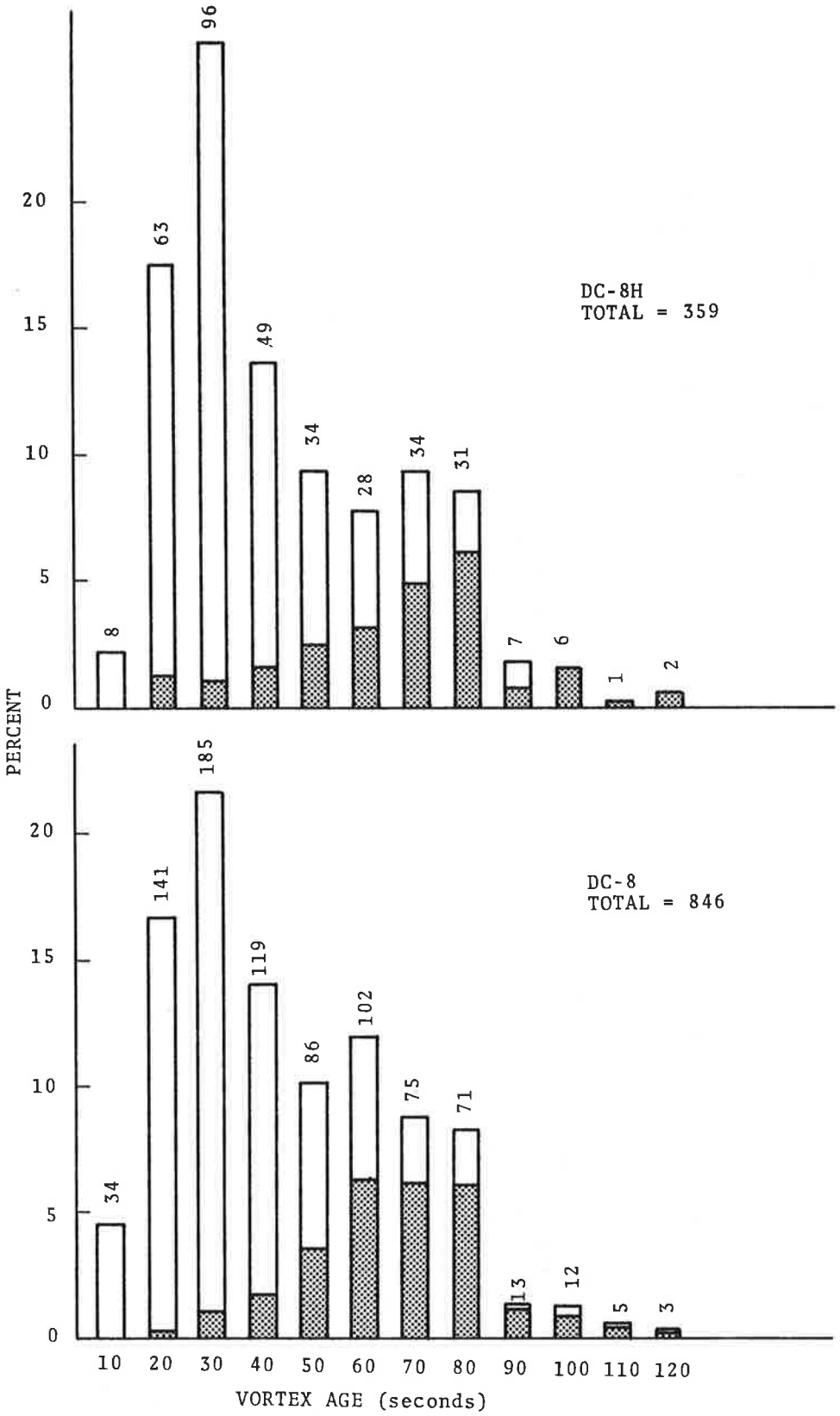

FIGURE 60. RESIDENCE TIME DATA FOR DC-8H (TOP) AND DC-8 (BOTTOM) AIRCRAFT

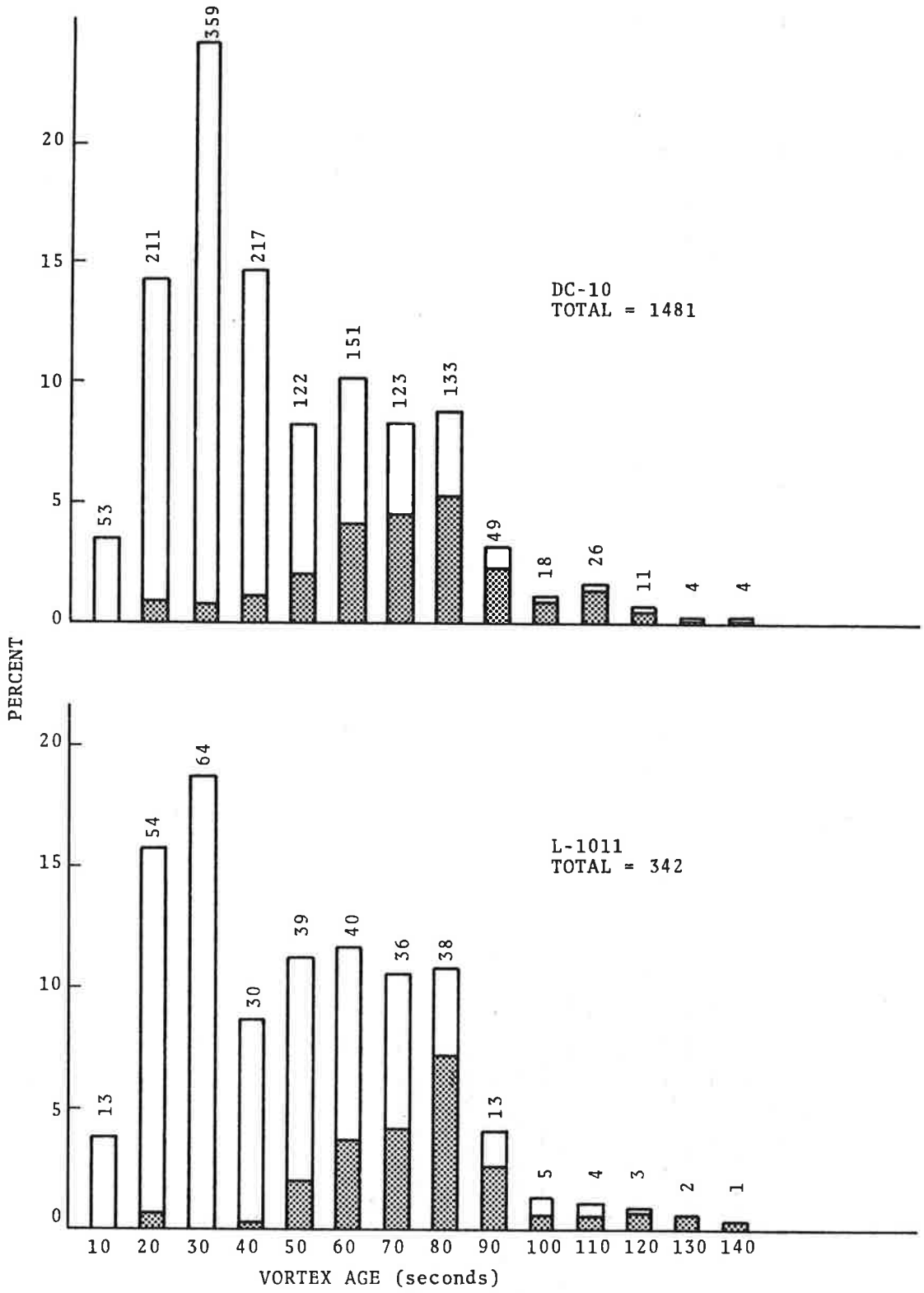

FIGURE 61. RESIDENCE TIME DATA FOR DC-10 (TOP) AND L-1011 (BOTTOM) AIRCRAFT

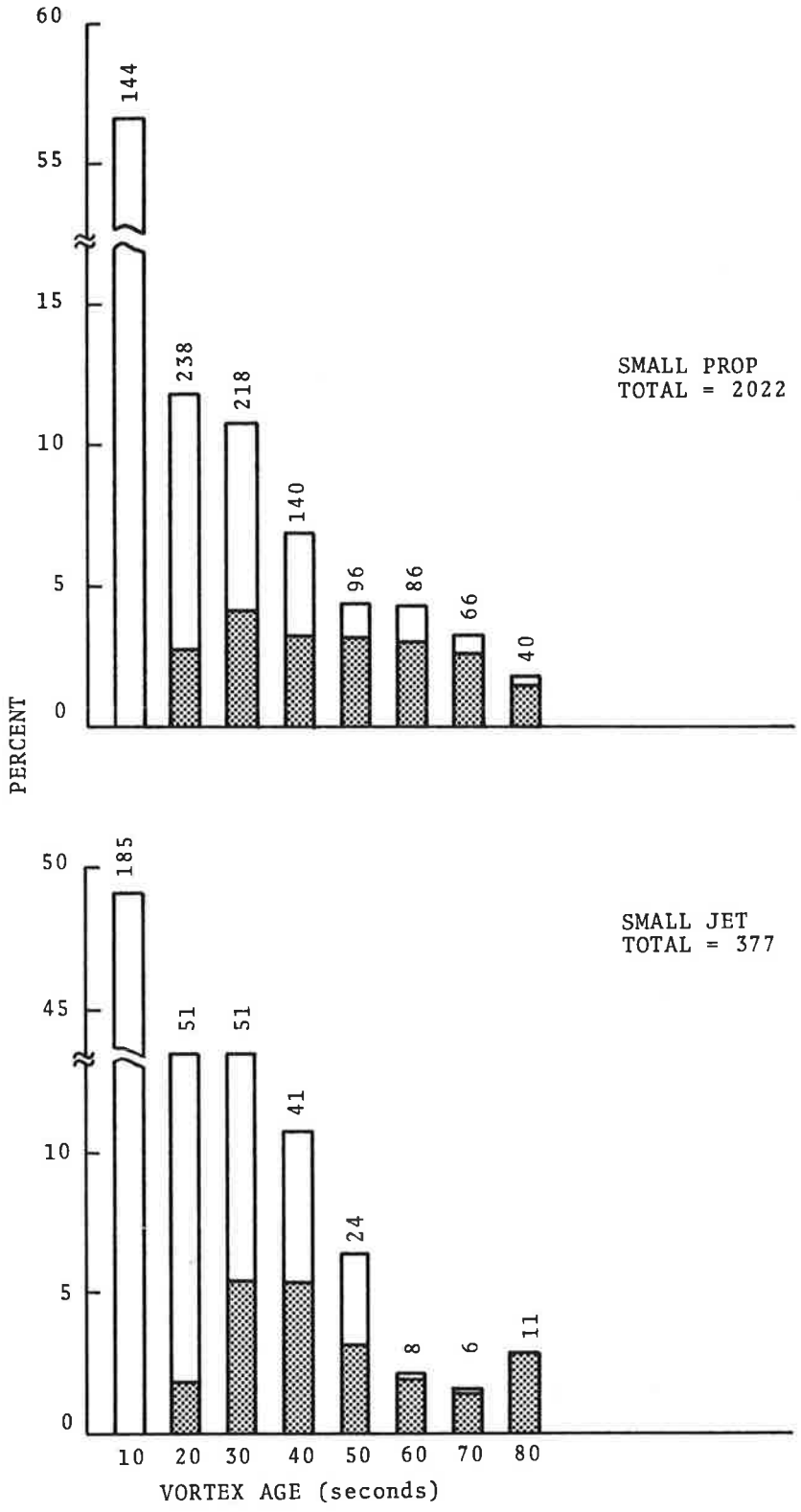

FIGURE 62. RESIDENCE TIME DATA FOR SMALL PROP (TOP) AND SMALL JET (BOTTOM) AIRCRAFT